

1 Scenario set-up and the new CMIP6-based climate-related forcings provided
2 within the third round of the Inter-Sectoral Model Intercomparison Project
3 (ISIMIP3b, group I and II)

4

5 Katja Frieler^{1,2}, Stefan Lange¹, Jacob Schewe¹, Matthias Mengel¹, Simon Treu^{1,2}, Christian
6 Otto¹, Jan Volkholz¹, Christopher P.O. Reyer¹, Stefanie Heinicke¹, Colin Jones³, Julia L.
7 Blanchard⁴, Cheryl S. Harrison⁵, Colleen M. Petrik⁶, Tyler D. Eddy⁷, Kelly Ortega-Cisneros⁸,
8 Camilla Novaglio⁴, Ryan Heneghan⁹, Derek P. Tittensor¹⁰, Olivier Maury¹¹, Matthias
9 Büchner¹, Thomas Vogt¹, Dánnell Quesada-Chacón¹, Kerry Emanuel¹², Chia-Ying Lee¹³,
10 Suzana J. Camargo^{13,14}, Linn Hamester¹, Jonas Jägermeyr^{14,15,1}, Sam Rabin^{16,a,b}, Jochen Klar¹,
11 Iliusi D. Vega del Valle¹, Lisa Novak¹, Inga J. Sauer¹, Gitta Lasslop¹⁷, Sarah Chadburn¹⁸,
12 Eleanor Burke¹⁹, Angela Gallego-Sala²⁰, Noah Smith²¹, Jinfeng Chang²², Stijn Hantson²³,
13 Chantelle Burton¹⁹, Anne Gädeke¹, Fang Li²⁴, Simon N Gosling²⁵, Hannes Müller
14 Schmied^{17,26}, Fred Hattermann¹, Thomas Hickler¹⁷, Rafael Marcé²⁷, Don Pierson²⁸, Wim
15 Thiery²⁹, Daniel Mercado-Bettín²⁷, Robert Ladwig³⁰, Ana I. Ayala²⁸, Matthew Forrest¹⁷,
16 Michel Bechtold³¹, Robert Reinecke³², Inge de Graaf³³, Jed O. Kaplan³⁴, Alexander Koch³⁵,
17 Matthieu Lengaigne¹¹, Rohini Kumar³⁶, Maryna Strokhal³⁷

18

19

20 Affiliations:

21 ¹Potsdam Institute for Climate Impact Research, 14473 Potsdam, Germany

22 ²University of Potsdam, Institute for Environmental Science and Geography, 14476
23 Potsdam, Germany

24 ³National Centre for Atmospheric Science and School of Earth and Environment, University
25 of Leeds, Leeds, LS29JT, UK

26 ⁴Institute for Marine and Antarctic Studies, University of Tasmania, Hobart, Tasmania,
27 Australia

28 ⁵Department of Ocean and Coastal Science and Center for Computation and Technology,
29 Louisiana State University, Baton Rouge, Louisiana, USA

30 ⁶Scripps Institution of Oceanography, University of California San Diego, CA, USA

31 ⁷Centre for Fisheries Ecosystems Research, Fisheries & Marine Institute, Memorial
32 University, St. John's, NL, Canada

33 ⁸Marine and Antarctic Research for Innovation and Sustainability, Department of Biological
34 Sciences, University of Cape Town, Rondebosch, Cape Town, 7701, South Africa

35 ⁹School of Environment and Science, Griffith University, Brisbane, Queensland, Australia

36 ¹⁰Department of Biology, Dalhousie University, Halifax, Nova Scotia, Canada, B3H 4R2

- 37 ¹¹IRD, Univ Montpellier, CNRS, Ifremer, INRAE, MARBEC, Sète, France
- 38 ¹²Lorenz Center, Massachusetts Institute of Technology, Cambridge, MA, USA
- 39 ¹³Lamont-Doherty Earth Observatory, Columbia University, Palisades, New York, USA
- 40 ¹⁴Columbia Climate School, Columbia University, New York, NY 10025, USA
- 41 ¹⁵NASA Goddard Institute for Space Studies, New York, NY 10025, USA
- 42 ¹⁶Climate and Global Dynamics Laboratory, National Center for Atmospheric Research
43 Boulder, CO 80302, USA
- 44 ¹⁷Senckenberg Leibniz Biodiversity and Climate Research Centre (SBIK-F), Frankfurt am
45 Main, Germany.
- 46 ¹⁸Department of Mathematics, University of Exeter, Exeter UK
- 47 ¹⁹Met Office Hadley Centre, Fitzroy Road, Exeter, UK
- 48 ²⁰Geography Department, University of Exeter, Exeter, UK
- 49 ²¹College of Engineering, Mathematics and Physical Sciences, University of Exeter, Exeter
50 EX4 4QF, UK.
- 51 ²²College of Environmental and Resource Sciences, Zhejiang University, Hangzhou, China
- 52 ²³Faculty of Natural Sciences, Universidad del Rosario, Bogotá, Colombia
- 53 ²⁴International Center for Climate and Environment Sciences, Institute of Atmospheric
54 Physics, Chinese Academy of Sciences, Beijing, China
- 55 ²⁵School of Geography, University of Nottingham, Nottingham, UK
- 56 ²⁶Institute of Physical Geography, Goethe University Frankfurt, Frankfurt am Main,
57 Germany
- 58 ²⁷Blanes Centre for Advanced Studies (CEAB-CSIC), Blanes, Spain
- 59 ²⁸Department of Ecology and Genetics, Uppsala University, Norbyvägen 18 D, 752 36
60 Uppsala, Sweden
- 61 ²⁹Vrije Universiteit Brussel, Department of Water and Climate, Brussels, Belgium
- 62 ³⁰Department of Ecoscience, Aarhus University, C.F. Møllers Allé 3, 8000 Aarhus C,
63 Denmark
- 64 ³¹KU Leuven, Department of Earth and Environmental Sciences, Leuven, Belgium
- 65 ³²Johannes Gutenberg-University Mainz, Mainz, Germany
- 66 ³³Earth Systems and Global Change Group, Wageningen University and Research,
67 Wageningen, The Netherlands
- 68 ³⁴Department of Earth Sciences and Institute for Climate and Carbon Neutrality, The
69 University of Hong Kong, Hong Kong
- 70 ³⁵Simon Fraser University, Burnaby, British Columbia, CA
- 71 ³⁶Department of Computational Hydrosystems, Helmholtz Centre for Environmental
72 Research—UFZ, Leipzig 04318, Germany
- 73 ³⁷Wageningen University & Research, Wageningen, Netherlands

74 ^aformerly at: Institute of Meteorology and Climate Research / Atmospheric Environmental
75 Research, Karlsruhe Institute of Technology, Garmisch-Partenkirchen, Germany
76 ^bformerly at: Department of Environmental Sciences, Rutgers University, New Brunswick,
77 New Jersey, USA

78
79 Correspondence to: Katja Frieler (katja.frieler@pik-potsdam.de)
80

81 **Abstract.** This paper describes the climate-related forcings (CRFs), i.e. change in climate
82 comprising the atmosphere and the ocean, coastal water levels, and atmospheric
83 composition (CO₂ and methane concentrations),) provided as input data provided within
84 the 'b' part of the third simulation round of the Inter-Sectoral Impact Model
85 Intercomparison Project (ISIMIP3b). While ISIMIP3a comprises historical impact models
86 simulations forced by observational ~~CRF and D~~direct ~~H~~human ~~F~~forcings (DHF), such as
87 changes in population and asset distributions, land use, fishing efforts, agricultural and
88 water management driven by socio-economic development or climate protection
89 strategies, and observational CRF, the ISIMIP3b CRFs are based on climate model
90 simulations generated within the sixth phase of the Coupled Model Intercomparison
91 Project (CMIP6). In a first set of experiments covering the pre-industrial (1601–1849) and
92 historical period (1850–2014) (ISIMIP3b, group I) the CMIP6-based CRFs for the ~~historical~~
93 period are combined with historical observation-based DHF also considered in ISIMIP3a
94 ~~(e.g. land use patterns, water and agricultural management, and fishing efforts)~~. These
95 group I simulations allow for the quantification of impacts of historical climate change by
96 comparison to simulations where the observational DHF are combined with simulated pre-
97 industrial CRFs. In addition, the impacts of observed changes in CRFs can be compared to
98 the impacts of simulated changes in CRFs by comparing the ISIMIP3a simulations to the
99 ISIMIP3b, group I simulations. The second group of experiments (ISIMIP3b, group II)
100 comprises future projections assuming constant observational direct human forcings at
101 2015 levels to estimate the impact of climate change given today's ~~DHF~~direct ~~human~~
102 ~~influences~~ for the low emission scenario SSP1-2.6, the high and the very high emission
103 scenarios SSP3-7.0, SSP5-8.5, and reference simulations based on pre-industrial CRF,
104 respectively. The very high emissions scenarios and the assumption of fixed present day
105 ~~DHF~~direct ~~human~~ forcings particularly allow for testing the scalability of impacts in terms
106 of global temperature change. The provided CRFs comprise atmospheric CO₂ and CH₄
107 concentrations, atmospheric and oceanic climate data, coastal water levels, tropical
108 cyclone (TC) tracks and their associated wind speed and precipitation fields. In addition to
109 the CRFs data, this paper describes the experiments belonging to group I and II and the

110 rationale behind them. Another set of future projections accounting for changing DHFs
111 (ISIMIP3b, group III) is in preparation and will be described in another paper.

112

113

114 **Introduction**

115 This is the second paper of a series of three papers describing the experiments of the
116 third simulation round of the Inter-Sectoral Impact Model Intercomparison Project ISIMIP
117 (isimip.org). The project provides a common scenario framework for cross-sectorally
118 consistent climate impact simulations. Here, the term ‘experiment’ is used as synonym for
119 ‘scenario-setup’, i.e. the specification of the impact model simulations in terms of the
120 applied input data or additional assumptions determining the simulations. This is
121 following the use of the term within other model intercomparison projects such as the
122 Coupled Model Intercomparison project CMIP (CMIP Model and Experiment
123 Documentation) and a longer tradition within ISIMIP. Within ISIMIP the experiments are
124 determined by the underlying set of CRFs and DHF. The CRF is different from the ‘climate
125 forcing’ considered within climate models. For the impact models the associated climate
126 change represents the forcing. In addition, some of the impacts (e.g. changes in natural
127 vegetation and crop yields) also directly depend on CO₂ concentrations (CO₂ fertilization
128 effect, increased water use efficiency). Others (coastal infrastructure models) need
129 information about sea level rise as input. Following the terminology of the IPCC AR6,
130 where climate-related systems are defined as the “climate system including the ocean and
131 the cryosphere as physical or chemical systems” (B. O’Neill et al., 2022), we label this group
132 of forcings as Climate-Related Forcings (CRF) that cover all the inputs listed in Table 1. This
133 group is distinguished from the Direct Human Forcing induced by socio-economic
134 development, mitigation strategies or human adaptation measures such as land use
135 changes, changes in agricultural and water management, population and assets
136 distributions. While this paper only introduced the CRF for the ISIMIP3b, group I + II
137 experiments a list of inputs belonging to this second group of forcings can be found in
138 Frieler et al., (2024).

139 **Currently, operational simulation protocols exist for the following sectors: Agriculture,**
140 **Biomes, Energy, Fire, Food security and nutrition, Groundwater, Labour, Lakes global,**
141 **Lakes regional, Fisheries and marine ecosystems global, Fisheries and marine ecosystems**
142 **local, Peatland, Permafrost, Water global, Water regional. Additional protocols for Coastal**
143 **systems, Regional forests, Temperature-related mortality, health indicators, Terrestrial**
144 **biodiversity, and Water quality sectors are under development.**

145

146

147 In its third round it covers i) model evaluation and climate impact attribution experiments
148 based on observation-based [CRFclimate](#) and [DHFdirect human forcings \(DHF\)](#) (ISIMIP3a,
149 [Table 1 of the associated protocol paperfirst paper](#), (Frieler et al., 2024), ii) climate impact
150 simulations driven by simulated [CRFclimate-related forcings \(CRF\) based on climate model](#)
151 [simulations generated within thebased the](#) sixth phase of the Coupled Climate Model
152 Intercomparison Project (CMIP6) ([see Table 1, this paper](#)) assuming ISIMIP3a
153 observational DHF in the historical period and fixed 2015 DHF for the future simulations
154 (ISIMIP3b, group I+II, this paper), and iii) an upcoming set of CMIP6-based future
155 projections where DHF vary according to given Shared Socioeconomic Pathways (SSPs) (no
156 adaptation scenarios) and in response to climate change impacts (adaptation scenarios)
157 (ISIMIP3b, group III). So while this paper only describes the ISIMIP3b CRF, [the first paper](#)
158 [described the historical DHF used within ISIMIP3b, and](#) the third paper will only address
159 the [future](#) DHFs [for group III](#) that are still under development while the CRF of the group
160 III simulations will be identical to the future CRF described here.

161
162 Similar to the Coupled Model Intercomparison Project (CMIP) (Eyring et al., 2016) all
163 simulations will be freely available (*ISIMIP Repository*, 2020) to allow for follow-up analysis.
164 The consistent design of the simulations does not only allow for the comparison of climate
165 impact simulations within each sector, but also enables the bottom-up integration of
166 impacts across sectors. Thus, it provides a unique basis for the estimation of the effects of
167 climate change on, e.g., the economy, displacement and migration, health, or water
168 quality resolving the mechanisms along different impact channels and fully exploiting the
169 process-understanding represented in the biophysical impact models.

170
171 Compared to [the CMIP5-based](#) ISIMIP2b, the ISIMIP3b CRF represent the following
172 updates: i) climate forcing data based on phase 6 of the Coupled Model Intercomparison
173 Project (CMIP6) (Eyring et al., 2016) and post-processed by an improved bias adjustment
174 and statistical downscaling method (see section **3.2**), and ii) [provision of](#) large ensembles
175 of potential realisations of tropical cyclone tracks, wind and precipitation fields derived
176 from two different modelling approaches assuming CMIP6 boundary conditions, while in
177 ISIMIP2b only one approach was used and precipitation fields were not included. In
178 addition, we plan to provide coastal water levels at high temporal resolution (upcoming).
179 The approach to generate the data is also described here.

180
181 The development of the ISIMIP3b protocol was coordinated by the ISIMIP-Cross-Sectoral
182 Science Team (CSST) at the Potsdam Institute for Climate Impact Research (PIK) along the
183 same decision process as for ISIMIP3a (Frieler et al., 2024).

184
185
186
187
188
189
190
191
192
193
194
195
196
197
198
199
200
201
202
203
204
205
206
207
208
209
210
211
212
213
214
215
216
217
218
219
220

This paper is accompanied by a simulation protocol (*ISIMIP3b Simulation Protocol*, 2026) providing all technical details such as file and variable naming conventions, as well as sector-specific output variables to be reported by the participating modelling teams. ~~This paper refers to the protocol version of December 21st, 2023. However, a~~As the protocol may still be updated due to addition of new variables, correction of errors, or the inclusion of new sectors, contributors to ISIMIP should always refer to protocol.isimip.org for the most up to date reference for planned impact model simulations.

The ISMIP3a and ISIMIP3b protocols have been jointly developed and participation in ISIMIP3 requires contribution to both ISIMIP3a and ISIMIP3b, using the same impact model versions in order to allow for the evaluation of the impact models future projections in ISIMIP3b.

~~†The paper provides a catalogue where interested modellers can find the data to run their models according to the ISIMIP3b protocol.~~

~~In section 1 the following, we describe selected scenarios and the rationale behind the individual scenario set-ups chosen within the community-driven decision process (section 1). In section 2 the second section, we then introduce the individual climate-related forcing data sets collected as input for the different modelling experiments in the second section covering atmospheric climate data including lightning and tropical cyclones tracks, wind and precipitation fields; ocean data; coastal water levels; and atmospheric CO₂ as well as CH₄ concentrations. WeThe paper does not analyse and discuss these data sets but only provides a brief documentation of the approaches, variable names, formats, references, sources, covered time period, etc., as a service to the community, without analysing and discussing these datasets, except for .-WeIt only shows and analyses the effects of an adjustment of the bias-adjustment method used to generate the ISIMIP3b atmospheric forcing data (see section 2.1).-Instead, †The paper is provides a intended to work as a catalogue where interested modellers can find the data to run their models according to the ISIMIP3b protocol. The paper only shows and analyses the effects of an adjustment of the bias-adjustment method used to generate the ISIMIP3b atmospheric forcing data (see section 2.1).~~

1 Experiments and underlying rationale

The selection of the scenarios is a community-driven process constrained by the availability of climate model simulations (~~multi-GCM ensemble~~ of simulations by multiple

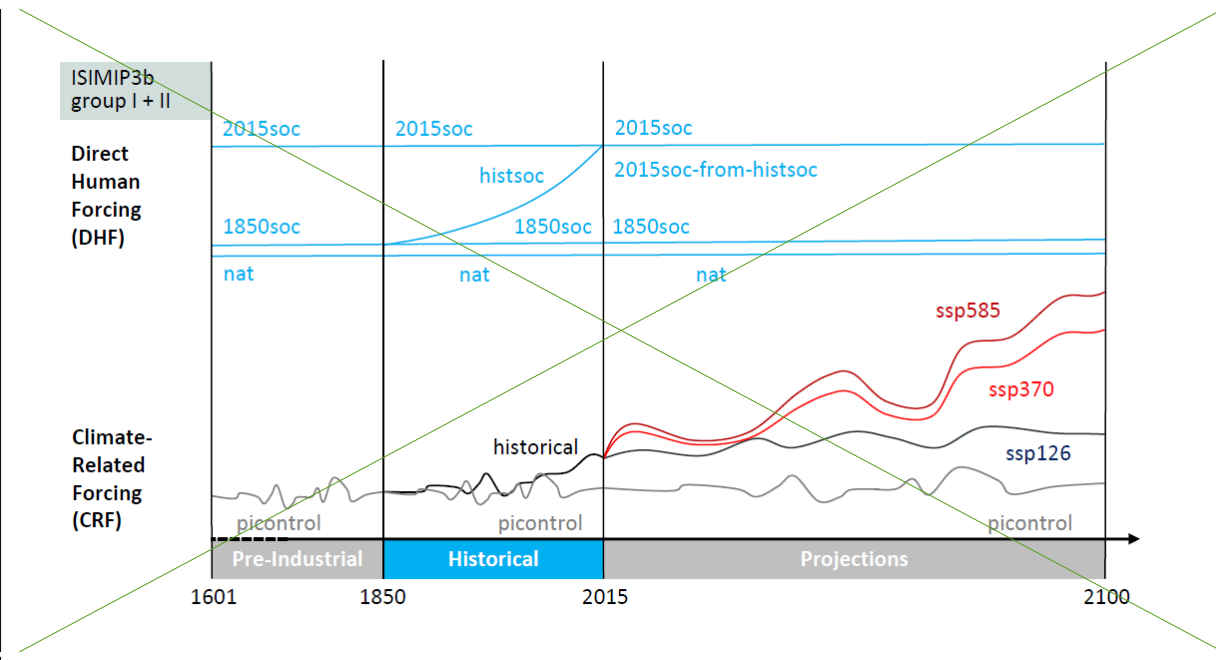
221 | General Circulation Models (GCMs) per scenario) and socio-economic background
222 | information (such as land use patterns, populations and GDP data etc. additionally
223 | required as 'Direct Human Forcing' for the ISIMIP3b, group III impact model simulations
224 | that will be introduced in an upcoming paper). These criteria have made CMIP6-
225 | ScenarioMIP the reference point for the selection (B. C. O'Neill et al., 2016). The selection
226 | of ISIMIP3b scenarios (see **Figure 1**) from the four ScenarioMIP Tier 1 scenarios was
227 | additionally driven by the aim to capture a wide range of possible futures from low to high
228 | emission scenarios and to provide ~~of~~ a long baseline simulation assuming pre-industrial
229 | climate conditions that allows for a robust estimation of reference return levels of
230 | extreme events. This is why the original selection comprised the pre-industrial baseline
231 | ('picontrol'), the historical simulations ('historical'), SSP1-2.6 representing the 'low end of
232 | the range of future forcing pathways in the IAM literature', and SSP5-8.5 representing the
233 | 'high end of the range of future pathways in the IAM literature' (B. C. O'Neill et al., 2016).
234 | Given recent mitigation efforts, some estimates of recoverable coal reserves, and
235 | decreasing prices for renewable energies the emissions underlying SSP5-8.5 have been
236 | criticised for being unplausibly high (Hausfather & Peters, 2020). Based on these
237 | discussions, the 'medium to high end of the range of future forcing pathway' SSP3-7.0 (B.
238 | C. O'Neill et al., 2016) has been added to the ISIMIP3b scenario set-up. While this scenario
239 | is described as 'average no climate protection policy' by Hausfather & Peters (2020), we
240 | highlight that we explicitly do not describe it as a 'business as usual scenario' and that this
241 | was not the framing within ScenarioMIP either. Instead SSP3-7.0 differs from the other
242 | scenarios with regard to particularly high aerosol emissions and high decreases in forest
243 | areas going beyond the assumptions in the other scenarios. So it has been shown that the
244 | increase of global mean precipitation with global warming is much weaker in SSP3-7.0
245 | than in the other scenarios is based on rather extreme assumptions about land use
246 | changes and aerosol emissions e.g. leading to a scaling of precipitation with global mean
247 | temperature that diverges from the scaling identified in the other scenarios (Shiogama et
248 | al., 2023). In addition, SSP5-8.5 is explicitly kept in the ISIMIP3b ensemble as its
249 | particularly strong warming signal allows testing to what degree the simulated impacts of
250 | climate may scale with global mean temperature, which could allow for a translation of
251 | impacts to other emission scenarios. In addition, even under lower emission scenarios,
252 | global warming levels as the ones reached under SSP5-8.5 in 2100 will eventually be
253 | reached later in time as long as emissions are not reduced to zero. These impacts of high
254 | warming levels would not be captured when only considering lower emission scenarios
255 | ending in 2100.

257 However, in such a setting it has to be taken into account that ssp370 is different from the
258 other scenarios with regard to particularly high aerosol emissions and high decreases in
259 forest areas going beyond the assumptions in the other models. So it has been shown
260 that the increase of global mean precipitation with global warming is much weaker in
261 SSP3-7.0 than in the other scenarios (Shiogama et al., 2023).

262
263 All ISIMIP experiments are determined by the underlying set of CRFs and DHF, where each
264 package of CRF and DHF has a specific label that will then be included in the output file
265 names to allow for an identification of the experiments they belong to. The individual
266 experiments are defined by the combination of both types of forcing data sets, where the
267 associated specifiers are indicated in brackets in the subheadings naming the
268 experiments (CRF specifier + DHF specifier). The different combinations of the default sets
269 of ISIMIP3b CRFs ('picontrol', 'historical', 'ssp126', 'ssp370', and 'ssp585') and DHF ('histsoc',
270 '2015soc', '1901soc', '1850soc', 'nat', and '2015soc-from-histsoc') are sketched in **Figure 1**
271 and described in more detail below.

272
273 The CRF data described in this paper are mandatory; i.e. if impact models consider this
274 forcing, the specified dataset must be used; if an alternative input data set is used instead,
275 the run cannot be considered an ISIMIP3b, group I + II simulation. The DHF for the
276 historical period is identical to the ISIMIP3a DHF listed in **Table 1** of Frieler et al. (2024)
277 where we also indicate whether the data set is mandatory or optional. Optional forcing
278 data could be used but is not mandatory. In addition, the protocol includes a set of
279 sensitivity experiments that are described as deviations from the default runs and labelled
280 by the baseline CRF and DHF settings and a third specifier indicating the deviation from
281 this default setting. The ISIMIP3b group I+II sensitivity scenario set-ups include
282 experiments with fixed levels of atmospheric CO₂ concentrations ('2015co2'), high levels in
283 CO₂ concentrations in combination with low levels of climate change ('ssp585co2'), and
284 runs with lightning data that vary in response to climate change ('varlightning'), while
285 lightning is fixed at present day levels in the default runs. These sensitivity experiment
286 runs are not depicted in **Figure 1** but listed in **Table 2**.

289



290

291

292

293

294

295

296

297

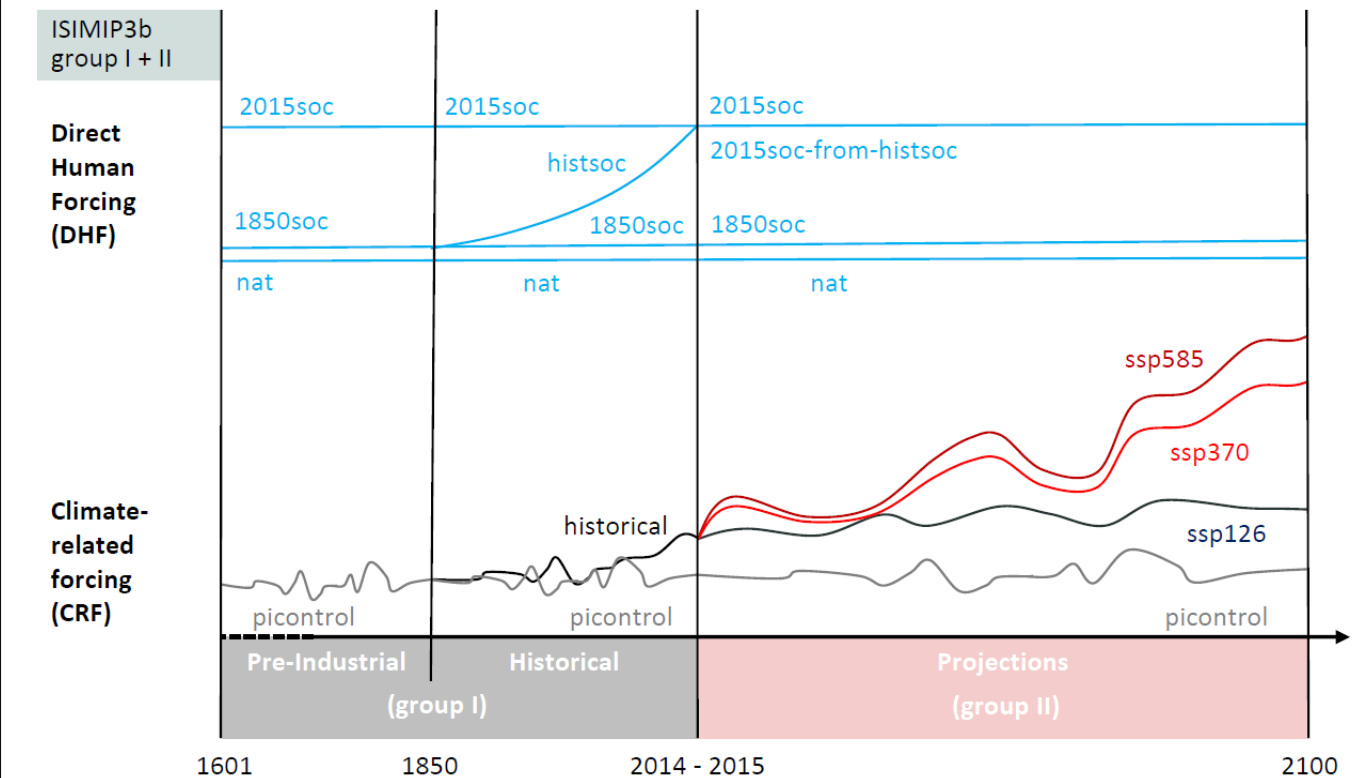


Figure 1: Illustration of the default ISIMIP3b forcing data sets. Each ISIMIP3b experiment is defined by a combination of a CRF data set with a DHF data set. The considered combinations are listed in **Table 2** and the underlying rationale is described in section **1.1** and **1.2**. **Table 1** lists all data sets defining the considered CRFs while the DHFs are based on the same datasets as in ISIMIP3a. Potentially required spin-up procedures are not included in the Figure, but described in section **1.1**.

298 The ISMIP3b simulations are divided into two groups. Group I comprises the simulations
 299 from 1601 - 1849 (pre-industrial) and 1850 - 2014 (historical) assuming simulated pre-
 300 industrial and historical CRFs and different constant ('nat', '1850soc', and '2015soc') or
 301 varying ('histsoc') levels of DHF based on the same observational data used in ISIMIP3a
 302 (see **Figure 1**). Group II comprises the future projections assuming constant 2015 levels of
 303 DHF (see **Figure 1**) including a baseline with pre-industrial CRF (grey line in the future
 304 projections part of **Figure 1**). All experiments are introduced in more detail below (section
 305 **1.1** for group I and **1.2** for group II).

307 In contrast to ISIMIP3a, the CRFs provided for ISIMIP3b currently only comprise
 308 atmospheric (see section **2.1**) and oceanic climate data (see section **2.4**), tropical cyclone
 309 tracks with associated wind and precipitation fields (see section **2.2**), and CO₂ and
 310 methane concentration (see section **2.5**). We do not yet provide associated coastal water
 311 levels (see section **2.2.3** for planned work), ~~and lightning data (see **Table 511**)~~. Impact
 312 simulations that rely on the missing forcings cannot be generated within ISIMIP3b yet, but
 313 we are currently developing their setup and will provide the forcings as soon as possible.
 314 The ISIMIP3b atmospheric and oceanic climate data ~~are~~ derived from five different
 315 ~~General Circulation Models (GCMs)~~ generated within the Coupled Model Intercomparison
 316 project, phase 6 (CMIP6).

318 **Table 1: Climate-Related Forcing datasets for ISIMIP3b.**

Forcing	Status	Source, description
Climate-related forcings ('picontrol', 'historical', 'ssp126', 'ssp370', 'ssp585')		
Atmospheric forcings ('picontrol', 'historical', 'ssp585', 'ssp370', 'ssp126')		
Gridded atmospheric climate forcing	mandatory	Bias-adjusted data (pre-industrial climate, historical climate, and future projections for the SSP1-2.6, SSP3-7.0, and SSP5-8.5 scenarios) generated by GFDL-ESM4, IPSL-CM6A-LR, MPI-ESM1-2-HR, MRI-ESM2-0, and UKESM1-0-LL within CMIP6 (Lange & Büchner, 2021), see section 2.1
Local atmospheric climate forcing for lakes	mandatory	Atmospheric data extracted from the data sets above for 72 lakes that have been identified within the lake sector as locations (grid cell of the ISIMIP 0.5° grid, ISIMIP3 local lake sites) where models can be calibrated based on observed temperature profiles and hypsometry within ISIMIP3b

		(depth and area) (Lange & Büchner, 2021)
Tropical cyclone tracks with wind and precipitation fields	mandatory	<p>Available on request (see section 2.2), samples of synthetic tropical cyclone tracks derived from the five CMIP6 GCMs considered within ISIMIP generated by two different statistical downscaling approaches, see section 2.2 and Meiler et al., (2025) for a comparison of the approaches.</p> <p>MIT approach (Emanuel et al., 2008, 2025):</p> <ul style="list-style-type: none"> ● pre-industrial climate from IPSL-CM6A-LR, MPI-ESM1-2-HR and MRI-ESM2-0 (all 1850--2014), and from UKESM1-0-LL (1950--2100) ● historical climate from IPSL-CM6A-LR, MPI-ESM1-2-HR, UKESM1-0-LL and GFDL-ESM4 (all 1850--2014), and from MRI-ESM2-0 (1950--2014). ● Future climate: <u>ssp126 (2061--2100)</u>, <u>ssp370 (2015--2100)</u> and <u>ssp585 (2015--2100)</u> from IPSL-CM6A-LR, MPI-ESM1-2-HR, MRI-ESM2-0, UKESM1-0-LL, and <u>ssp585 (2061--2100)</u> from GFDL-ESM4. <p>Two different configurations (SD and CRH, see section 2.2) of the Columbia HAZard model (CHAZ, Leet et al. (2018, 2025):</p> <ul style="list-style-type: none"> ● pre-industrial climate (1601-2100) from GFDL-ESM4, IPSL-CM6A-LR, MPI-ESM1-2-HR, MRI-ESM2-0, and UKESM1-0-LL. ● historical climate (1850--2014) from GFDL-ESM4, IPSL-CM6A-LR, MPI-ESM1-2-HR, MRI-ESM2-0, and UKESM1-0-LL ● future climate (2015--2100): <u>ssp126</u>, <u>ssp370</u>, <u>ssp585</u> from GFDL-ESM4, IPSL-CM6A-LR, MPI-ESM1-2-HR, MRI-ESM2-0, and UKESM1-0-L <p>For tracks generated by the MIT approach, we also provide wind and precipitation fields (Quesada-Chacón et al., 2025a, 2025b).</p>
Lightning	mandatory	Flash Rate Monthly Climatology not changing with climate change (Cecil, 2006)

Oceanic forcings ('picontrol', 'historical', 'ssp585', 'ssp370', 'ssp126')		
Oceanic climate forcing	mandatory	Uncorrected data (pre-industrial climate, historical climate, and future projections for the SSP1-2.6, SSP3-7.0, and SSP5-8.5 scenarios) generated by GFDL-ESM4, IPSL-CM6A-LR, MPI-ESM1-2-HR, and UKESM1-0-LL within CMIP6 (Büchner, 2024), see section 2.4
Coastal water levels		
Coastal water levels	mandatory	This data set has not been generated yet. However, in section 2.3 we describe a method to generate relative sea level projections that smoothly extend tide gauge observations into the future building on a Bayesian model (Perrette & Mengel, 2025). For ISIMIP3, we plan to extend the framework to all coastlines and directly use ISIMIP GCM output for the global thermodynamic and local aerodynamic components, adjusting the gridded simulations to associated observations to ensure a consistent transition from the historical period. Ice sheet and glacier contributions are incorporated through spatial fingerprints, while unresolved vertical land motion processes are estimated from residuals at tide gauges and extrapolated where no observations are available. We are also developing an approach to extend the sea level projections to daily maximum water levels derived from the ISIMIP3 atmospheric forcings (daily mean sSurface aAir pPressure and daily mean nNear-sSurface wWind sSpeed).
Atmospheric composition or fluxes		
Atmospheric CO ₂ concentration	mandatory	Büchner & Reyer (2022) based on the following sources: 1850–2005: Meinshausen et al. (2011); 2006–2014: Global annual CO ₂ from NOAA Global Monthly Mean CO ₂ (Lan et al., 2023); 2015–2100: Meinshausen et al. (2020)
Atmospheric CH ₄ concentration	mandatory	Büchner & Reyer (2022) based on the following sources: 1850–2014: Meinshausen et al. (2017); 2015–2100: Meinshausen et al. (2020)
Climate-Related Forcings for the sensitivity experiment 'varlightning', using above forcing data except for:		

Lightning data ('varlightning')		
Varying lightning according to climate change	mandatory	Lightning data has been generated for the ssp126, ssp370, and ssp850 climate projections from UKESM1-0-LL (Kaplan et al., 2023)
Climate-Related Forcings for the 'de-biased' sensitivity experiment		
Global oceanic forcings		
Oceanic forcings based on de-biased atmospheric forcings	mandatory	<u>These data sets have not been generated yet. However, in section 2.4.2 we propose an approach to de-bias the oceanic forcings based on the ocean biogeochemistry model NEMO-PISCES forced by a de-biased version of the IPSL-CM6A-LR-based atmospheric forcing as an option to fulfil the demand for de-biased ocean data we would like to follow.</u> Not available yet, simulated by the ocean-biogeochemistry model ocean-biogeochemistry NEMO-PISCES forced by a de-biased version of the IPSL-CM6A-LR-based atmospheric forcing (see section 2.4.2)
Regional oceanic forcings		
De-biased oceanic forcing based on observed oceanic data for individual variables and regions	mandatory	<u>The regional models of the fisheries and marine ecosystem sector have applied regional bias-adjustments within their impact simulations that are described in section 2.4.3 and that make these simulations part of the 'de-biased' sensitivity experiment in the sector (see Table 2) while the default experiments are based on the raw oceanic forcings.</u> Not centrally provided, see section 2.4.3

319

320

321 **1.1 ISIMIP3b, group I: Climate-model based impact model simulations for** 322 **the period from 1601 to 2015**

323

324 The group I experiments cover the years 1601–1849 with pre-industrial CRFs ('picontrol')
325 and fixed 1850 direct human forcings ('1850soc') described in the grey column 3 of the
326 ISIMIP3b scenario **Table 2** as well as the subsequent years 1850–2014 considering pre-
327 industrial and historical CRF climate-related forcings ('picontrol' or 'historical') and different
328 assumptions about DHFdirect human forcings ('histsoc', '2015soc', '1850soc', and 'nat') as

329 described in the grey column 4 of **Table 2**. The reasoning behind the individual
330 experiments are introduced below.

331
332 **Pre-industrial reference simulations (picontrol + histsoc, picontrol + 2015soc,**
333 **picontrol + 2015soc-from-histsoc, picontrol + 1850soc, picontrol + nat; default):** To
334 estimate the impacts of historical and future changes in the CRFs, the protocol includes
335 reference simulations based on pre-industrial CRFs and DHF identical to those considered
336 in the climate change scenario runs. These reference simulations represent large samples
337 (at least 250 years) of impact distributions based on stable pre-industrial CRFs (picontrol)
338 and constant DHFs (see ‘picontrol + 1850soc’, ‘picontrol + 2015soc’, and ‘picontrol + nat’
339 experiments in **Table 2**). Compared to the often used much shorter historical reference
340 periods, this allows for a more robust fitting of extreme value distributions such as
341 Gumbel distributions to simulation of e.g. annual maximum discharge to estimate
342 reference 100 year return levels. ~~In order to allow for the fitting of extreme value~~
343 ~~distributions such as Gumble or Generalized Extreme Value (GEV) distributions to, e.g. annual~~
344 ~~maximum discharge to estimate reference 100 year return levels of certain impacts, the runs are~~
345 ~~designed to include~~includes the generation of large samples (at least 250 years) of impact
346 ~~distributions distribution based on stable pre-industrial CRFs (picontrol) and constant DHFs (see~~
347 ~~‘picontrol + 1850soc’, ‘picontrol + 2015soc’, and ‘picontrol + nat’ experiments in Table 2).~~

348 In addition, the protocol includes a reference experiment for the historical period (1850--
349 2014) with DHF changing over time (histsoc) and 1850--2014 pre-industrial CRF (picontrol),
350 while fixed 2015 DHF is considered afterwards (2015--2100) (‘picontrol + 2015soc-from-
351 histsoc’). This run may be different from the ‘picontrol + 2015soc’ simulation for this time
352 window because of the lagged effects of increasing DHF from 1850 to 2014. The ‘histsoc’
353 DHF is identical to ISIMIP3a (Frieler et al., 2024).

354 The complete pre-industrial reference runs are divided in two parts. Only the first parts
355 from the start until 2014 belong to group I (grey fields in [Table 2](#)~~the table~~), while the
356 second parts covering the period 2015--2100 belong to group II (red parts of ~~the t~~**Table**
357 [2](#)).

358
359 Comparing these reference simulations to the scenario experiments using historical CRFs
360 (historical + histsoc, historical + 2015soc, historical + 1850soc, historical + nat; default (see
361 below)) allows for the estimation of the effects of simulated historical climate change
362 conditional on the assumed DHF. The historical CRFclimate-related forcing (‘historical’)
363 starts from the pre-industrial climate simulation in 1850, i.e. the ‘picontrol’ and ‘historical’
364 versions of the experiments have a common starting point. As some impact indicators
365 may have ‘internal’ trends not necessarily forced by external drivers (e.g. re-growth of

366 forests), the comparison of the 1850–2014 impact simulations forced by the ‘historical’
367 CRF to parallel simulations using the ‘picontrol’ CRF is more appropriate to estimate the
368 effects of historical climate change than comparing an early period of the historical impact
369 simulation to the end of the historical period. The comparison of the simulations
370 assuming ‘historical’ CRF with the reference simulations based on ‘picontrol’ CRF does not
371 allow for a separation of the impacts of the natural and anthropogenic historical climate
372 forcing. To allow for a quantification of the effects of the anthropogenic CRFs, we also
373 support historical reference simulation accounting for the natural CRF only (‘hist-nat’
374 simulations generated within the Detection and Attribution Model Intercomparison
375 Project (DAMIP) as sub-MIP of CMIP6, (Gillett et al., 2016)). While this set-up is not an
376 official part of the ISIMIP3b protocol, we provide the associated bias-adjusted CRF as
377 secondary climate input data (Lange et al., 2023).

378 For models requiring a spin-up, the ‘picontrol’ CRFs should be used in combinations with
379 DHF i) at 1850 levels to spin-up for the ‘1850soc’ and ‘histsoc’ experiments, ii) at 2015 levels
380 to initialise the ‘2015soc’ experiment, and iii) set to zero to start the ‘nat’ experiments. For
381 the spin-up all years of the ‘picontrol’ CRF should be copied as often as needed. The
382 ‘picontrol + 1850soc’ run from 1601–1849 is part of the regular experiments that should
383 be reported and hence the spin-up has to be finished before this pre-industrial period.

384 ~~To allow for a quantification of the impacts of the anthropogenic CRFs, we also support~~
385 ~~historical reference simulation assuming only natural CRF (‘hist-nat’ simulations generated~~
386 ~~within the Detection and Attribution Model Intercomparison Project (DAMIP) as sub-MIP~~
387 ~~of CMIP6, (Gillett et al., 2016) by providing the associated bias-adjusted CRF as secondary~~
388 ~~climate input data (Lange et al., 2023). However, associated simulations are not an official~~
389 ~~part of ISIMIP3b and not described in the associated protocol.~~

390
391 **Standard historical simulations based on historical climate-related forcing and**
392 **observed changes in direct human forcing (historical + histsoc; default):** This
393 experiment covering the historical period (1850–2014) is determined ~~are forced~~ by
394 historical (‘historical’) CRFs and DHFs evolving according to observations (ISIMIP3a ‘histsoc’
395 DHF). The ISIMIP3b ‘historical + histsoc’ experiment is comparable to the default ‘obsclim +
396 histsoc’ experiment ~~run used~~ considered within ISIMIP3a but based on simulated CRFs.
397 The simulated climate is different from the observed realisation due to differences in the
398 internal variability of the observed and simulated historical climate and potential deficits
399 in the climate model simulations or the observational data. A comparison between the
400 default ISIMIP3b ‘historical + histsoc’ impact model simulations to the associated ISIMIP3a
401 results allows for a quantification of the effects of the discrepancies between the observed
402 and simulated CRFs on the considered impact indicators. This simulation ~~experiment~~ can

403 | be initialised from the spin-up of the associated pre-industrial reference simulations in
404 | case a spin-up is needed.

405

406 | **Simulations with historical climate-related forcing and fixed 2015 direct human**
407 | **forcing (historical + 2015soc; default):** This historical experiment is similar to the
408 | standard historical experiment except that it is forced by fixed 2015 DHF. It is introduced
409 | into the 'first priority' scenario-set-up to generate an ensemble of historical cross-
410 | sectorally consistent impact simulations that is as large as possible by not excluding
411 | impact models that are not able to handle varying DHF. If a spin-up is needed the
412 | associated simulationexperiment can be initialised from the spin-up of the associated
413 | pre-industrial reference simulation (picontrol + 2015soc, default) described at the
414 | beginning of this section.

415

416 | **Simulations with historical climate-related forcing and fixed 1850 direct human**
417 | **forcing (historical + 1850soc; default):** This historical experiment is also similar to the
418 | standard historical experiment but it is forced by the fixed 1850 DHFs. It corresponds to
419 | the 'obsclim + 1901soc' experimentsimulation of ISIMIP3a. Here in ISIMIP3b we consider
420 | the year 1850 instead of 1901 used in ISIMIP3a as this is the year where the 'historical'
421 | climate simulations with observed natural and human forcings start, i.e. a branch from the
422 | pre-industrial climate simulations assuming constant pre-industrial forcings ('picontrol').
423 | The 'historical + 1850soc, default' impact model simulations allow for the quantification of
424 | the 'pure effect of climate change' over the historical period. In contrast, the comparison
425 | of the 'historical + 1850soc, default' impacts simulations to the 'historical + histsoc'
426 | simulations allows for the quantification of the 'pure effect of historical changes in DHF'. If
427 | a spin-up is required it does not have to be newly generated as it is identical to the spin-up
428 | for the default 'picontrol + 1850soc', 'picontrol + histsoc', and 'historical + histsoc'
429 | simulationexperiments and described in the beginning of this section.

430

431 | **Simulations with historical climate-related forcing and no direct human forcings**
432 | **(historical + nat; default):** Considering no DHFdirect human forcings (nature run) allows
433 | quantifying the effect of the simulated historical climate change conditional on otherwise
434 | natural conditions, i.e. no direct human influences on land use, water management etc..
435 | This experiment is introduced as a companion experiment— to the 'obsclim + nat'
436 | experimentsimulations of ISIMIP3a. The comparison with the three historical simulations
437 | with constant DHFdirect human forcings allows for testing; to what degree the impact of
438 | climate change on the simulated natural or human systems is conditional on the
439 | underlying DHFdirect human forcing. This experiment is only included for the biomes and

440 fisheries and marine ecosystems fisheries sectors as models from other sectors usually
441 need some basic information such as vegetation patterns that are not available for
442 natural-only conditions. The biomes models generate their own natural-only vegetation
443 patterns based on their dynamic representation of vegetation. A spin-up does not have to
444 be newly generated but is identical to the spin-up for the 'picontrol + nat' experiment
445 described above.

446

447 **'De-biased' sensitivity simulations within the marine ecosystems and fisheries sector**
448 **(FishMIP) with de-biased historical oceanic forcings and no or histsoc direct human**
449 **forcings (historical + nat, historical + histsoc; de-biased):** So far, the default oceanic
450 forcing is not bias-adjusted as globally the observational data are ~~too sparse~~ to ~~be~~ ~~used~~
451 be used in a similar empirical way as for the bias-adjustment of the atmospheric forcing.
452 However, the biases in the forcing are expected to also induce biases in the historical and
453 future impact simulations. To quantify these effects and to test a suggested bias-
454 adjustment method based on comprehensive ocean-biogeochemistry model simulations
455 forced by bias-adjusted atmospheric forcings we include a sensitivity experiment where
456 the default ~~CRFclimate-related forcing~~ is replaced by input data generated by a dynamical
457 de-biasing approach (Lengaigne et al., 2025) using the NEMO-PISCES physical-
458 biogeochemical ocean model (Madec, 2015), which is the oceanic component of the IPSL-
459 CM6A-LR climate model. Thus, the forcing data will first be generated for IPSL-CM6A-LR,
460 but later extended to other ISIMIP-GCMs as described in subsection **2.4.2**.

461 In contrast, the oceanic forcing for the regional component of the marine ecosystems and
462 fisheries sector have been bias-adjusted by regional observational oceanic data as
463 described in subsection **2.4.3**. In this case most models only use the bias-adjusted inputs
464 and not the raw ones. Nevertheless the experiments are labeled as 'de-biased' sensitivity
465 experiments to ensure a consistent naming across scales.

466

467 **1.2 ISIMIP3b, group II: Climate-model based future impact model** 468 **simulations with constant 2015 direct human forcings**

469

470 The ISIMIP3b, group II simulations comprise a set of future impact projections (2015--
471 2100) using fixed levels of ~~DHFdirect human forcings~~ as considered in the historical
472 simulations ('2015soc', '1850soc', and 'nat') or reached at the end (2014) of the historical
473 period in the 'historical + histsoc' runs ('2015soc-from-histsoc'). These runs are described in
474 the red cells of **Table 24**.

475

476 **Pre-industrial reference simulations (picontrol + 2015soc, picontrol + 2015soc-from-**
477 **histsoc, picontrol + 1850soc, picontrol + nat; default):** These simulations are included
478 into the ISIMIP3, group II part of the protocol to allow for the estimation of the effect of
479 climate change by comparing the future impact projections to simulations assuming the
480 same background DHF but pre-industrial levels of CRF (see description of baseline
481 simulations in section 1.1).

482
483 **Future impact projections assuming SSP-RCP-based climate-related forcings starting**
484 **from ‘historical + histsoc’ simulations (ssp126 + 2015soc-from-histsoc, ssp370 +**
485 **2015soc-from-histsoc, ssp585 + 2015soc-from-histsoc; default):** ~~This~~ these experiment runs
486 represents an expansion continuation of the group I ‘historical + histsoc’ experiment
487 based on simulations assuming fixed 2015 DHF direct human forcings for the future. Note
488 that this experiment is different from the experiment with fixed 2015 DHF for the future
489 where the associated impact simulations starting from the ‘historical + 2015soc’ group I
490 simulation experiment (see description below).

491
492 These experiments have been introduced to describe the impacts of different scenarios of
493 changes in the climate-related systems on today’s natural systems and societies, i.e.
494 assuming present day population levels and distributions, land use patterns, water, and
495 agricultural management measures etc.. In many cases, the projected changes in natural
496 and human systems can be interpreted as the pure effect of the prescribed changes in the
497 climate-related systems. However, they could also partly result from lagged effects of the
498 historical changes in DHFs (‘histsoc’), CRF (‘historical’), or natural temporal trends induced
499 e.g. by re-growth of forests. To be able to separate natural trends from the effects of
500 changing CRFs, these the associated simulations can be compared to reference impact
501 simulations with pre-industrial CRF climate-related forcings forced with the same
502 DHF direct human forcings (‘picontrol + 2015soc-from-histsoc’, see description in group I
503 section).

504
505 **Future impact projections assuming SSP-RCP-based climate-related forcings starting**
506 **from historical simulations with constant 2015 direct human forcings (ssp126 +**
507 **2015soc, ssp370 + 2015soc, ssp585 + 2015soc; default):** These experiments
508 expand continue the ‘historical + 2015soc’ experiments from ISIMIP3b, group I using
509 DHF direct human forcings that are held constant at 2015 levels for the historical period
510 into the future. Although the DHF in the future period is identical to the future simulations
511 described above, the difference in historical forcing may affect the impact simulations in
512 the future period. These simulations are also considered first priority as some of the

513 impact models may not be able to handle varying ~~DHFdirect human forcings~~ and
514 therefore can only perform these experiments. Models participating in the '2015soc-from-
515 histsoc' experiments described above are also asked to complete the '2015soc' runs to
516 generate an as large as possible ensemble of consistent impact model simulations with as
517 many members as possible.

518
519 **Future impact projections assuming SSP-RCP-based climate-related forcings starting**
520 **from historical simulations assuming constant 1850 direct human forcings (ssp126 +**
521 **1850soc, ssp370 + 1850soc, ssp585 + 1850soc; default):** These experiments continue the
522 default 'historical + 1850soc' experiments considered in ISIMIP3b, group I. They are
523 included to estimate the impact of changes in the climate-related systems conditional on
524 1850 levels of ~~DHFdirect human forcings~~ that can be compared to the impact conditional
525 on today's levels of ~~DHFdirect human forcings~~ ('2015soc').

526
527 **Future impact projections assuming SSP-RCP-based climate-related forcings starting**
528 **from historical simulations assuming no direct human forcings (ssp126 + nat, ssp370**
529 **+ nat, ssp585 + nat; default):** These experiments continue the default 'historical + nat'
530 experiments in ISIMIP3b, group I. They are included to estimate the effect of changes in
531 the climate-related systems (here climate change itself and increasing CO₂ concentrations)
532 assuming no ~~DHFdirect human forcings~~.

533
534 **CO₂ sensitivity simulations (ssp126 + 2015soc-from-histsoc, ssp370 + 2015soc-from-**
535 **histsoc, ssp585 + 2015soc-from-histsoc, ssp585 + 2015soc, ssp585 + 1850soc, ssp585 +**
536 **nat; 2015co2):** To separate the effects of increasing atmospheric CO₂ concentrations (in
537 particular the CO₂ fertilisation or water use efficiency effects on vegetation) from the
538 effects of other changes in the climate-related systems, the ISIMIP3b protocol includes
539 sensitivity experiments where atmospheric CO₂ concentrations are held constant at 2015
540 levels. For SSP1-2.6 and SSP3-7.0, they are only introduced as deviations from the default
541 '2015soc-from-histsoc' experiments while for SSP5-8.5 the effect can also be quantified
542 conditional on all levels of direct human influences considered in the previous
543 experiments.

544 **Future lightning sensitivity simulations (ssp126 + 2015soc-from-histsoc, ssp370 +**
545 **2015soc-from-histsoc, ssp585 + 2015soc-from-histsoc; varlightning):** To study the
546 effects of future changes in lightning flash rates as opposed to using a stationary lightning
547 climatology, the ISIMIP3b protocol includes sensitivity experiments where future lightning
548 flash rates change along the RCPs. The future lightning data sensitivity experiment is
549 introduced as a deviation from the default '2015soc-from-histsoc' experiment and only for

550 one climate model (UK-ESM). This sensitivity experiment has been introduced for the fire
551 sector.

552 **Climate sensitivity simulations under high levels of CO₂ (ssp126 + 2015soc-from-**
553 **histsoc, ssp585co2):** To study the effects of high atmospheric CO₂ concentration without
554 accompanying changes in climate, the ISIMIP3b protocol includes a sensitivity experiment
555 where the atmospheric CO₂ concentration are prescribed according to RCP8.5, while the
556 other ~~CRFclimate-related forcings~~, in particular the atmospheric forcings are from SSP1-
557 2.6. The future climate sensitivity experiment is introduced as a deviation from the default
558 'ssp126 + 2015soc-from-histsoc' experiment. This sensitivity experiment has been
559 introduced for the peat sector.

560 **'De-biased' sensitivity simulations within the marine ecosystems and fisheries sector**
561 **(FishMIP) with de-biased oceanic forcings and no or 2015soc direct human forcings**
562 **for reference simulations based on pre-industrial oceanic forcing (picontrol + nat,**
563 **picontrol + 2015soc-from-histsoc; de-biased) and the associated simulations**
564 **accounting for different levels of climate change (ssp126 + nat, ssp370 + nat, ssp858 +**
565 **nat, ssp126 + 2015soc-from-histsoc, ssp370 + 2015soc-from-histsoc, ssp585 + 2015soc-**
566 **from-histsoc):** These simulations represent the future extensions of the 'de-biased' group
567 I simulations described above. They are designed to test the dynamical bias-adjustment
568 suggested for the global oceanic forcings under different levels of climate change (ssp126,
569 ssp370, ssp585). The regional impact projections within the sector are also based on de-
570 biased oceanic forcings and are therefore also labeled as 'de-biased' sensitivity
571 experiments to ensure a consistent labeling across scales.

572

573 |

574 **Table 2: ISIMIP3b climate-model based experiments.** The table provides a
 575 comprehensive list of all ISIMIP3b, group I (grey) and group II (red) experiments defined
 576 by the assumed ~~climate-related forcings (CRF)~~ and ~~direct human forcings (DHF)~~. Here, the
 577 ~~CRF climate-related forcings~~ are only described by the climate (oceanic and atmospheric)
 578 forcings and the assumed CO₂ and CH₄ concentrations that have a direct influence on the
 579 simulated impacts independent of climate. Coastal water levels are not mentioned in the
 580 description as we do ~~forcings as we do not provide~~ the associated input data ~~coastal water~~
 581 ~~levels yet.~~

Experiment specified by the combination of CRF + DHF priority	Short description	Period: Pre-industrial 1601–1849	Period: Historical 1850–2014	Period: Future 2015–2100
pre-industrial control + 2015soc-from-histsoc 1st priority	CRF: No changes in climate the- climate-related systems, CO ₂ and CH ₄ fixed at 1850 levels	picontrol	picontrol	picontrol
	DHF: Varying management before 2015, then fixed at 2015 levels thereafter	1850soc	histsoc	2015soc-from-histsoc
pre-industrial control + 2015soc 1st priority	CRF: No changes in climate the- climate-related systems, CO ₂ and CH ₄ fixed at 1850 levels	Does not have to be simulated as the following periods already provide 251 simulation years assuming stable baseline CRF and DHF. ensi	picontrol	picontrol
	DHF: Fixed at 2015 levels for all periods		2015soc	2015soc
pre-industrial control + 1850soc	CRF: No changes in climate the- climate-related systems, CO ₂ and CH ₄ fixed at 1850	Does not have to be simulated as the following periods already provide 251 simulation years	picontrol	picontrol

2nd priority	levels	assuming stable baseline CRF and DHF.		
	DHF: Fixed at 1850 levels for all periods		1850soc	1850soc
pre-industrial control + nat 2nd priority	CRF: No changes in climate the climate-related systems , CO ₂ and CH ₄ fixed at 1850 levels	Does not have to be simulated as the following periods already provide 251 simulation years assuming stable baseline CRF and DHF.	picontrol	picontrol
	DHF: No direct human influences		nat	nat
RCP2.6 + 2015soc-from-histsoc 1st priority	CRF: Simulated historical climate changes in climate-related systems , CO ₂ and CH ₄ concentrations as observed in the historical period, then simulated SSP1-2.6-based climate change and CO₂ and CH₄ also changing according to SSP1-2.6 changes in the climate-related systems	Identical to picontrol + 1850soc-run-described-above	historical	ssp126
	DHF: Varying management before 2015, then fixed at 2015 levels thereafter		histsoc	2015soc-from-histsoc
RCP2.6 + 2015soc 1st priority	CRF: Simulated historical climate changes in climate-related systems , CO ₂ and	Identical to "picontrol + 2015soc"-run	historical	ssp126

	<p>CH₄ concentrations as observed in the historical period, <u>then simulated SSP1-2.6-based climate change and CO₂ and CH₄ also changing according to SSP1-2.6</u>then simulated SSP1-2.6-based CRF changes in the climate-related systems</p>			
	<p>DHF: Fixed at 2015 levels for all periods</p>		2015soc	2015soc
<p>RCP2.6₊ 1850soc 2nd priority</p>	<p>CRF: Simulated historical <u>climate change</u>changes in climate-related systems, CO₂ and CH₄ concentrations as observed in the historical period, <u>then simulated SSP1-2.6-based climate change and CO₂ and CH₄ also changing according to SSP1-2.6</u>then simulated SSP1-2.6-based CRF changes in the climate-related systems</p>	<p>Identical to "picontrol + 1850soc" run</p>	historical	ssp126
	<p>DHF: Fixed at 1850 levels for all</p>		1850soc	1850soc

	periods			
RCP2.6+ nat 2nd priority	CRF: Simulated historical <u>climate change</u> changes in climate-related systems, CO ₂ and CH ₄ concentrations as observed in the historical period, <u>then simulated SSP1-2.6-based climate change</u> and CO ₂ and CH ₄ also changing according to SSP1-2.6 <u>then simulated SSP1-2.6-based CRF changes in the climate-related systems</u>	Identical to "picontrol + nat" run	historical	ssp126
	DHF: No direct human influences		nat	nat
CO₂ sensitivity RCP2.6+ 2015soc-from-histsoc 2nd priority	CRF: Simulated historical <u>climate change</u> changes in climate-related systems, CO ₂ and CH ₄ concentrations as observed in the historical period, <u>then simulated SSP1-2.6-based climate change</u> and CH ₄ also changing according to SSP1-2.6, <u>but then simulated SSP1-</u>	Identical to "picontrol + 1850soc" run	"histsoc" version of the historical <u>period</u> of the RCP2.6 experiments, <u>as described above</u>	ssp126 Sensitivity experiment: 2015co2

	<p>2.6-based CRF-changes in the climate-related systems but fixed 2015 CO₂ concentrations</p> <p>DHF: Varying management before 2015, then fixed at 2015 levels thereafter</p>			
<p>RCP7.0 +</p> <p>2015soc-from-histsoc</p> <p>1st priority</p>	<p>CRF: Simulated historical <u>climate change</u> changes in climate-related systems, CO₂ and CH₄ concentrations as observed in the historical period, <u>then simulated SSP3-7.0-based climate change and CO₂ and CH₄ also changing according to SSP3-7.0</u> then simulated <u>SSP3-7.0-based CRF-changes in the climate-related systems</u></p> <p>DHF: Varying management before 2015, then fixed at 2015 levels thereafter</p>	Identical to "picontrol + 1850soc" run	"histsoc" version of the historical <u>period</u> of <u>the</u> RCP2.6 experiment	<p>ssp370</p> <p>2015soc-from-histsoc</p>
<p>RCP7.0 +</p> <p>2015soc</p>	<p>CRF: Simulated historical <u>climate change</u> changes in climate-related</p>	Identical to "picontrol + 2015soc" run	Identical to "historical + 2015soc" run	ssp370

<p>1st priority</p>	<p>systems, CO₂ and CH₄ concentrations as observed in the historical period, <u>then simulated SSP3-7.0-based climate change and CO₂ and CH₄ also changing according to SSP3-7.0</u>then-simulated SSP3-7.0-based CRF-changes in the climate-related systems</p>		<p>described-above</p>	
<p>RCP7.0 + 1850soc 2nd priority</p>	<p>CRF: Simulated historical <u>climate change</u>changes in climate-related systems, CO₂ and CH₄ concentrations as observed in the historical period, then simulated SSP3-7.0-based climate change and CO₂ and CH₄ also changing according to SSP3-7.0<u>then-simulated SSP3-7.0-based changes in the climate-related systems</u></p>	<p>Identical to "picontrol + 1850soc"run</p>	<p>Identical to "historical + 1850soc"run described-above</p>	<p>2015soc</p> <p>ssp370</p>

	DHF: Fixed at 1850 levels for all periods			1850soc
RCP7.0 + nat 2nd priority	CRF: Simulated historical <u>climate change</u> changes in climate-related systems, CO ₂ and CH ₄ concentrations as observed in the historical period, <u>then simulated SSP3-7.0-based climate change and CO₂ and CH₄ also changing according to SSP3-7.0</u> then simulated SSP3-7.0-based CRF changes in the climate-related systems	Identical to "picontrol + nat" run	Identical to "historical + nat" run <u>described above</u>	ssp370
	DHF: No direct human influences			nat
CO₂ sensitivity RCP7 + 2015soc-from-histsoc 2nd priority	CRF: Simulated historical <u>climate change</u> changes in climate-related systems, CO ₂ and CH ₄ concentrations as observed in the historical period, <u>then simulated SSP3-7.0-based climate change and CH₄ also</u>	Identical to "picontrol + 1850soc" run	Identical to "historical + histsoc" run <u>described above</u>	ssp370 Sensitivity experiment: 2015co2

	<p><u>changing according to SSP3-7.0, then simulated SSP3-7.0-based CRF changes in the climate-related systems</u> but CO₂ concentrations fixed at 2015 levels</p>			
	<p>DHF: Varying management before 2015, then fixed at 2015 levels thereafter</p>			<p>2015soc-from-histsoc</p>
<p>RCP8.5 + 2015soc-from-histsoc 1st priority</p>	<p>CRF: Simulated historical <u>climate change changes in climate-related systems</u>, CO₂ and CH₄ concentrations as observed in the historical period, <u>then simulated SSP5-8.5-based climate change and CO₂ and CH₄</u> also <u>changing according to SSP5-8.5 then simulated SSP5-8.5-based CRF changes in the climate-related systems</u></p>	<p>Identical to "picontrol + 1850soc"-run</p>	<p>Identical to "historical + histsoc"-run described above</p>	<p>ssp585</p>
	<p>DHF: Varying management before 2015, then fixed at 2015 levels thereafter</p>			<p>2015soc-from-histsoc</p>

<p>RCP8.5 + 2015soc 1st priority</p>	<p>CRF: Simulated historical <u>climate changes in climate-related systems</u>, CO₂ and CH₄ concentrations as observed in the historical period, <u>then simulated SSP5-8.5-based climate change and CO₂ and CH₄ also changing according to SSP5-8.5 then simulated SSP5-8.5-based CRF changes in the climate-related systems</u></p> <p>DHF: Fixed at 2015 levels for all periods</p>	<p>Identical to "picontrol + 2015soc" run</p>	<p>Identical to "historical + 2015soc" run described above</p>	<p>ssp585</p>
<p>RCP8.5 + 1850soc 2nd priority</p>	<p>CRF: Simulated historical <u>climate changes in climate-related systems</u>, CO₂ and CH₄ concentrations as observed in the historical period, <u>then simulated SSP5-8.5-based climate change and CO₂ and CH₄ also changing according to SSP5-8.5 then simulated SSP5-8.5-based</u></p>	<p>Identical to "picontrol + 1850soc" run</p>	<p>Identical to "historical + 1850soc" run described above</p>	<p>ssp585</p>

	<p>changes in the climate-related systems</p> <p>DHF: Fixed at 1850 levels for all periods</p>			<p>1850soc</p>
<p>RCP8.5 +</p> <p>nat</p> <p>2nd priority</p>	<p>CRF: Simulated historical <u>climate change</u>changes in climate-related systems, CO₂ and CH₄ concentrations as observed in the historical period, <u>then simulated SSP5-8.5-based climate change and CO₂ and CH₄ also changing according to SSP5-8.5</u>then simulated SSP5-8.5-based changes in the climate-related systems</p> <p>DHF: No direct human influences</p>	Identical to "picontrol + nat" -run	Identical to "historical + nat" -run	<p>ssp585</p>
<p>CO₂ sensitivity RCP8.5 +</p> <p>2015soc-from-histsoc</p> <p>1st priority</p>	<p>CRF: Simulated historical <u>climate change</u>changes in climate-related systems, CO₂ and CH₄ concentrations as observed in the historical period, <u>then simulated</u></p>	Identical to "picontrol + 1850soc" -run	Identical to "historical + histsoc" -run	<p>ssp585</p> <p>Sensitivity experiment: 2015co2</p>

	<p><u>SSP5-8.5-based climate change and CH₄ also changing according to SSP5-8.5then-simulated-SSP5-8.5-based CRF-changes-in-the-climate-related systems,</u> but CO₂ concentrations fixed at 2015 levels</p>			
	<p>DHF: Varying management before 2015, then fixed at 2015 levels thereafter</p>			<p>2015soc-from-histsoc</p>
<p>CO₂ sensitivity RCP8.5 ±</p> <p>2015soc</p> <p>1st priority</p>	<p>CRF: Simulated historical <u>climate changechanges-in-climate-related-systems,</u> CO₂ and CH₄ concentrations as observed in the historical period, <u>then simulated SSP5-8.5-based climate change and CH₄ also changing according to SSP5-8.5then-simulated-SSP5-8.5-based-CRFchanges-in-the-climate-related-systems,</u> but CO₂ concentrations fixed at 2015</p>	<p>Identical to "picontrol + 2015soc"-run</p>	<p>Identical to "historical + 2015soc"-run</p>	<p>ssp585</p> <p>Sensitivity experiment: 2015co2</p>

	levels			
	DHF: Fixed at 2015 levels for all periods			2015soc
CO₂ sensitivity RCP8.5 ± 1850soc 2nd priority	CRF: Simulated historical <u>climate change</u> changes in climate-related systems , CO ₂ and CH ₄ concentrations as observed in the historical period, <u>then simulated SSP5-8.5-based climate change and CH₄ also changing according to SSP5-8.5</u> then simulated SSP5-8.5-based CRF changes in the climate-related systems , but CO ₂ concentrations fixed at 2015 levels	Identical to "picontrol + 1850soc" run	Identical to "historical + 1850soc" run	ssp585 Sensitivity experiment: 2015co2
	DHF: Fixed at 1850 levels for all periods			1850soc
CO₂ sensitivity RCP8.5 ± nat 1st priority	CRF: Simulated historical <u>climate change</u> changes in climate-related systems , CO ₂ and CH ₄ concentrations as observed in the historical period, <u>then simulated</u>	Identical to "picontrol + nat" run	Identical to "historical + nat" run	ssp585 Sensitivity experiment: 2015co2

	<p><u>SSP5-8.5-based climate change and CH₄ also changing according to SSP5-8.5 then simulated SSP5-8.5-based CRF changes in the climate-related systems, but CO₂ concentrations fixed at 2015 levels</u></p> <p>DHF: No direct human influences</p>			<p>nat</p>
<p>Lightning sensitivity RCP2.6 ±</p> <p>2015soc-from-histsoc</p> <p>2nd priority</p>	<p>CRF: Simulated historical <u>climate change changes in climate-related systems, CO₂ and CH₄ concentrations as observed in the historical period, then simulated SSP1-2.6-based climate change and CO₂ and CH₄ also changing according to SSP1-2.6 then simulated SSP1-2.6-based CRF changes in the climate-related systems, in contrast to the default experiment the SSP1-2.6-based</u></p>	<p>Identical to "picontrol + 1850soc" run</p>	<p>Identical to "historical + histsoc" run</p>	<p>ssp126</p> <p>Sensitivity experiment: varlightning</p>

	<p><u>climate change</u> <u>also</u> includes <u>ing</u> <u>varying</u> future lightning which in the default case is considered fixed at climatological levels</p>			
	<p>DHF: Varying management before 2015, then fixed at 2015 levels thereafter</p>			<p>2015soc-from-histsoc</p>
<p>Lightning sensitivity RCP7.0 +</p> <p>2015soc-from-histsoc</p> <p>2nd priority</p>	<p>CRF: Simulated historical <u>climate change</u> <u>changes in</u> <u>climate-related systems</u>, CO₂ and CH₄ concentrations as observed in the historical period, <u>then simulated SSP3-7.0-based climate change and CO₂ and CH₄ also changing according to SSP3-7.0, then simulated SSP3-7.0-based CRF changes in the climate-related systems in contrast to the default experiment the SSP3-7.0-based climate change also includes varying future</u></p>	<p>Identical to "picontrol + 1850soc"-run</p>	<p>Identical to "historical + histsoc"-run</p>	<p>ssp370</p> <p>Sensitivity experiment: varlightning</p>

	<p><u>lightning which in the default case is considered fixed at climatological levels</u> including varying future lightning which in the default case is considered fixed at climatological levels</p> <p>DHF: Varying management before 2015, then fixed at 2015 levels thereafter</p>			
<p>Lightning sensitivity RCP8.5 ± 2015soc-from-histsoc 2nd priority</p>	<p>CRF: Simulated historical <u>climate changechanges in climate-related systems</u>, CO₂ and CH₄ concentrations as observed in the historical period, <u>then simulated SSP5-8.5-based climate change and CO₂ and CH₄ also changing according to SSP5-8.5, then simulated SSP5-8.5-based CRF changes in the climate-related systems in contrast to the default experiment the</u></p>	<p>Identical to "picontrol + 1850soc" run</p>	<p>Identical to "historical + histsoc"- run</p>	<p>2015soc-from-histsoc</p> <p>ssp585 Sensitivity experiment: varlightning</p>

	<p><u>SSP5-8.5-based climate change also includes varying future lightning which in the default case is considered fixed at climatological levels including varying future lightning which in the default case is considered fixed at climatological levels</u></p>			
	<p>DHF: Varying management before 2015, then fixed at 2015 levels thereafter</p>			<p>2015soc-from-histsoc</p>
<p>Climate sensitivity, RCP2.6 with RCP8.5 CO₂ + 2015soc-from-histsoc 2nd priority</p>	<p>CRF: Simulated <u>historical climate change</u> erical changes in climate-related systems, CO₂ and CH₄ concentrations as observed in the historical period, then <u>CH₄ and CO₂</u> evolves according to SSP5-8.5 while <u>climate change is prescribed according to the all other CRFs change according to default SSP1-2.6 forcing data</u></p>	<p>Identical to "picontrol + 1850soc" run</p>	<p>Identical to "historical + histsoc" run</p>	<p>ssp126 Sensitivity experiment: ssp585co2</p>

	DHF: Varying management before 2015, then fixed at 2015 levels thereafter			2015soc-from-histsoc
Bias sensitivity, de-biased oceanic data for pre-industrial control <u>+</u>	CRF: De-biased pre-industrial oceanic forcing, CO ₂ fixed at 1850 levels	Not covered	picontrol	picontrol Sensitivity experiment: de-biased
nat 2nd priority	DHF: no direct human influences	Not covered	nat	nat
Bias sensitivity, de-biased oceanic data for SSP1-2.6 <u>+</u>	CRF: De-biased simulated historical oceanic forcing, <u>CO₂ concentrations as observed in the historical period,</u> then de-biased simulated SSP1-2.6-based oceanic forcing <u>and CO₂ concentrations also changing according to SSP1-2.6</u>	Not covered	historical	ssp126 Sensitivity experiment: de-biased
nat 2nd priority	DHF: no direct human influences	Not covered	nat	nat
Bias sensitivity, de-biased oceanic data for SSP3-7.0 <u>+</u>	CRF: De-biased simulated historical oceanic forcing, <u>CO₂ concentrations as observed in the historical period,</u> then de-biased	Not covered	historical	ssp370 Sensitivity experiment: de-biased
nat				

2nd priority	simulated SSP3-7.0-based oceanic forcing and CO ₂ concentrations also changing according to SSP3-7.0			
	DHF: no direct human influences	Not covered	nat	nat
Bias sensitivity, de-biased oceanic data for SSP5-8.5 + nat 2nd priority	CRF: <u>De-biased simulated historical oceanic forcing, CO₂ concentrations as observed in the historical period, then de-biased simulated SSP5-8.5-based oceanic forcing and CO₂ concentrations also changing according to SSP5-8.5</u> De-biased simulated historical oceanic forcing, then de-biased simulated SSP5-8.5-based oceanic forcing	Not covered	historical	ssp585 Sensitivity experiment: de-biased
	DHF: No direct human influences	Not covered	nat	nat
Bias sensitivity, de-biased oceanic data for pre-	CRF: De-biased pre-industrial oceanic forcing, CO ₂ fixed at 1850	Not covered	picontrol	picontrol Sensitivity experiment: de-biased

industrial control₊ 2015soc-from-histsoc 2nd priority	levels			
	DHF: Varying direct human influences before 2015, then fixed at 2015 levels thereafter	Not covered	histsoc	2015soc-from-histsoc
Bias sensitivity, de-biased oceanic data for SSP1-2.6₊ 2015soc-from-histsoc 2nd priority	CRF: <u>De-biased simulated historical oceanic forcing, CO₂ concentrations as observed in the historical period, then de-biased simulated SSP1-2.6-based oceanic forcing and CO₂ concentrations also changing according to SSP1-2.6</u> De-biased simulated historical oceanic forcing, then de-biased simulated SSP1-2.6-based oceanic forcing	Not covered	historical	ssp126 Sensitivity experiment: de-biased
	DHF: Varying direct human influences before 2015, then fixed at 2015 levels thereafter	Not covered	histsoc	2015soc-from-histsoc
Bias sensitivity, de-biased oceanic data for SSP3-	CRF: <u>De-biased simulated historical oceanic forcing, CO₂ concentrations as</u>	Not covered	historical	ssp370 Sensitivity experiment: de-biased

<p>7.0 +</p> <p>2015soc-from-histsoc</p> <p>2nd priority</p>	<p><u>observed in the historical period, then de-biased simulated SSP3-7.0-based oceanic forcing and CO₂ concentrations also changing according to SSP3-7.0</u>De-biased simulated historical oceanic forcing, then de-biased simulated SSP3-7.0-based oceanic forcing</p>			
	<p>DHF: Varying direct human influences before 2015, then fixed at 2015 levels thereafter</p>	<p>Not covered</p>	<p>histsoc</p>	<p>2015soc-from-histsoc</p>
<p>Bias sensitivity, de-biased oceanic data for SSP5-8.5 +</p> <p>2015soc-from-histsoc</p> <p>2nd priority</p>	<p>CRF: <u>De-biased simulated historical oceanic forcing, CO₂ concentrations as observed in the historical period, then de-biased simulated SSP5-8.5-based oceanic forcing and CO₂ concentrations also changing according to SSP5-8.5</u>De-biased simulated historical oceanic forcing, then de-</p>	<p>Not covered</p>	<p>historical</p>	<p>ssp585</p> <p>Sensitivity experiment: de-biased</p>

	biased-simulated- SSP5-8.5-based- oceanic-forcing			
	DHF: Varying direct human influences before 2015, then fixed at 2015 levels thereafter	Not covered	histsoc	2015soc-from-histsoc

582

583

584

585

586

587

588

589

590

591

592

593

594

595

596

597

598

599

600

601

602

603

604

605

606

607

~~Table 2: ISIMIP3b climate-model based experiments. The table provides a comprehensive list of all ISIMIP3b, group I (grey) and group II (red) experiments defined by the assumed climate-related forcings (CRF) and direct human forcings (DHF). Here the climate-related forcings are only described by the climate (oceanic and atmospheric) and CO₂ forcings as we do not provide coastal water levels yet.~~

2 Climate-related forcing data

2.1 Bias-adjusted and statistically downscaled atmospheric climate forcing

For ISIMIP3b we provide the daily atmospheric forcings for the same variables as in ISIMIP3a on the default 0.5° grid (see **Table 3**). These variables are from the output of CMIP6 climate model simulations, selected and processed as described below. We use the climate simulations from the picontrol (for pre-industrial conditions), historical (for historical conditions), ssp126, ssp370, and ssp585 (for future conditions under the scenarios SSP1-2.6, SSP3-7.0, and SSP5-8.5, respectively) CMIP6 experiments.

Table 3: Climate-related atmospheric forcing data provided within ISIMIP3b. The upper limits of [precipitation \(pr\)](#) and [snowfall \(prsn\)](#) correspond to 600 mm day⁻¹ and 300 mm day⁻¹, respectively, while the lower and upper limits of [Near-Surface Air Temperature \(tas\)](#), [Daily Maximum Near-Surface Air Temperature \(tasmax\)](#) and [Daily Minimum Near-Surface Air Temperature \(tasmin\)](#) correspond to -90°C and +70°C, respectively.

Variable	Variable specifier	Unit (maximum range, inner bounds if considered)	Resolution	Datasets
Near-Surface Relative Humidity	hurs	% ([1, 100], [0.01, 99.99])	0.5° grid, daily	Bias-adjusted and downscaled from GFDL-ESM4, IPSL-CM6A-LR, MPI-ESM1-2-HR, MRI-ESM2-0, and UKESM1-0-LL simulations generated for CMIP6.
Near-Surface Specific Humidity	huss	kg kg ⁻¹ ([0.0000001, 0.1])	0.5° grid, daily	Derived from bias-adjusted and downscaled hurs, ps, and tas from GFDL-ESM4, IPSL-CM6A-LR, MPI-ESM1-2-HR, MRI-ESM2-0, and UKESM1-0-LL simulations generated for CMIP6.
Precipitation (including snowfall)	pr	kg m ⁻² s ⁻¹ ([0, 600/86400], [0.1/86400, ∞])	0.5° grid, daily	Bias-adjusted and downscaled from GFDL-ESM4, IPSL-CM6A-LR, MPI-ESM1-2-HR, MRI-ESM2-0, and UKESM1-0-LL simulations generated for CMIP6.
Snowfall	prsn	kg m ⁻² s ⁻¹ ([0, 300/86400]) Maximum range and inner bounds of unitless snowfall ratio (prsnratio = prsn/pr): ([0,1],	0.5° grid, daily	Derived from bias-adjusted and downscaled pr and prsnratio from GFDL-ESM4, IPSL-CM6A-LR, MPI-ESM1-2-HR, MRI-ESM2-0, and UKESM1-0-LL simulations

		[0.0001,0.9999])		generated for CMIP6.
Surface Air Pressure	ps	Pa ([480, 110000])	0.5° grid, daily	Bias-adjusted and downscaled from GFDL-ESM4, IPSL-CM6A-LR, MPI-ESM1-2-HR, MRI-ESM2-0, and UKESM1-0-LL simulations generated for CMIP6.
Surface Downwelling Longwave Radiation	rlds	W m ⁻² ([40, 600])	0.5° grid, daily	Bias-adjusted and downscaled from GFDL-ESM4, IPSL-CM6A-LR, MPI-ESM1-2-HR, MRI-ESM2-0, and UKESM1-0-LL simulations generated for CMIP6.
Surface Downwelling Shortwave Radiation	rsds	W m ⁻² ([0, 500]) Maximum range and inner bounds of normalized rsds used during bias adjustment: ([0,1], [0.0001, 0.9999])	0.5° grid, daily	Bias-adjusted and downscaled from GFDL-ESM4, IPSL-CM6A-LR, MPI-ESM1-2-HR, MRI-ESM2-0, and UKESM1-0-LL simulations generated for CMIP6.
Near-Surface Wind Speed	sfcwind	m s ⁻¹ ([0.1, 50], [0.01, ∞])	0.5° grid, daily	Bias-adjusted and downscaled from GFDL-ESM4, IPSL-CM6A-LR, MPI-ESM1-2-HR, MRI-ESM2-0, and UKESM1-0-LL simulations generated for CMIP6.
Near-Surface Air Temperature	tas	K ([183.15, 343.15])	0.5° grid, daily	Bias-adjusted and downscaled from GFDL-ESM4, IPSL-CM6A-LR, MPI-ESM1-2-HR, MRI-ESM2-0, and UKESM1-0-LL simulations

				generated for CMIP6.
Daily Maximum Near-Surface Air Temperature	tasmax	K ([183.15, 343.15]) Maximum range and inner bounds considered for tasrange: ([0.01, ∞[, [0.01,∞[) Maximum range and inner bounds considered for unitless tasskew: ([0,1], [0.0001,0.9999])	0.5° grid, daily	Derived from bias-adjusted and downscaled tasrange = tasmax - tasmin and tasskew = (tas - tasmin) / (tasmax - tasmin) from GFDL-ESM4, IPSL-CM6A-LR, MPI-ESM1-2-HR, MRI-ESM2-0, and UKESM1-0-LL simulations generated for CMIP6.
Daily Minimum Near-Surface Air Temperature	tasmin	K ([183.15, 343.15]) Maximum range and inner bounds considered for tasrange: ([0.01, ∞[, [0.01,∞[) Maximum range and inner bounds considered for unitless tasskew: ([0,1], [0.0001,0.9999])	0.5° grid, daily	Derived from bias-adjusted and downscaled tasrange = tasmax - tasmin and tasskew = (tas - tasmin) / (tasmax - tasmin) from GFDL-ESM4, IPSL-CM6A-LR, MPI-ESM1-2-HR, MRI-ESM2-0, and UKESM1-0-LL simulations generated for CMIP6.

608

609 For the pre-industrial conditions, 500 years of picontrol output data are used and
610 harmonised across [General Circulation Models \(GCMs\)](#) with respect to the time range they
611 cover. This is possible because picontrol data only carry nominal year labels without
612 historical reference points (see original nominal start and end years in **Table 4**). We
613 changed the GCM-specific picontrol time ranges listed to 1601–2100. ~~This is possible because~~
614 ~~picontrol data only carry nominal year labels. We shift the GCM-specific picontrol time ranges~~
615 ~~listed in Table 4 to 1601–2100.~~ For the historical and future climate conditions, we provide
616 input data for 1850–2014 and 2015–2100, respectively, in line with the time ranges
617 covered by the corresponding CMIP6 experiments. The common time axis is important as
618 the use of the input data should be harmonised across all sectors. In particular, the year-

619 by-year combination of the pre-industrial [CRFclimate-related forcing](#) with the historical
 620 [DHFdirect human forcing](#) should be done in the same way across all sectors and models.

621
 622 **Selection of climate models.** To limit the number of mandatory impact simulations and
 623 hence lower the barrier to participation in ISIMIP3b, we provide climate input data for only
 624 five selected CMIP6 climate models. The basic characteristics of the five GCMs are listed in
 625 **Table 4**. The models were selected based on data availability at the selection time (late
 626 2019 to early 2020), performance in the historical period, structural independence,
 627 process representation and equilibrium climate sensitivity (ECS).

628
 629 **To be included in ISIMIP3b, a GCM had to provide daily data for all variables listed in**
 630 **Table 3 except for [near-surface specific humidity \(huss\)](#) (which was derived from [near-](#)**
 631 **[surface relative humidity \(hurs\)](#), [surface air pressure \(ps\)](#) and [near-surface air](#)**
 632 **[temperature \(tas\)](#), see below), **ps if sea level pressure (psl) was available, so a proxy****
 633 **for ps could be computed based on psl and tas, and [near-surface wind speed \(sfcwind\)](#)**
 634 **if zonal and meridional near-surface wind components (uas, vas) were available, so a**
 635 **proxy for sfcwind could be computed based on uas and vas.** Those daily data had to cover
 636 500 picontrol years and all years of the historical, SSP1-2.6, SSP3-7.0, and SSP5-8.5. In
 637 addition, we favoured GCMs that provided the additional input data needed for the
 638 tropical cyclone modelling (**Table 5**) and the fisheries and marine ecosystems sector
 639 (FishMIP; **Table 10**).

640
 641 **Table 4:** Characteristics of CMIP6 climate models used in ISIMIP3b. Columns show (from
 642 left to right) the climate model acronym, the horizontal grid size (longitude x latitude) of
 643 the original atmospheric output data, the ensemble member used, the nominal time
 644 range covered by the picontrol data used, the [equilibriumeffectiveequilibrium](#) climate
 645 sensitivity (ECS) according to (Meehl et al., 2020), and the main model reference paper and
 646 the CMIP6 simulation data publications used. For definitions of climate model acronyms
 647 and modelling groups see (Durack, n.d.).

GCM	Grid size	Member	picontrol	ECS	References
GFDL-ESM4	288 x 180	r1i1p1f1	0001- 0500	2.6 °C	Dunne et al. (2020); Krasting et al. (2018); John et al. (2018)
IPSL-CM6A-LR	144 x 143	r1i1p1f1	1870- 2369	4.6 °C	Boucher et al. (2018, 2019, 2020)
MPI-ESM1-2-	384 x	r1i1p1f1	1850-	3.0°	Jungclaus et al. (2019); Mauritsen et al.

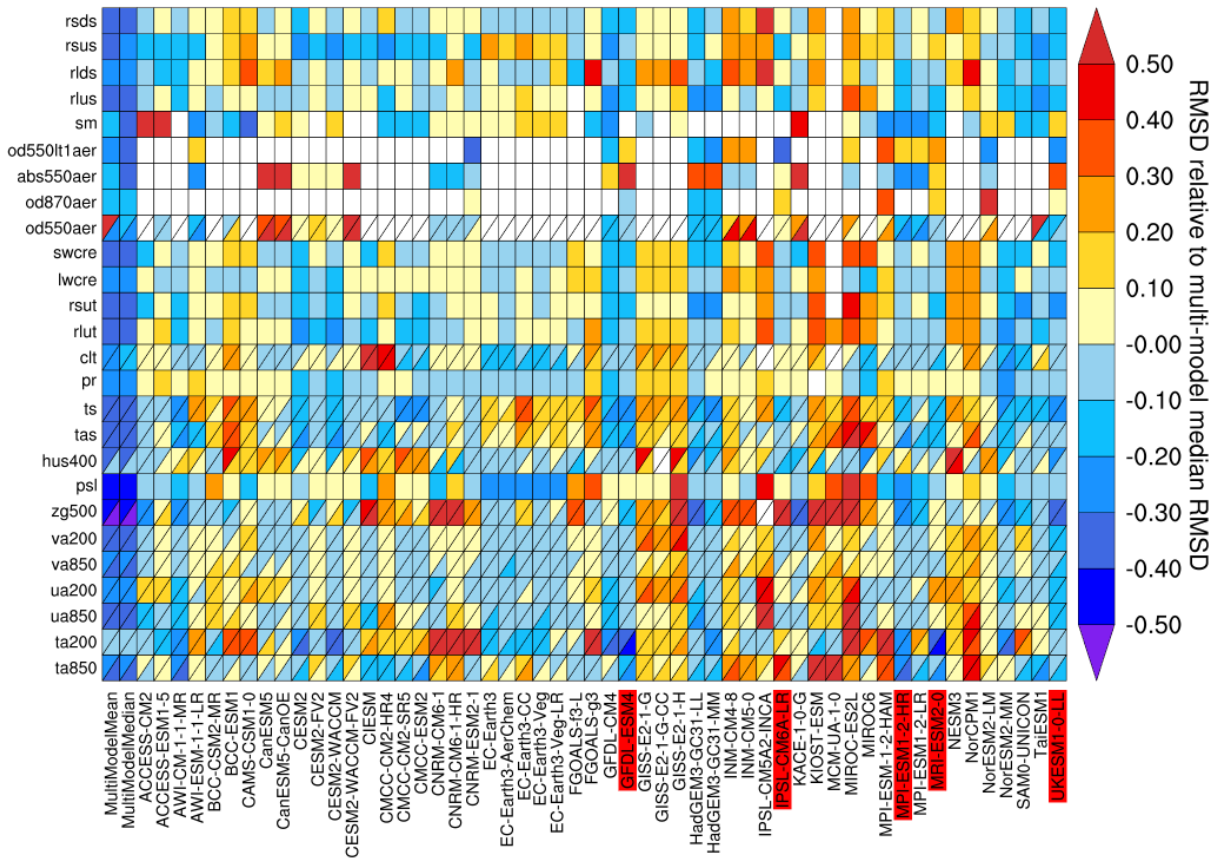
HR	192		2349	C	(2019); Schupfner et al. (2019)
MRI-ESM2-0	320 x 160	r1i1p1f1	1850– 2349	3.2° C	Yukimoto, Kawai et al. (2019) Yukimoto, Koshiro et al. (2019a, 2019b)
UKESM1-0-LL	192 x 144	r1i1p1f2	1960– 2459	5.3° C	Good et al. (2019); Sellar et al. (2019); Tang et al. (2019)

648

649

650 According to a skill analysis (see **Figure 2**), the GCMs ACCESS-CM2, AWI-CM-1-1-MR,
651 CESM2, CESM2-WACCM, CMCC-ESM2, EC-Earth3-AerChem, GFDL-CM4, GFDL-ESM4,
652 HadGEM3-GC31-LL, HadGEM3-GC31-MM, MPI-ESM1-2-HR, MPI-ESM1-2-LR, MRI-ESM2-0,
653 NorESM2-MM, SAM0-UNICON, TaiESM1, and UKESM1-0-LL perform relatively well in
654 reproducing the main historically observed characteristics of the atmosphere. From that
655 list, only GFDL-ESM4, MPI-ESM1-2-HR, MRI-ESM2-0, and UKESM1-0-LL provided all required
656 daily data at the time of model selection. Another model that fulfilled all those data
657 requirements and shows an average performance in the historical period is IPSL-CM6A-LR.
658 These five GCMs were selected to be used in ISIMIP3b. With the exception of GFDL-ESM4,
659 these models also provide the data needed for tropical cyclone modelling. GFDL-ESM4 is
660 the model providing the most comprehensive oceanic bio-geochemical forcings for
661 FishMIP while other models cover less and partly other oceanic variables (see **Table 816**).
662 Three of the climate models (GFDL-ESM4, IPSL-CM6A-LR, UKESM1-0-LL) are successors of
663 models already used in ISIMP2b and in the ISIMIP Fast Track.

664



665

666

667 **Figure 2:** Relative space-time root-mean-square deviation (RMSD) calculated from the
 668 climatological seasonal cycle of the CMIP6 historical simulations (1980–1999) compared to
 669 observational datasets, for various CMIP6 GCMs (columns) and climate variables (rows), similar to
 670 Fig. 6 of Bock et al. (2020). A relative performance is displayed, with blue shading showing being
 671 better and yellow and red shading showing worse model performance than
 672 the median RMSD of all model results of the CMIP6 ensemble. A diagonal split of a grid square
 673 shows the relative error with respect to the reference data set (lower right triangle) and an
 674 alternative data set (upper left triangle), as listed in Table 5 of Bock et al. (2020). White boxes are
 675 used when data are not available for a given model and variable. Models selected for ISIMIP3b are
 676 highlighted in red. Variables are (from top to bottom): Surface Downwelling Shortwave Radiation
 677 (rsds), Surface Upwelling Shortwave Radiation (rsus), Surface Downwelling Longwave Radiation
 678 (rlds), Surface Upwelling Longwave Radiation (rlus), Soil Moisture (sm), Ambient Fine Aerosol
 679 Optical Depth at 550 nm (od550lt1aer), Ambient Aerosol Absorption Optical Thickness at 550 nm
 680 (abs550aer), Ambient Aerosol Optical Depth at 870 nm (od870aer), Ambient Aerosol Optical
 681 Thickness at 550 nm (od550aer), Shortwave Cloud Radiative Effect (swcre), Longwave Cloud
 682 Radiative Effect (lwcre), Top-of-Atmosphere Outgoing Shortwave Radiation (rsut), Top-of-
 683 Atmosphere Outgoing Longwave Radiation (rlut), Total Cloud Cover Percentage (clt), Precipitation
 684 (pr), Surface Temperature (ts), Near-Surface Air Temperature (tas), Specific Humidity at 400 hPa
 685 (hus400), Sea Level Pressure (psl), Geopotential Height at 500 hPa (zg500), Northward Wind at 200
 686 hPa (va200), Northward Wind at 850 hPa (va850), Eastward Wind at 200 hPa (ua200), Eastward

687 Wind at 850 hPa (ua850), Air Temperature at 200 hPa (ta200), and Air Temperature at 850 hPa
688 (ta850). Produced with ESMValTool v2.0 (Andela et al., 2020b, 2020a; Righi et al., 2020).

689

690 The five GCMs are structurally independent in terms of their ocean and atmosphere model
691 components. Furthermore, all of them have a coupled climate and carbon cycle and in
692 some cases, fully interactive chemistry and aerosol components. We favoured models that
693 applied prognostic couplings between processes and model domains wherever possible
694 to maximise the coverage of simulated feedbacks.

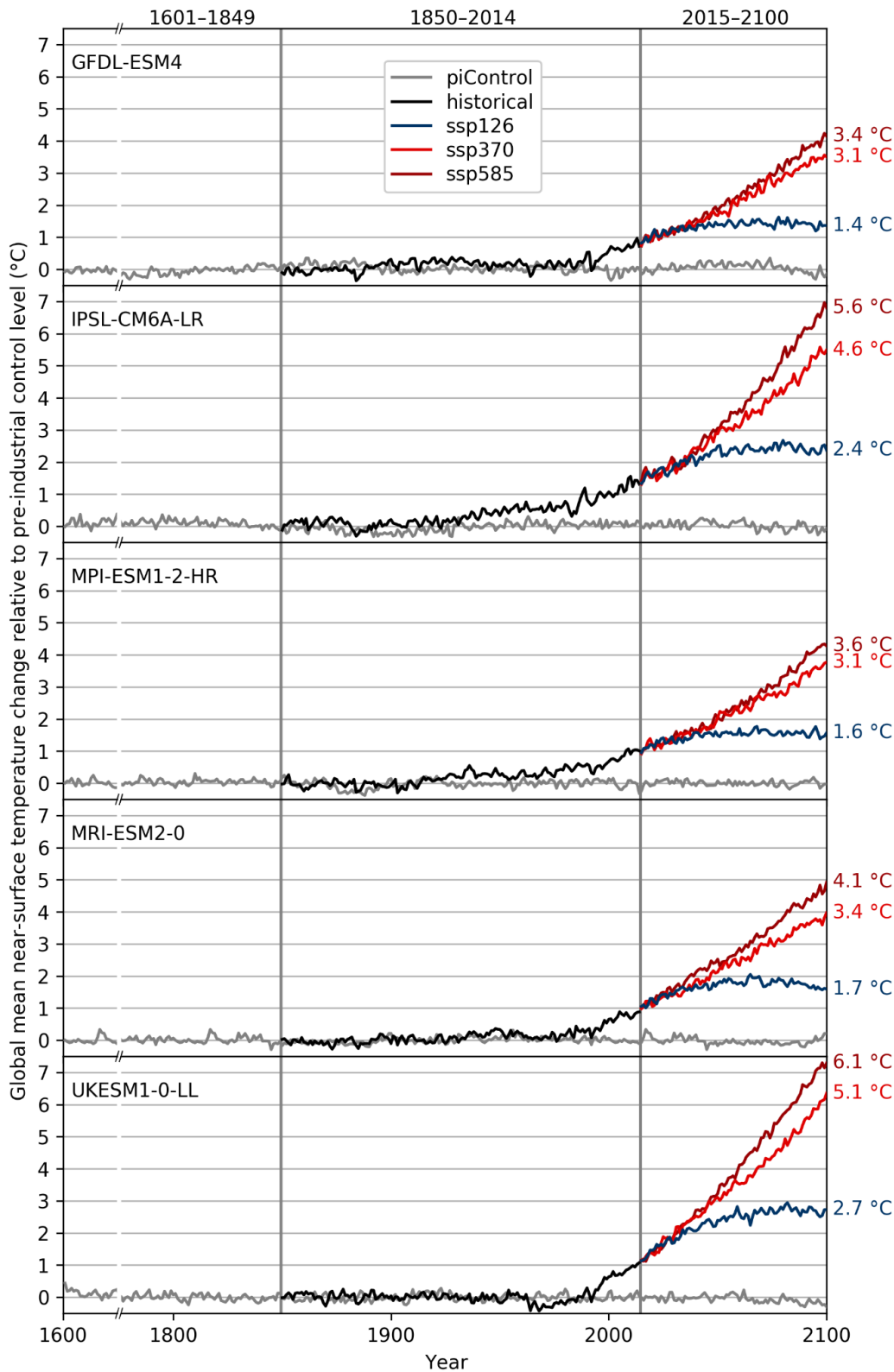
695

696 The five GCMs provide a good representation of both the mean and the range of the full
697 CMIP6 multi-model ensemble ECS. According to Meehl et al. (2020), the CMIP6 multi-
698 model mean ECS is 3.7°C, which is precisely met by the mean ECS of the five ISIMIP3b
699 GCMs. The transient climate response (TCR) of 2.0°C is also precisely met. This provides an
700 improvement over ISIMIP2b, [in the sense of the selected GCM subset reflecting the](#)
701 [statistics of the larger CMIP ensemble](#). In [ISIMIP2b that case](#) the mean ECS for the full
702 CMIP5 was 3.2°C compared with a mean ECS of 3.72°C for the four ISMIP2b GCMs (see
703 Table S1 and S2 in Jägermeyr et al. (2021)). The ISIMIP3b ensemble includes three models
704 with below-average ECS (GFDL-ESM4, MPI-ESM1-2-HR, MRI-ESM2-0) and two models with
705 above-average ECS (IPSL-CM6A-LR, UKESM1-0-LL) (see **Table 412**). In line with their ECS
706 values, we find GFDL-ESM4 and UKESM1-0-LL to project the weakest and strongest global
707 warming, respectively, under any future scenario considered (see **Figure 3**). Under SSP5-
708 8.5, the global mean near-surface temperature in 2100 is about 3°C larger in UKESM1-0-LL
709 than in GFDL-ESM4. Under SSP1-2.6, the projections are about 1.5°C apart. The ensemble
710 mean warming of the ISIMIP3b CMIP6 models is significantly higher than the warming of
711 the ISIMIP2b CMIP5 models, across global land area by an average of 0.3°C, but over the
712 main breadbasket cropland regions by more than 0.5°C between 1983–2013 and 2069–
713 2099, under both SSP1-2.6 and SSP5-8.5 (Table S1 in (Jägermeyr et al., 2021)). This is in line
714 with the higher median ECS in CMIP6 compared to CMIP5; indeed, some CMIP6 models
715 have an ECS above the assessed likely (2.5°C to 4°C) and very likely (2°C to 5°C) ranges in
716 the IPCC's sixth assessment report (AR6) (Forster et al., 2021). **The reasons for these**
717 **higher estimates of ECS are complex, with cloud feedback processes playing an important**
718 **role (Zelinka et al., 2020). While the plausibility of the very high ECS estimates has been**
719 **questioned, recent studies indicate CMIP6 models with high ECS tend to simulate cloud**
720 **properties better than low ECS models (Bock & Lauer, 2024); also, unaccounted natural**
721 **variability may have biased the IPCC's assessed ranges somewhat low (Liang et al., 2024;**
722 **Watanabe et al., 2024).**

723

724 The ISIMIP3b ensemble reflects the spread in ECS of the overall CMIP6 ensemble, with two
725 models above the AR6 likely range and one of these (UKESM1-0-LL) above the very likely
726 range. The strong warming response of these models should be kept in mind when
727 conducting ISIMIP3b-based impacts studies. However, depending on the region and
728 variable of interest, the high ECS does not necessarily have any bearing on the magnitude
729 or realism of projected regional impacts, and any further selection of models should not
730 be based solely on ECS but on the models' suitability for the impacts variables in question
731 (Swaminathan et al., 2024). In many applications, results can be harmonized by describing
732 the simulated impacts in terms of global mean temperature changes instead of time for
733 the different emission scenarios.

734



735
 736 **Figure 3:** Time series of annual global mean near-surface temperature change relative to pre-
 737 industrial levels (1601–1849 average) as simulated with GFDL-ESM4, IPSL-CM6A-LR, MPI-ESM1-2-
 738 HR, MRI-ESM2-0 and UKESM1-0-LL (from top to bottom). Colour coding indicates the underlying
 739 CMIP6 experiments (grey: pre-industrial control, black: historical, blue: SSP1-2.6, light red: SSP3-
 740 7.0, dark red: SSP5-8.5) with corresponding time periods given at the top. Numbers to the right of

741 the plot represent end-of-century warming levels under the different future scenarios, expressed
742 as the global multi-year mean near-surface temperature change from 1601–1849 to 2070–2100.
743

744 **Bias adjustment and statistical downscaling.** To make the GCM-based climate forcing
745 usable for the impact modellers we apply a bias adjustment ensuring that the GCM
746 simulations match the observed distribution of climate data over the historical reference
747 period (1979–2014). In addition to the bias adjustment a statistical downscaling to our
748 standard 0.5° grid is included in the pre-processing of the surface and near-surface
749 atmospheric variables (see **Table 311**). The method used for the bias adjustment and
750 statistical downscaling (BASD) in ISIMIP3b is version 2.5 of ISIMIP3BASD (Lange, 2019b,
751 2021a).

752
753 ISIMIP3BASD has several advantages compared to the method used for bias adjustment
754 and statistical downscaling in ISIMIP2b (Frieler et al., 2017; Lange, 2017, 2018). First, it
755 clearly separates the adjustment of biases in climate model output at 1° or 2° resolution,
756 whatever is closest to the original output data, from the statistical downscaling to the
757 target resolution of 0.5°. Compared to ISIMIP2b, where climate model output was first
758 spatially interpolated to the target resolution and then bias-adjusted, the new approach
759 avoids the associated underestimation of improves the spatial variability at the target
760 resolution (Lange, 2019b). Second, the new quantile mapping method preserves trends in
761 each quantile of the distribution of the daily data and adjusts biases in distribution
762 quantiles of the daily data more accurately than the ISIMIP2b bias adjustment methods
763 (Lange, 2019b).

764
765 For trend preservation, we first produce pseudo-future pseudo-observations by shifting
766 the historically observed daily data by the simulated future climate change. Here, the
767 signal of climate change is the difference or the ratio between the inverse empirical
768 cumulative distribution function of the historical period and the respective distribution
769 functions of each 36-year period of the future. Using the difference ensures additive trend
770 preservation and using the ratio ensures multiplicative trend preservation under bias
771 adjustment. We apply additive trend preservation for near-surface air temperature (tas),
772 sea level pressure (psl, see **Table 36**), and surface downwelling longwave radiation (rlds).
773 We apply primarily multiplicative trend preservation for precipitation including snowfall
774 (pr), near-surface wind speed (sfcWind), and the range (tasrange = tasmax - tasmin)
775 between the daily maximum and minimum near-surface air temperatures (tasmax and
776 tasmin, respectively) that can transition smoothly to additive trend preservation for data
777 with large negative biases in the historical period (Lange, 2019b). In a second step, the

778 future simulations are mapped onto the ~~pseudo~~-future pseudo-observations by quantile
779 mapping. Both steps, the generation of the ~~pseudo~~-future pseudo-observations and the
780 quantile mapping of the future simulations onto the pseudo-observations, are applied for
781 each day of the year separately. The distributions include data from the 31 days around
782 the considered day and all years of the reference or future period, respectively. This
783 means a sample size of 31x36 values for each day of the year. Through this approach the
784 bias adjustment implicitly also adjusts the multi-year mean annual cycle and a mix of year-
785 to-year and day-to-day variability (Haerter et al., 2011).

786

787 In addition, the method adjusts the frequency of daily data falling outside of the inner
788 bounds specified in **Table 311** (e.g. the dry day frequency, i.e. the number of days with
789 precipitation below 0.1 mm day⁻¹).

790

791 Four variables were adjusted and downscaled indirectly: near-surface specific humidity
792 (huss) was derived from adjusted and downscaled near-surface relative humidity (hurs),
793 surface air pressure (ps), and near-surface air temperature (tas) using the equations of
794 Buck et al. (1981) as described in Weedon et al. (2010), snowfall (prsn) was derived from
795 adjusted and downscaled precipitation including snow (pr) and the snowfall ratio
796 (prsnratio = prsn / pr), and daily maximum and daily minimum near-surface air
797 temperatures (tasmax and tasmin, respectively) were derived from adjusted and
798 downscaled tas, and the tasrange = tasmax - tasmin and skewness of the daily
799 temperature cycle tasskew = (tas - tasmin) / (tasmax - tasmin).

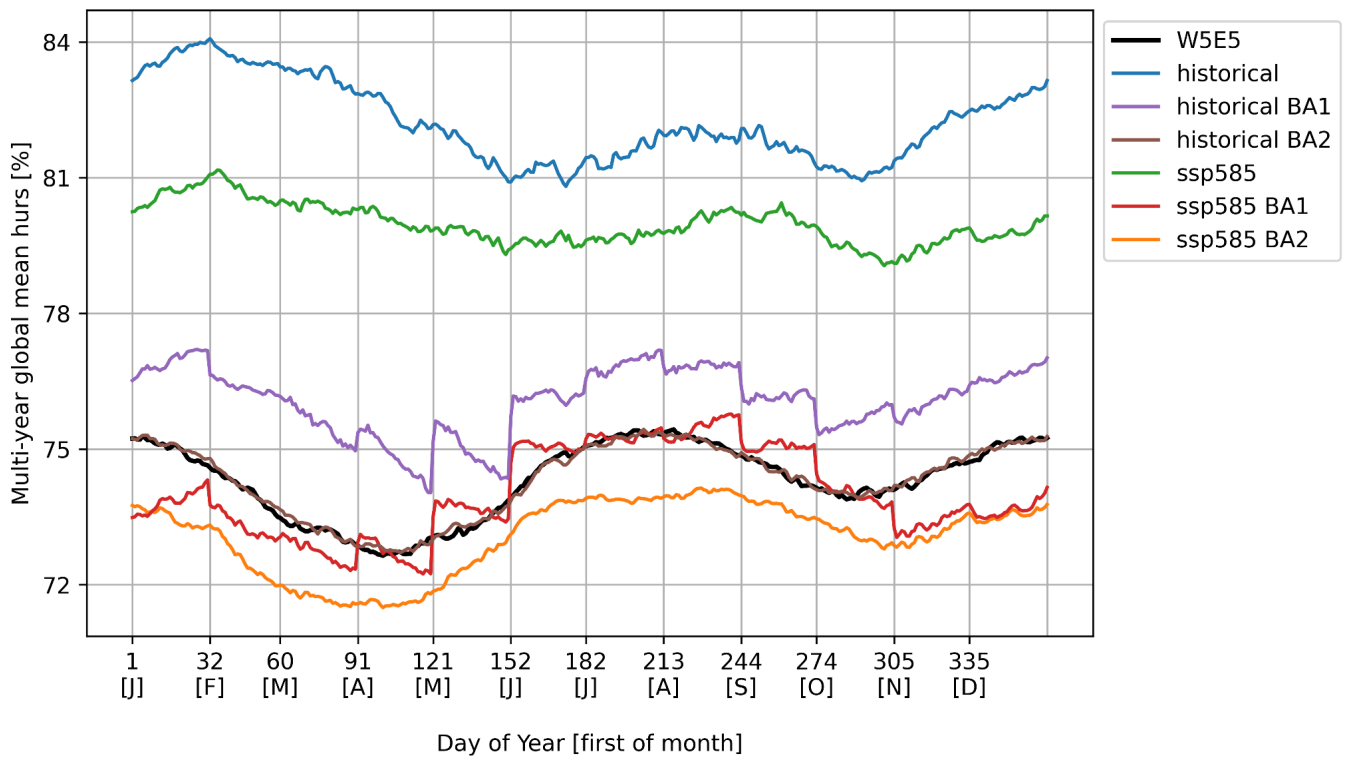
800

801 The basic characteristics of ISIMIP3BASD (version 1.0) are described in Lange (2019b).
802 However, the method finally used to generate the forcing data now provided within
803 ISIMIP3b (ISIMIP3BASD version 2.5) deviates from the original version in some aspects. In
804 the following we describe the most important updates of the procedure relative to the one
805 described in Lange (2019b). For a complete list of differences between the two versions of
806 the BASD method and the full history of which feature was added in which update, see the
807 CHANGELOG included in the archive of code version 2.5 (Lange, 2021a).

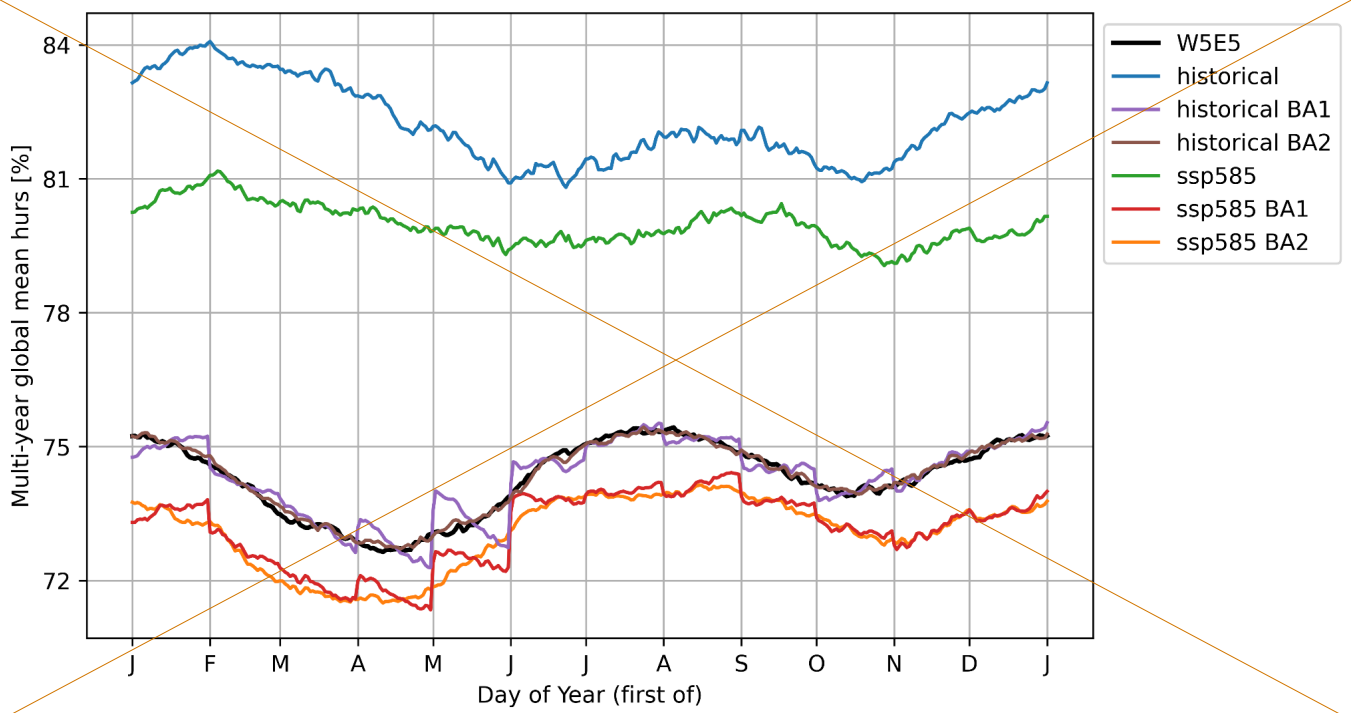
808

809 In Lange (2019b) the bias-adjustment was applied on a monthly basis, i.e. the ~~pseudo~~-
810 future pseudo-observations and the quantile mapping described above was applied to all
811 daily January data, February data and so forth. This approach can introduce discontinuities
812 at the transition from one month to another (see **Figure 4**). That is why for ISIMIP3b the
813 adjustment is done in the running window mode with steps of one day and a window
814 width of 31 days as described above. This approach resolves the discontinuity issue (see

815 | **Figure 4**), as suggested by Themeßl et al. (2012); Thrasher et al. (2012); Gennaretti et al.
816 | (2015); and Grenier (2018).
817



818



819

$$\begin{aligned}
& P_{fut}^{obs} = \{ \\
& P_{fut}^{\square} \text{ if } P_{hist}^{\square} = P_{hist}^{obs}, \\
& 0 + (P_{hist}^{obs} - 0)(P_{fut}^{\square} - 0) / (P_{hist}^{\square} - 0) \text{ if } P_{fut}^{\square} \leq P_{hist}^{\square} > P_{hist}^{obs}, \\
& 1 - (1 - P_{hist}^{obs})(1 - P_{fut}^{\square}) / (1 - P_{hist}^{\square}) \text{ if } P_{fut}^{\square} \geq P_{hist}^{\square} < P_{hist}^{obs}, \\
& P_{hist}^{obs} + P_{fut}^{\square} - P_{hist}^{\square} \text{ otherwise.}
\end{aligned} \tag{1}$$

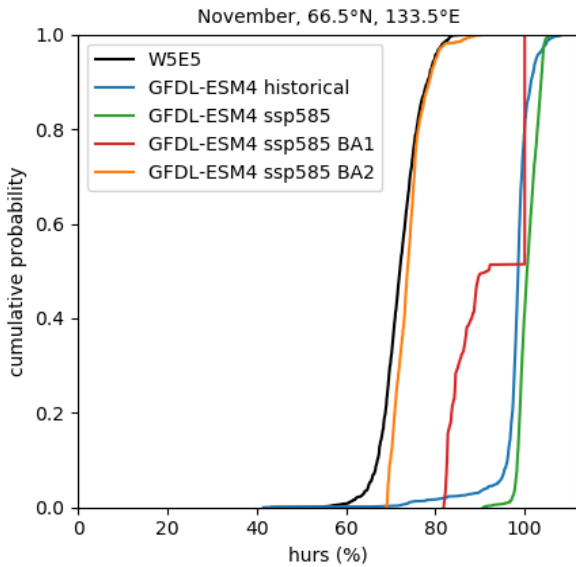
In this revised relation, the otherwise case applies if $P_{fut}^{\square} < P_{hist}^{\square} < P_{hist}^{obs}$ or $P_{fut}^{\square} > P_{hist}^{\square} > P_{hist}^{obs}$. Hence it applies to the aforementioned edge case, where it produces a less extreme future pseudo-observed relative frequency of $0.0 + 0.9 - 0.8 = 0.1$. Equation (8) of Lange (2019b) was revised analogously to equation (9).

Furthermore, we refined the method used to generate future pseudo-observations (step 5 of the bias adjustment method algorithm of Lange (2019b)) for all variables with at least one bound: In v1.0, the future pseudo-observations were generated by transferring simulated trends in all distribution quantiles to the observational reference data. That included trends in, e.g., precipitation quantiles below the wet-day threshold. However, in some cases, the trend transfer turned many dry days into wet days, with a profound impact on the shape of the distribution of future pseudo-observed wet-day precipitation. As a result, simulated trends in wet-day precipitation intensity were not well preserved. In v2.5, trend transfers are restricted to values within threshold. This particularly improves the preservation of trends in wet-day precipitation intensities.

We also modified the bias adjustment method for Near-Surface Relative Humidity (hurs) because ISIMIP3BASD v1.0 turned out to produce unrealistic distributions of hurs under climate change if there are too many cases of supersaturation ($hurs \geq 100\%$) in the simulated data. This is the case for several of the CMIP6 GCMs selected for ISIMIP3b, particularly in high-latitude winter: While no supersaturations are found in the observational reference data, the GCM simulates many supersaturations in the historical reference period and even more so in a future period, under SSP5-8.5 (see **Figure 5**). ISIMIP3BASD v1.0 preserves this projected trend and hence produces future bias-adjusted hurs data with many supersaturations. In v2.5, this trend is no longer preserved. Instead, the supersaturation probability is fixed at the observed level, which is zero or very close to zero in all seasons and grid cells for W5E5. Future pseudo-observations of hurs are generated by applying the revised (see above) equation (8) of Lange (2019b) to all hurs values after capping them at 100%. The new approach was motivated by findings from Ruosteenoja et al. (2017, 2018). They analysed hurs data from CMIP5 and showed that (i) supersaturations in those data are mostly spurious, resulting from, e.g., inconsistencies in

885 the interpolation of temperature and specific humidity to the near-surface level, and (ii)
 886 climatological mean value trends of hurs become more consistent with trends in relative
 887 humidity from the lowest model level if hurs is capped at 100% before trends are
 888 calculated.

889



890

891

892 **Figure 5:** Empirical cumulative distribution functions of near-surface relative humidity in high-
 893 latitude winter (November, 66.5°N, 133.5°E) for GFDL-ESM4 historical (1979–2014) and SSP5-8.5
 894 (2065–2100), with historical simulated data in blue, future simulated data in green, future bias-
 895 adjusted data in red and orange, and observational reference data in black. The simulated climate
 896 change signal is well preserved with ISIMIP3BASD v2.5 using a fixed supersaturation ($\text{hurs} \geq$
 897 100%) probability and equation (1) applied to all hurs values after capping them at 100% to
 898 generate future pseudo-observations (orange, BA2). In contrast, the simulated climate change
 899 signal is not well preserved if the supersaturation probability is allowed to change and equations
 900 (8) and (9) of Lange (2019b) are used to generate future pseudo-observations of hurs (red, BA1).

901

902 In addition, while ISIMIP3BASD v1.0 applies parametric quantile mapping to all climate
 903 variables, we used a nonparametric approach for the bias adjustment of near-surface
 904 relative humidity (hurs), the snowfall ratio (prsnratio), surface downwelling shortwave
 905 radiation (rsds), and the skewness of the daily temperature (tasskew) since the parametric
 906 quantile mapping method previously used for those variables suffered from occasionally
 907 unstable beta distribution fits.

908

909 Moreover, the parametric quantile mapping described in Lange (2019b) does not only
 910 adjust biases in quantiles of the simulated daily data but also adjusts biases in the

911 | likelihood of individual events, as in Switanek et al. (2017). To avoid overfitting artifacts
912 we did not adjust event likelihoods for ISIMIP3b.

913

914 Finally, the diurnal temperature range (tasrange) was ultimately bias-adjusted using a
915 Weibull distribution, not a Rice distribution as described in (Lange, 2019b) because the
916 Weibull distribution fits the data better in most cases, in particular in the upper tail.

917

918 For further details of the application of ISIMIP3BASD v2.5 for ISIMIP3b, including the exact
919 Python commands and application periods used per CMIP6 experiment, see the ISIMIP3b
920 bias adjustment fact sheet (Lange, 2021b).

921

922 In addition, we use a new observational target dataset. Instead of using the EWEMBI
923 dataset (E2OBS, WFDEI and ERAI data merged and bias-corrected for ISIMIP; (Lange,
924 2019a)) in ISIMIP3b we adjust the climate forcing data to version 2.0 of the W5E5 dataset
925 (WFDE5 over land merged with ERA5 over the ocean; (Lange et al., 2021)). The data cover
926 the entire globe at 0.5° horizontal and daily temporal resolution from 1979 to 2019. W5E5
927 v2.0 is derived by applying version 2.0 of the WATCH Forcing Data methodology (WFDE5;
928 (Cucchi et al., 2020)) to ERA5 reanalysis data (Hersbach et al., 2020) and precipitation data
929 from version 2.3 of the Global Precipitation Climatology Project (GPCP; (Adler et al., 2003)).

930

931 The statistical downscaling method did not change between v1.0 and v2.5 of
932 ISIMIP3BASD, i.e. for ISIMIP3b we use the approach described by Lange (2019b). This
933 method adds the spatiotemporal variability that is missing at the low spatial resolution at
934 which the bias adjustment is done (1° or 2°, depending on the GCM), compared to the
935 target resolution of the downscaling (0.5°). The method is a modified version of the MBCn
936 algorithm from Cannon (2018), which in turn is a stochastic, multivariate, non-parametric
937 quantile mapping method. We use it to transfer the statistical relationship between low-
938 resolution and high-resolution W5E5 data to the GCM output that was previously bias-
939 adjusted using low-resolution W5E5 data. In comparison to the approach used in ISIMIP2b
940 (a spatial interpolation to the target resolution followed by a bias adjustment at that
941 resolution), the approach used in ISIMIP3b is less prone to inflate temporal variability and
942 deflate spatial variability, i.e. the ISIMIP3b approach produces more realistic
943 spatiotemporal variability patterns at the target resolution (Lange, 2019b).

944

945 |

946 **2.2 Tropical cyclones**

947

948 **Table 5:** Information about tropical cyclone tracks and windfields provided as climate-
 949 related forcing data within ISIMIP3b.

Variable	Variable specifier	Unit	Resolution	Datasets
Time associated with a given location of the storm centre	time	hours since 1950-01-01 00:00	along-track, 2-hourly (MIT model) 6-hourly (CHAZ model)	MIT (Emanuel et al., 2008) and -CHAZ (Lee et al., 2018)
Latitudinal coordinate of storm centre	lat	degrees north	along-track, 2-hourly (MIT model) 6-hourly (CHAZ model)	MIT (Emanuel et al., 2008) and -CHAZ (Lee et al., 2018)
Longitudinal coordinate of storm centre	lon	degrees east	along-track, 2-hourly (MIT model) 6-hourly (CHAZ model)	MIT (Emanuel et al., 2008) and -CHAZ (Lee et al., 2018)
Central pressure	pres	hPa	along-track, 2-hourly	MIT (Emanuel et al., 2008)
Maximum 1-minute sustained wind speed	windspat ialmax	ms⁻¹knots	along-track, 2-hourly (MIT model) 6-hourly (CHAZ model)	MIT (Emanuel et al., 2008) and -CHAZ (Lee et al., 2018)
Radius of maximum wind speeds	rmw	km	along-track, 2-hourly	MIT (Emanuel et al., 2008)
Wind speed on the 850 hPa pressure level	ua850 va850	ms⁻¹knots (MIT model), ms⁻¹ (CHAZ model)	along-track, 2-hourly (MIT model) 6-hourly (CHAZ model)	MIT (Emanuel et al., 2008) and -CHAZ (Lee et al., 2018)
Temperature on the 600 hPa pressure level	ta600	K	along-track, 2-hourly (MIT model) 6-hourly (CHAZ model)	MIT (Emanuel et al., 2008) and -CHAZ (Lee et al., 2018)
Frequency of TC occurrence	freqyear	count per year	annual	MIT (Emanuel et al., 2008)

Gridded lifetime maximum 1-minute sustained wind speed	windlifetimemax	mm s ⁻¹	Per storm on a 300 arc-seconds (~10 km) grid	Wind fields calculated with Holland and Emanuel-Rotunno wind profiles (Holland, 1980, 2008) for <u>MIT both sets of synthetic tracks (CHAZ and MIT)</u>
Maximum 24-hourly rainfall total during the whole storm duration	maxrain	mm	per storm on a 300 arc-seconds (~10 km) grid	Maximum 24-hourly rainfall (Zhu et al., 2013) calculated for Holland and Emanuel-Rotunno wind profiles for <u>MIT both sets of synthetic tracks (CHAZ and MIT)</u>

950

951 We provide large ensembles of potential realisations of TC tracks and intensities that are
 952 consistent with the large-scale atmospheric and oceanic conditions simulated by four of
 953 the five the 5 ISIMIP3b GCMs (see **Table 64**) and for a selection of scenarios considered in
 954 ISIMIP3b (see **Table 1**). ~~We provide gridded wind (maximum 1-minute sustained wind~~
 955 ~~speeds during the whole duration of the TC) and rainfall (maximum 24-hourly amounts of~~
 956 ~~rain during the whole duration of the TC) fields at a spatial resolution of 300 arc-seconds~~
 957 ~~(approximately 10 km) by the same approaches also applied to the historically observed~~
 958 ~~tracks [Citation error], section 3.2).~~

959 The tracks are generated by two different statistical-dynamical approaches, the MIT
 960 approach and the CHAZ approach detailed below. ~~— that, forced by data from the~~
 961 ~~ISIMIP3b GCMs listed in data (see Table 64), these allow generating large ensembles of~~
 962 ~~potential realisations of numerous a large number of synthetic storms. For the MIT,~~
 963 ~~approach, we provide gridded wind (maximum 1-minute sustained wind speeds during~~
 964 ~~the whole duration of the TC) and rainfall (maximum 24-hourly amounts of rain during the~~
 965 ~~whole duration of the TC) fields at a spatial resolution of 300 arc-seconds (approximately~~
 966 ~~10 km) using the same approaches also applied to the historically observed tracks (Frieler~~
 967 ~~et al., 2024), section 3.2).~~

968 Both methods to generate the TC tracks are assessed in Meiler et al. (2025). The
 969 modeling approaches consist of a genesis, a track, and an intensity module:

970 ~~The MIT approach.~~ Within MIT (Emanuel et al., 2008), the time-evolving state of the
 971 atmosphere and ocean surface given by the GCMs is randomly (uniformly distributed in
 972 time and space) seeded by weak proto-cyclones (genesis module). The seed disturbances
 973 are assumed to move with the GCM-provided large-scale flow in which they are
 974 embedded, plus a westward and poleward component owing to planetary curvature and

975 rotation (track module). Their intensity is calculated using the Coupled Hurricane Intensity
976 Prediction System (CHIPS; (Emanuel et al., 2004)), a simple axisymmetric hurricane model
977 coupled to a reduced upper ocean model to account for the effects of upper ocean mixing
978 of cold water to the surface (intensity module). Applied to the synthetically generated
979 tracks, this model simulates which of the seeded proto-cyclones develop into TCs,
980 reaching maximum 1-minute sustained wind speeds of at least 35 knots, or dissipate due
981 to unfavourable environments. The probabilistic seeding of proto-cyclones is repeated
982 until the desired number of storms per year is reached (in our case, 1500). For each year,
983 the share of proto-cyclones that dissipated in the process is used to derive an estimate of
984 annual TC occurrences (**freqyear**). Extensive comparisons to historical events (Emanuel et
985 al., 2008) have revealed that the statistical properties of the simulated events are
986 consistent with historical TC genesis.

987 ~~1500 tracks were generated globally and~~ For each year of the ISIMIP3b period 1850—
988 2100 (except for GFDL-ESM4, where tracks were only generated for 1850—2014 and 2061—
989 2100, and MRI-ESM2-0 for 1950—2100, see **Table 1**), ~~1500 tracks were generated, globally.~~
990 Depending on the application, a simple subsampling (Meiler et al., 2022) or a more
991 advanced bias-correction and emulation procedure (Geiger et al., 2021) might be
992 necessary to extract properly-sized sets of potential realisations from the MIT ensembles.

993 The “ISIMIP3b tropical cyclone tracks MIT” dataset shall only be used for noncommercial
994 purposes, including teaching and research at universities, colleges and other educational
995 institutions, research at non-profit research institutions, and personal non-profit
996 purposes. It is accessible through the ISIMIP data portal after agreeing to the
997 corresponding license.

998 For using the tracks for commercial purposes, including but not restricted to consulting
999 activities, software or data products, and a commercial entity participating in research
1000 projects, please contact Kerry Emanuel (MIT, email: emanuel@mit.edu) for an appropriate
1001 license.

1002 ~~The MIT track data shall be used for non-commercial research or academic purposes only.~~
1003 ~~Data can be made available by the ISIMIP team upon written consent by Kerry Emanuel~~
1004 ~~(MIT, email: emanuel@mit.edu).~~

1005 **The CHAZ approach.** CHAZ (Lee et al., 2018) seed disturbances are also initialised
1006 randomly, but, in contrast to the MIT model, the global seeding rate and the local
1007 probabilities are derived from two versions of a TC genesis index (TCGI, (Tippett et al.,
1008 2011) (genesis module)) and intended to represent the environmental conditions instead
1009 of being adjusted to produce a prescribed number of TCs. It is noted that CHAZ’s
1010 projection of global and basin-wide TC annual frequency is sensitive to the choice of the
1011 particular variable used to represent moisture in its genesis module. Simulations using
1012 column relative humidity (CRH) as the moisture variable tend to project an overall increase
1013 in global TC frequency, while those using saturation deficit (SD) show a decrease
1014 (Camargo et al., 2014; Lee et al., 2020). Both parameters describe how far the atmosphere

1015 is from saturation, and they have very similar spatial patterns in the present climate, so
1016 historical data cannot be used to determine which variable is the best choice to represent
1017 the climate. These two configurations reflect the uncertainty of TC frequency projections
1018 (Sobel et al., 2021). Here we provide CHAZ downscaling using both choices of moisture
1019 variable to account for this uncertainty.

1020 Similar to MIT, CHAZ then moves the synthetic storms by advection of the environmental
1021 steering flow plus a beta drift (track module). The evolution of synthetic storm intensity is
1022 calculated using the surrounding atmospheric conditions through an empirical multiple
1023 linear regression model plus a stochastic component (intensity module, (Lee et al., 2015,
1024 2016)). The stochastic component accounts for internal storm dynamics that do not
1025 depend explicitly on the environment. While, in MIT, TC occurrence frequency is provided
1026 as an additional variable, in CHAZ, this information is implicitly contained in the number of
1027 TCs that were seeded by the genesis module and that reached TC strength according to
1028 the intensity module.

1029 For ISIMIP3b, 20 different CHAZ realisations of the genesis and subsequent tracks are
1030 generated with 40 ensemble members each from the intensity module [for the historical
1031 period and for all RCP-SSP combinations considered within ISIMIP3b](#). For each of the 20
1032 realisations, we compute wind and rain fields for the first ensemble member from the
1033 intensity ensemble. The design of 20 realisations allows CHAZ to generate similar
1034 numbers (~1800) of synthetic storms per year per GCM as the MIT models over the
1035 historical period. The exact number of storms per year in CHAZ varies by GCM, by
1036 scenario, by the choice of humidity variables in CHAZ's genesis component (Lee et al.,
1037 2020). On average, CHAZ generates 1817, 1802, 1820, 1810, 1842 storms per year for
1038 GFDL-ESM4, IPSL-CM6A-LR, MPI-ESM1-2-HR, MRI-ESM2-0, and UKESM1-0-LL, respectively.
1039 The CHAZ model has been shown to capture the statistical properties of the observed
1040 storms when forced by a global reanalysis data (Lee et al., 2018). Its CMIP6 downscaling
1041 results are reported in Fosu et al. (2024). Sobel et al. (2019) used both models to study
1042 cyclone risk [forat](#) Mumbai, India and showed that MIT and CHAZ generate comparable
1043 return periods (frequency of exceedance) of maximum wind speeds at landfall. However, a
1044 frequency bias-correction might still be necessary, depending on the application (Meiler et
1045 al., 2022).

1046 [The "ISIMIP3b tropical cyclone tracks \(CHAZ\)" dataset shall only be used for
1047 noncommercial purposes, including teaching and research at universities, colleges and
1048 other educational institutions, research at non-profit research institutions, and personal
1049 non-profit purposes. It is accessible through the ISIMIP data portal after agreeing to the
1050 corresponding license.](#)

1051 [For using the tracks for commercial purposes, including but not restricted to consulting](#)
 1052 [activities, software or data products, and a commercial entity participating in research](#)
 1053 [projects, please contact Chia-Ying Lee \(Columbia University, email: \[cl3225@columbia.edu\]\(mailto:cl3225@columbia.edu\)\)](#)
 1054 [for an appropriate license.](#)

1055 .
 1056 ~~The track data generated by the CHAZ approach shall be used for non-commercial~~
 1057 ~~research or academic purposes only. Data can be made available by the ISIMIP team upon~~
 1058 ~~written consent by Chia-Ying Lee (Columbia University, email: cl3225@columbia.edu).~~

1060 **Table 6:** Climate input data interpolated to 2° horizontal resolution and provided without
 1061 bias adjustment for tropical cyclone modelling with MIT and CHAZ.

Variable	Variable specifier	Unit	Resolution	Datasets
Sea Water Potential Temperature	thetao	°C	2° grid, model specific levels (m from surface to 200 m depth), monthly	GFDL-ESM4 , IPSL-CM6A-LR, MPI-ESM1-2-HR, MRI-ESM2-0, and UKESM1-0-LL simulations generated for CMIP6.
Sea Surface Temperature	tos	°C	2° grid over the ocean, monthly	GFDL-ESM4 , IPSL-CM6A-LR, MPI-ESM1-2-HR, MRI-ESM2-0, and UKESM1-0-LL simulations generated for CMIP6.
Surface Temperature	ts	K	2° grid covering land and ocean areas, monthly	GFDL-ESM4 , IPSL-CM6A-LR, MPI-ESM1-2-HR, MRI-ESM2-0, and UKESM1-0-LL simulations generated for CMIP6. ts may differ from tos in regions of sea ice where tos refers to temperatures under the ice while ts refers to temperatures at the surface.
Air Temperature	ta	K	2° grid; 15 pressure levels (from 1000 to 30 hPa), monthly	GFDL-ESM4 , IPSL-CM6A-LR, MPI-ESM1-2-HR, MRI-ESM2-0, and UKESM1-0-LL simulations generated for CMIP6.
Specific Humidity	hus	kg kg ⁻¹	2° grid; 15 pressure levels (from 1000	GFDL-ESM4 , IPSL-CM6A-LR, MPI-ESM1-2-HR, MRI-ESM2-0,

			to 30 hPa), monthly	and UKESM1-0-LL simulations generated for CMIP6.
Relative Humidity at 600 hPa	hur	%	2° grid, monthly	GFDL-ESM4 , IPSL-CM6A-LR, MPI-ESM1-2-HR, MRI-ESM2-0, and UKESM1-0-LL simulations generated for CMIP6.
Precipitable water (water vapour content vertically integrated through the atmospheric column)	prw	kg m ⁻²	2° grid, monthly	GFDL-ESM4 , IPSL-CM6A-LR, MPI-ESM1-2-HR, MRI-ESM2-0, and UKESM1-0-LL simulations generated for CMIP6.
Sea Level Pressure	psl	Pa	2° grid, monthly	GFDL-ESM4 , IPSL-CM6A-LR, MPI-ESM1-2-HR, MRI-ESM2-0, and UKESM1-0-LL simulations generated for CMIP6.
Eastward Wind	ua	m s ⁻¹	2° grid; 200, 250, 850 hPa; monthly	GFDL-ESM4 , IPSL-CM6A-LR, MPI-ESM1-2-HR, MRI-ESM2-0, and UKESM1-0-LL simulations generated for CMIP6.
Northward Wind	va	m s ⁻¹	2° grid; 200, 250, 850 hPa; monthly	GFDL-ESM4 , IPSL-CM6A-LR, MPI-ESM1-2-HR, MRI-ESM2-0, and UKESM1-0-LL simulations generated for CMIP6.
Eastward Wind	ua	m s ⁻¹	2° grid; 250, 850 hPa; daily	GFDL-ESM4 , IPSL-CM6A-LR, MPI-ESM1-2-HR, MRI-ESM2-0, and UKESM1-0-LL simulations generated for CMIP6.
Northward Wind	va	m s ⁻¹	2° grid; 250, 850 hPa; daily	GFDL-ESM4 , IPSL-CM6A-LR, MPI-ESM1-2-HR, MRI-ESM2-0, and UKESM1-0-LL simulations generated for CMIP6.

1062

1063

2.3 Coastal water levels

Table 7: Coastal water level specifications

Variable	Variable specifier	Unit	Resolution	Datasets
Coastal water levels	cwl	m	custom coastal grid Hourly or daily maxima	planned

We do not yet provide coastal water levels as forcing data for ISIMIP3b. However, we plan to generate time series of coastal water levels from 1900 to 2100 at hourly resolution or for daily maxima. The data set and method will be described in a separate manuscript. Similar to the hourly water level dataset of ISIMIP3a (see section 3.3 of Frieler et al. (2024) and Treu et al. (2023)), we will combine longer-term annual sea level change with estimates of short-term coastal water level variation. Concerning the long-term sea level change component, we ~~go beyond~~will further develop the ISIMIP2b approach (Frieler et al., 2017) and use tide gauge, satellite, vertical land motion and global climate model data to constrain a model with observations and IPCC AR6 projections in a Bayesian setting building on Perrette & Mengel (2025). ~~The Perrette & Mengel (2025) model Modelled global contributions from ice sheets and fingerprints are translated to regional sea level rise via fingerprints. A new aspect is that we include an estimation of vertical land motion to provide relative coastal water levels instead of geocentric coastal water levels. The model allows for smooth projections of relative sea level from observational time series collected at tide gauge stations with an explicit representation of the different components of sea level rise. To become usable for ISIMIP3 the approach we will a) extend the approach will be extended to all coastlines and b) use GCM output directly for the global thermosteric and local sterodynamic components (Gregory et al., 2019) of sea level rise, which are modeled by the GCMs. Extension to all coastlines is possible for the ice sheet, glacier and sterodynamic components as they rely on spatial fingerprints or GCM output. Processes driving vertical land motion that are not related to large scale climate processes are however more difficult to model. They are estimated from data as residual vertical land motion in Perrette & Mengel (2025). As we do not have data at all coastlines we will extrapolate in time and space the historical rates from tide gauge sites or apply zero rates for this component. Using the explicit component structure of the model, we replace the global thermosteric and the local sterodynamic parts by the output~~

1095 [from ISIMIP GCMs. To that end, we reference the gridded sterodynamic simulation data](#)
1096 [with observations of that component so that they smoothly emerge from the historical](#)
1097 [period. We do not adjust variability or trends of the GCM data. The method will provide](#)
1098 [relative sea level projections \(including vertical land motion\), which can be directly used in](#)
1099 [coastal impact studies.](#) We plan to estimate the short-term coastal water level variation by
1100 a machine-learning approach that is trained to reproduce simulations of the Global
1101 [TideSurge](#) and [SurgeTide](#) Model (GTSM) ~~model~~ driven by ERA5 reanalysis data (Muis et al.,
1102 2020) or simulations from HighResMIP (Muis et al., 2023). We are currently testing the
1103 dependency of the short-term water level variation on available atmospheric information
1104 at GCM resolution. If the predictive power is high enough we will use the findings to
1105 provide computationally efficient water level projections specific for the ISIMIP GCMs.

1107 **2.4 Ocean data**

1108
1109 In the default experiments, the ocean variables provided by the GCMs are not subject to
1110 bias-adjustment, unlike the atmospheric forcing data (section **2.4.1**). This is due to the
1111 absence of a comprehensive global observational oceanic dataset to serve as a reference
1112 for the adjustment.

1113 However, in order to mitigate potential biases in global impact model simulations
1114 stemming from biases in raw oceanic forcing data, we [plan to](#) provide a de-biased version
1115 to be used in a sensitivity experiment (see **Table 2**). They will be derived from an ocean-
1116 biogeochemistry model forced by bias-adjusted monthly atmospheric surface flux data
1117 from four of the five ISIMIP3b GCMs. The approach preserves the monthly variability of
1118 the underlying GCM while the daily variability is added from an independent simulation
1119 (see section **2.4.2**).

1120 For the regional impact model simulations, observational data for individual variables
1121 have either been applied directly (if the required forcing was observed) to rectify biases in
1122 regional oceanic forcings by the delta method or have first been translated into the
1123 required forcing variable by model simulations (see section **2.4.3**). ~~In the delta approach~~
1124 ~~absolute simulated deviations from reference levels are added to the observed reference~~
1125 ~~levels.~~ The regional bias-adjustment is independent from the generation of the global de-
1126 biased forcing data.

1127 In order to gauge the effects of these adjustments on the corresponding impact
1128 simulations, the protocol includes sensitivity experiments (**'de-biased'**) grounded on these
1129 adjusted ~~CRFclimate-related forcings~~ (see **Table 2**). The comparison of associated impact
1130 simulation to the default ones is expected to provide valuable insights into the effects of
1131 potential biases in the ~~CRFclimate-related forcings~~. The 'de-biased' experiments are

1132 considered a starting point to develop methods to bias-adjust the oceanic forcings in
 1133 further ISIMIP simulation rounds and make these simulations the default ones. Following
 1134 the ISIMIP ‘consistency framing’ the bias-adjustment should also preserve the daily
 1135 variability of the original GCM simulations to allow for a cross-sectoral integration on daily
 1136 time scale. .

1137 **2.4.1 Raw data without bias adjustment (default experiment)**

1138 In ISIMIP3b, a set of physical and biogeochemical ocean variables nearly identical to that
 1139 in ISIMIP3a is provided (see section 3.4, **Table 8** of Frieler et al. (2024) and **Table 8** below).
 1140 These variables are obtained from the CMIP6 GCMs, which also supply the atmospheric
 1141 forcing for ISIMIP3b, except for MRI-ESM2-0, which lacks bio-geochemical variables. In
 1142 other models, only certain individual variables are missing (see **Table 8**). Obtaining both
 1143 atmospheric and oceanic variables from the same set of GCMs ensures consistency
 1144 between the fisheries and marine ecosystems sector and other ISIMIP sectors. The
 1145 available variables in ISIMIP3b are interpolated from the native grids of the ocean models
 1146 to a regular 1° grid. This resolution is comparatively lower than that of the ISIMIP3a ocean
 1147 input data due to the generally reduced native resolution of CMIP6 GCM simulations
 1148 compared to the ocean model used to generate the oceanic forcings based on
 1149 observational atmospheric forcings for ISIMIP3a.
 1150

1151 **Table 8:** Oceanic climate-related forcing data provided within ISIMIP3b. Variables with
 1152 suffixes -bot, -surf, and -vint were obtained from the seafloor, the top layer of the ocean,
 1153 and vertical integration, respectively.

Variable	Variable specifier	Unit	Resolution	Datasets
Mass concentration of total phytoplankton expressed as chlorophyll	chl	kg m ⁻³	1° grid, vertically resolved, monthly	GFDL-ESM4, IPSL-CM6A-LR, MPI-ESM1-2-HR, UKESM1-0-LL
Sea floor depth	deptho	m	1° grid, constant	GFDL-ESM4, IPSL-CM6A-LR, MPI-ESM1-2-HR, UKESM1-0-LL
Downward flux of particulate organic carbon	expc-bot	mol m ⁻² s ⁻¹	1° grid, monthly	GFDL-ESM4, IPSL-CM6A-LR, MPI-ESM1-2-HR, UKESM1-0-LL

Particulate organic carbon content	intpoc	kg m ⁻²	1° grid, monthly	GFDL-ESM4, MPI-ESM1-2-HR, UKESM1-0-LL
Net primary organic carbon production by all types of phytoplankton	intpp	mol m ⁻² s ⁻¹	1° grid, monthly	GFDL-ESM4, IPSL-CM6A-LR, MPI-ESM1-2-HR, UKESM1-0-LL
Net primary organic carbon production by diatoms	intppdiat	mol m ⁻² s ⁻¹	1° grid, monthly	GFDL-ESM4, IPSL-CM6A-LR, UKESM1-0-LL
Net Primary Organic Carbon Production by Other Phytoplankton	intppmisc	mol m ⁻² s ⁻¹	1° grid, monthly	GFDL-ESM4, IPSL-CM6A-LR, UKESM1-0-LL
Net Primary Mole Productivity of Carbon by Picophytoplankton	intpppico	mol m ⁻² s ⁻¹	1° grid, monthly	GFDL-ESM4
Net Primary Organic Carbon Production of Carbon by Diazotrophs	intppdiaz	mol m ⁻² s ⁻¹	1° grid, monthly	GFDL-ESM4, MPI-ESM1-2-HR
Mixed layer depth defined by delta rho = 0.125	mlotstmax	m	1° grid, monthly	IPSL-CM6A-LR, MPI-ESM1-2-HR, UKESM1-0-LL
Dissolved oxygen concentration	o2, o2-bot, o2-surf	mol m ⁻³	1° grid, vertically resolved, ocean bottom and surface fields, monthly	GFDL-ESM4, IPSL-CM6A-LR, MPI-ESM1-2-HR, UKESM1-0-LL
pH	ph, ph-bot, ph-surf	1	1° grid, vertically resolved, ocean bottom and surface fields, monthly	GFDL-ESM4, IPSL-CM6A-LR, MPI-ESM1-2-HR, UKESM1-0-LL
Total phytoplankton carbon	phyc,	mol m ⁻³	1° grid,	GFDL-ESM4, IPSL-CM6A-LR,

concentration	phyc-vint		vertically resolved and vertically integrated, monthly	MPI-ESM1-2-HR, UKESM1-0-LL
Concentration of diatoms expressed as carbon in sea water	phydiat, phydiat-vint	mol m ⁻³	1° grid, vertically resolved and vertically integrated, monthly	GFDL-ESM4, IPSL-CM6A-LR, UKESM1-0-LL
Concentration of diazotrophs expressed as carbon in Sea Water	phydiaz, phydiaz-vint	mol m ⁻³	1° grid, vertically resolved and vertically integrated, monthly	GFDL-ESM4, MPI-ESM1-2-HR
Mole Content of Miscellaneous Phytoplankton Expressed as Carbon in Sea Water	phymisc, phymisc-vint	mol m ⁻²	1° grid, vertically resolved and vertically integrated, monthly	GFDL-ESM4, IPSL-CM6A-LR, MPI-ESM1-2-HR, UKESM1-0-LL
Mole Concentration of Picophytoplankton Expressed as Carbon in Sea Water	phypico, phypico-vint	mol m ⁻³	1° grid, vertically resolved and vertically integrated, monthly	GFDL-ESM4
Net Downward Shortwave Radiation at Sea Water Surface	rsndts	W m ⁻²	1° grid, monthly	GFDL-ESM4, IPSL-CM6A-LR, MPI-ESM1-2-HR
Sea Ice Area Fraction	siconc	%	1° grid, monthly	GFDL-ESM4, IPSL-CM6A-LR, MPI-ESM1-2-HR, UKESM1-0-LL
Sea water salinity	so, so-bot, so-surf	0.001	1° grid, vertically resolved, ocean bottom and	GFDL-ESM4, IPSL-CM6A-LR, MPI-ESM1-2-HR, UKESM1-0-LL

			surface fields, monthly	
Sea water potential temperature	thetao	°C	1° grid, vertically resolved, monthly	GFDL-ESM4, IPSL-CM6A-LR, MPI-ESM1-2-HR, UKESM1-0-LL
Ocean model cell thickness	thkcello	m	1° grid, vertically resolved, monthly	GFDL-ESM4, IPSL-CM6A-LR, MPI-ESM1-2-HR, UKESM1-0-LL
Sea water potential temperature at sea floor (bottom)	tob	°C	1° grid, monthly	GFDL-ESM4, IPSL-CM6A-LR, MPI-ESM1-2-HR, UKESM1-0-LL
Sea surface temperature	tos	°C	1° grid, monthly	GFDL-ESM4, IPSL-CM6A-LR, MPI-ESM1-2-HR, UKESM1-0-LL
Sea water zonal velocity	uo	m s ⁻¹	1° grid, vertically resolved, monthly	IPSL-CM6A-LR, MPI-ESM1-2-HR, UKESM1-0-LL
Sea water meridional velocity	vo	m s ⁻¹	1° grid, vertically resolved, monthly	IPSL-CM6A-LR, MPI-ESM1-2-HR, UKESM1-0-LL
Concentration of mesozooplankton expressed as carbon in sea water	zmeso, zmeso-vint	mol m ⁻³	1° grid, vertically resolved and vertically integrated, monthly	GFDL-ESM4, IPSL-CM6A-LR, UKESM1-0-LL
Concentration of microzooplankton expressed as carbon in sea water	zmicro, zmicro-vint	mol m ⁻³	1° grid, vertically resolved and vertically integrated, monthly	GFDL-ESM4, IPSL-CM6A-LR, UKESM1-0-LL
Total Zooplankton Carbon	zooc,	mol m ⁻³	1° grid,	GFDL-ESM4, IPSL-CM6A-LR,

Concentration	zooc-vint		vertically resolved and vertically integrated, monthly	MPI-ESM1-2-HR, UKESM1-0-LL
---------------	------------------	--	--	----------------------------

1154

1155 **2.4.2 Bias-adjusted global ocean forcings ('de-biased' sensitivity experiment)**

1156 GCMs have been shown to have limitations in accurately representing various aspects of
1157 the present climate system (Eyring et al., 2023), (S  ferian et al., 2020), that are also expected
1158 to affect regional physical and biogeochemical oceanic projections (Li et al., 2016),
1159 (Tagliabue et al., 2021). In particular, biases in sea-surface temperature (SST, variable 'tos')
1160 and nutricline as well as thermocline depth influence oceanic primary productivity, which
1161 in turn has major influence on various marine ecosystem processes. Thus, reducing the
1162 substantial biases in GCMs' ocean variables through bias-adjustment is desirable.
1163 Typically, for bias-adjustment of atmospheric variables, statistical approaches are used
1164 where a transfer function is trained to map the simulated historical distribution of the
1165 relevant variables to the observed distribution and then applied to future simulations. Yet
1166 for oceanic variables, the scarcity of comprehensive sub-surface observational data
1167 globally does not allow for a similar, direct adjustment of the relevant variables. However,
1168 standalone ocean-biogeochemistry simulations, when driven by observation-based
1169 atmospheric reanalysis data, have been demonstrated to considerably alleviate SST-
1170 related biases and typically provide satisfactory simulations of the physical ocean and
1171 marine biogeochemistry for the historical period (e.g. Tsujino et al. (2020), Barrier et al.
1172 (2023). Thus, an alternative process-oriented bias-adjustment approach has been
1173 developed that relies on a comprehensive ocean-biogeochemistry model that is forced by
1174 bias-adjusted atmospheric forcings. The adjustment of the ISIMIP3b oceanic forcings
1175 builds on such a dynamical de-biasing approach (Lengaigne et al., 2025), which relies on
1176 conducting forced oceanic simulations using the NEMO-PISCES physical-biogeochemical
1177 ocean model (Madec, 2015), which is the oceanic component of the IPSL-CM6A-LR climate
1178 model. The ocean model needs to be forced with high-frequency (3-hourly) surface
1179 momentum, heat and freshwater fluxes. Since from the CMIP6 pre-industrial, historical,
1180 and future scenario simulations used in ISIMIP3b these variables are only available at
1181 monthly resolution, additional steps are necessary to generate climatological high-
1182 frequency fluxes first. In the following, we first describe these preparatory steps, and then
1183 the de-biasing strategy, in more detail.

1184

1185 | **High-frequency surface flux forcing.** Initially, a climatological simulation spanning the
1186 historical period from 1958 to 2022 is performed by forcing the ocean model NEMO-

1187 PISCES with a single repeating annual cycle representative of the 1990s' climate conditions
1188 sourced from the "Repeat Year Forcing" (RYF) from JRA55 reanalysis (Stewart et al., 2020).
1189 This simulation is driven using the CORE bulk formulae (Large W. G., 2004), incorporating
1190 all surface atmospheric variables at 3-hourly resolution from JRA55 RYF as inputs and
1191 storing 3-hourly momentum, heat and freshwater fluxes from this simulation. These 3-
1192 hourly JRA55 RYF fluxes are then added to the monthly seasonal flux anomalies available
1193 from the ISIMIP3b climate models for the pre-industrial (picontrol), historical (historical)
1194 and future SSP1-2.6 (ssp126), SSP3-7.0 (ssp370), and SSP5-8.5 (ssp585) scenarios. In this
1195 way, 3-hourly surface flux forcings are created for all ISIMIP3b scenarios. Notably, this
1196 procedure results in sub-monthly variability mirroring that of the JRA55 RYF, rather than
1197 the variability simulated by the coupled climate model. This means that any projected
1198 changes in sub-monthly variability due to climate change are not integrated in the final
1199 de-biased product. However, to date, marine ecosystem modellers have not analysed sub-
1200 monthly variability anyways (and most marine ecosystem models are not suited to
1201 account for sub-monthly variability of forcings), making this approach suitable.

1202 Alternatively, de-biased ocean simulations including GCM-based sub-monthly variability
1203 could be constructed by an alternative approach. In this scenario, 3-hourly surface
1204 atmospheric variables would be extracted directly from each GCM simulation, rather than
1205 from JRA55 RYF forced oceanic simulations. Forcing NEMO-PISCES with these variables
1206 using bulk formulae would once again produce the necessary 3-hourly surface fluxes, this
1207 time with variability consistent with the coupled GCM across all timescales. This approach
1208 however requires running a separate ocean simulation for each GCM and scenario to
1209 derive the surface fluxes, necessitating a much larger number of ocean model runs than
1210 the approach using JRA55 RYF. In addition, the 3-hourly input from the GCMs is not
1211 available for all scenarios without gaps.

1212
1213 **De-biasing strategy.** The 3-hourly surface fluxes, constructed as described above, then
1214 serve as input forcings for another set of NEMO-PISCES ocean model simulations which
1215 produce the final, bias-adjusted historical and future forcings for the marine ecosystem
1216 models. Since Notably, these ocean model simulations are not driven with bulk formulae
1217 but directly with surface fluxes (instead of bulk formulae), they enable an online
1218 implementation of the surface heat flux feedbacks triggered by climate change, which is
1219 important for realistically representing the effects of global warming into the forced ocean
1220 biogeochemistry model for historical and future simulations (Lengaigne et al., 2025). As
1221 described by Lengaigne et al. (2025), climate change alters surface fluxes both directly
1222 through the effect of greenhouse gases on atmospheric characteristics, such as wind
1223 speed or humidity; and through feedback effects related to changes in SST. For our bias-
1224 adjustment procedure, to maintain physical consistency, the part of the anomalous

1225 surface fluxes that directly depends on climate change-induced SST warming is separated
1226 from the part that does not. Only the latter part is used as a direct flux input to [NEMO-](#)
1227 ~~[PISCES](#)~~~~the ocean model~~, while the former is implemented within NEMO-PISCES as an
1228 online relaxation to the warming signal from the debiased historical and future
1229 simulations using a spatially and seasonally variable feedback damping coefficient. This
1230 SST feedback coefficient, derived from observed surface variables, represents the
1231 Newtonian cooling negative feedback related to latent heat fluxes through the Clausius-
1232 Clapeyron relationship and the negative feedback related to upward long-wave radiation
1233 through Stefan's law (Zhang & Li, 2014) and the positive downward longwave radiation
1234 feedback related to increasing temperature (Shakespeare & Roderick, 2022). Application of
1235 this approach to the [NEMO-PISCES](#) ocean model effectively reproduces the global SST
1236 changes simulated by CMIP6 models, as demonstrated in Lengaigne et al. (2025).

1237 In this way, physical and biogeochemical ocean simulations are generated for piconrol
1238 and historical climate forcings as well as for each of the future climate change scenarios,
1239 ensuring that the background climatological state is constrained by the reanalysis, while
1240 still accounting for both interannual and long-term climate variability simulated by the
1241 underlying GCM. Consequently, the resulting ocean-biogeochemistry simulations
1242 considerably mitigate the strong present-day climatological biases identified in the
1243 coupled models. Depending on data availability for the relevant monthly fluxes, this de-
1244 biasing procedure can be applied to any climate model. The set of variables included in
1245 the de-biased dataset will be a subset to the one in the raw GCM dataset (Table 8),
1246 detailed in Table 9.

1247
1248 Additionally, to generate observation-based oceanic forcings for ISIMIP3a, a reference
1249 simulation is also forced with the full JRA55 forcing (Tsujino et al., 2018) that includes
1250 observed inter-annual and decadal variability. This oceanic forcing is expected to be a
1251 valuable additional ~~[CRF](#)~~~~climate-related forcing~~ for impact model evaluation within
1252 ISIMIP3a akin to the GFDL-MOM6-COBALT2 reanalysis-driven historical dataset used in
1253 ISIMIP3a (Frieler et al., 2024). ~~The set of variables included in the de-biased dataset is a~~
1254 ~~subset to the one in the raw GCM dataset (Table 8), detailed in Table 9.~~

1257 | **Table 9:** Bias-adjusted ocean data to be used by global impact models in the ‘de-biased’
 1258 | sensitivity experiment in the fisheries and marine ecosystems sector

Variable	Variable specifier (variables in brackets are not directly available as model output but will have to be derived in post-processing)	Unit	Resolution	Forcing datasets
Mass concentration of total phytoplankton expressed as chlorophyll	chl	kg m ⁻³	1° grid, vertically resolved, monthly	JRA55+IPSL-CM6A-LR
Sea floor depth	deptho	m	1° grid, constant	JRA55+IPSL-CM6A-LR
Downward flux of particulate organic carbon	expc-bot	mol m ⁻² s ⁻¹	1° grid, monthly	JRA55+IPSL-CM6A-LR
Net primary organic carbon production by all types of phytoplankton	intpp	mol m ⁻² s ⁻¹	1° grid, monthly	JRA55+IPSL-CM6A-LR
Net primary organic carbon production by diatoms	intppdiat	mol m ⁻² s ⁻¹	1° grid, monthly	JRA55+IPSL-CM6A-LR
Net Primary Organic Carbon Production by Other Phytoplankton	intppmisc	mol m ⁻² s ⁻¹	1° grid, monthly	JRA55+IPSL-CM6A-LR
Mixed layer depth defined by delta rho = 0.125	mloitstmax	m	1° grid, monthly	JRA55+IPSL-CM6A-LR
Dissolved oxygen	o2, (o2-bot), o2-	mol m ⁻³	1° grid, vertically	JRA55+IPSL-CM6A-LR

concentration	surf		resolved, ocean bottom and surface fields, monthly	
pH	ph, (ph-bot), ph-surf	1	1° grid, vertically resolved, ocean bottom and surface fields, monthly	JRA55+IPSL-CM6A-LR
Total phytoplankton carbon concentration	phyc, (phyc-vint)	mol m ⁻³	1° grid, vertically resolved and vertically integrated, monthly	JRA55+IPSL-CM6A-LR
Concentration of diatoms expressed as carbon in sea water	phydiat, (phydiat-vint)	mol m ⁻³	1° grid, vertically resolved and vertically integrated, monthly	JRA55+IPSL-CM6A-LR
Mole Content of Miscellaneous Phytoplankton Expressed as Carbon in Sea Water	phymisc, (phymisc-vint)	mol m ⁻²	1° grid, vertically resolved and vertically integrated, monthly	JRA55+IPSL-CM6A-LR
Net Downward Shortwave Radiation at Sea Water Surface	rsndts	W m ⁻²	1° grid, monthly	JRA55+IPSL-CM6A-LR
Sea water salinity	so, (so-bot), so-surf	0.001	1° grid, vertically resolved, ocean bottom and surface fields, monthly	JRA55+IPSL-CM6A-LR
Sea water potential temperature	thetao	°C	1° grid, vertically resolved, monthly	JRA55+IPSL-CM6A-LR
Ocean model cell thickness	thkcello	m	1° grid, vertically resolved, monthly	JRA55+IPSL-CM6A-LR
Sea water potential	(tob)	°C	1° grid, monthly	JRA55+IPSL-CM6A-LR

temperature at sea floor (bottom)				
Sea surface temperature	tos	°C	1° grid, monthly	JRA55+IPSL-CM6A-LR
Sea water zonal velocity	uo	m s ⁻¹	1° grid, vertically resolved, monthly	JRA55+IPSL-CM6A-LR
Sea water meridional velocity	vo	m s ⁻¹	1° grid, vertically resolved, monthly	JRA55+IPSL-CM6A-LR
Concentration of mesozooplankton expressed as carbon in sea water	zmeso, (zmeso-vint)	mol m ⁻³	1° grid, vertically resolved and vertically integrated, monthly	JRA55+IPSL-CM6A-LR
Concentration of microzooplankton expressed as carbon in sea water	zmicro, (zmicro-vint)	mol m ⁻³	1° grid, vertically resolved and vertically integrated, monthly	JRA55+IPSL-CM6A-LR
Total Zooplankton Carbon Concentration	zooc, (zooc-vint)	mol m ⁻³	1° grid, vertically resolved and vertically integrated, monthly	JRA55+IPSL-CM6A-LR

1259

1260

2.4.3 Bias-adjusted regional ocean forcings ('de-biased' sensitivity experiment)

1261

1262

1263

1264

1265

1266

1267

1268

1269

1270

1271

Regional marine ecosystem models are most often calibrated to reproduce observed environmental variables when driven by observed sea surface and bottom temperature, primary production (phytoplankton production), and zooplankton biomass. However, [despite this calibration, that would still lead to biases may still occur](#) in the [ecosystem model's](#) historical simulations [when it is if the impact model was](#) forced by [- potentially biased - climate modelsimulated input](#) data instead of observational data. To reduce this effect the GCM-based input data has been adjusted such that the historical GCM simulations match observational data for certain regions (Eddy et al., 2025). The adjustment is based on the delta approach where simulated and observational forcing data X_{sim} and X_{obs} are averaged across a given historical reference period to determine the bias $\Delta = \text{mean}(X_{sim}) - \text{mean}(X_{obs})$ that is then subtracted from the simulated forcing

1272 data. This method preserves the trend in the forcing data and its internal variability. Some
 1273 ocean forcing variables are not an exact match with variables used in regional marine
 1274 ecosystem models. For example, sea water potential temperature (thetao), concentration
 1275 of diatoms (phydiat-vint), or concentration of mesozooplankton (zmeso-vint) may first be
 1276 converted to other indicators that are then used as input for the regional marine
 1277 ecosystem models. In these cases the derived indicator is corrected using the delta
 1278 method (see **Table 10**).

1279 **Table 10:** Bias-adjusted ocean data to be used by regional impact models in the ‘de-biased’
 1280 sensitivity experiment in the fisheries and marine ecosystems sector. [EwE: Ecopath with](#)
 1281 [Ecosim. See Ortega-Cisneros et al. \(2025\) for details about this and other ecosystem](#)
 1282 [models mentioned.](#)

Variable	Variable specifier	Unit	Resolution	Forcing datasets
Southern Benguela Current				
Net primary organic carbon production by all types of phytoplankton	intpp	mol m ⁻² s ⁻¹	1° grid, monthly	Corrected based on observed primary production for the southern Benguela current based on the delta method where the adjustment target is data from 1978 for the EwE model and 1990 for the Atlantis model
Sea water potential temperature	thetao	°C	1° grid, vertically resolved, monthly	Raw GCM temperature data converted to temperatures at 0-50, 50-100, 100-300 and 300-500 m according to the configuration for the southern Benguela Atlantis model, and 0-50 and 300-500 m for the EwE model.
Cook Strait				
Net primary organic carbon production by all types of phytoplankton	intpp	mol m ⁻² s ⁻¹	1° grid, monthly	Corrected based on observed primary production for Cook Strait using the delta method where observational target data is from 1950

East Bass Strait				
Net primary organic carbon production by all types of phytoplankton	intpp	mol m ⁻² s ⁻¹	1° grid, monthly	Corrected based on observed primary production for East Bass Strait using the delta method where observational target data is from 1994
East Bering Sea				
Concentration of diatoms expressed as carbon in sea water	phydiat-vint	mol m ⁻³	1/4° grid, vertically resolved and vertically integrated, monthly	Converted to phytoplankton size classes used in East Bering Sea mizer model then corrected using the delta method for the period 1982–1993
Concentration of diazotrophs expressed as carbon in sea water	phydiaz-vint	mol m ⁻³	1/4° grid, vertically resolved and vertically integrated, monthly	Converted to phytoplankton size classes used in East Bering Sea mizer model then corrected using the delta method for the period 1982–1993
Concentration of picoplankton expressed as carbon in sea water	phypico-vint	mol m ⁻³	1/4° grid, vertically resolved and vertically integrated, monthly	Converted to phytoplankton size classes used in East Bering Sea mizer model then corrected using the delta method for the period 1982–1993
Concentration of mesozooplankton expressed as carbon in sea water	zmeso-vint	mol m ⁻³	1/4° grid, vertically resolved and vertically integrated, monthly	Converted to zooplankton size classes used in East Bering Sea mizer model then corrected using the delta method for the period 1982–1993
Concentration of microzooplankton expressed as carbon in sea water	zmicro-vint	mol m ⁻³	1/4° grid, vertically resolved and vertically integrated, monthly	Converted to zooplankton size classes used in East Bering Sea mizer model then corrected using the delta method for the period 1982–1993
Sea surface temperature	tos	°C	1/4° grid, monthly	Corrected based on configuration for the East Bering Sea mizer model using

				the delta method for the period 1982–1993
Hawai'i				
Concentration of diatoms expressed as carbon in sea water	phydiat-vint	mol m ⁻³	1/4° grid, vertically resolved and vertically integrated, monthly	Converted to phytoplankton size classes used in Hawaii mizer model (Woodworth-Jefcoats, 2022) then corrected using the delta method
Concentration of diazotrophs expressed as carbon in sea water	phydiaz-vint	mol m ⁻³	1/4° grid, vertically resolved and vertically integrated, monthly	Converted to phytoplankton size classes used in Hawaii mizer model then corrected using the delta method
Concentration of picoplankton expressed as carbon in sea water	phypico-vint	mol m ⁻³	1/4° grid, vertically resolved and vertically integrated, monthly	Converted to phytoplankton size classes used in Hawaii mizer model then corrected using the delta method
Concentration of mesozooplankton expressed as carbon in sea water	zmeso-vint	mol m ⁻³	1/4° grid, vertically resolved and vertically integrated, monthly	Converted to zooplankton size classes used in Hawaii mizer model then corrected using the delta method
Concentration of microzooplankton expressed as carbon in sea water	zmicro-vint	mol m ⁻³	1/4° grid, vertically resolved and vertically integrated, monthly	Converted to zooplankton size classes used in Hawaii mizer model then corrected using the delta method
Sea water potential temperature	thetao	°C	1/4° grid, vertically resolved, monthly	Converted to temperature used in Hawaii Mizer model then corrected based on observed sea water potential temperature for Hawaii using the delta method from 1961–1980 with observed

				temperature data from the World Ocean Atlas
--	--	--	--	---

2.5 Future Lightning Data

For the 'varlightning' sensitivity experiment we provide temporally varying lightning density (strokes $\text{km}^{-2} \text{day}^{-1}$) for the period 2015--2100 on monthly resolution (monthly mean of daily lightning stroke density) and the standard 0.5° global grid. This dataset may be used in a range of applications, for example, to understand the influence of lightning on wildfire ignition or atmospheric composition.

The lightning density is derived from future climate simulations ~~of~~by UKESM1-0-LL and an empirical relationship between Convective Available Potential Energy (CAPE) and lightning strokes based on the WWLLN Global Lightning Climatology and time-series (WGLC) (Kaplan & Lau, 2021, 2022). Daily mean CAPE is calculated from non bias-adjusted air temperature, air pressure, and specific humidity on pressure levels from the surface to the top of the troposphere.

The relationship between daily CAPE and daily lightning is estimated by linear regression of log-transformed CAPE derived from the GCM-calculated CAPE during the period of overlapping model output and observed daily lightning from WGLC (2015-2020) for each gridcell and month of the year. Where <10 observations of daily lightning ~~are~~were available over the calibration period, we used global mean regression parameters.

The empirical relationships are applied to the daily CAPE data from the UKESM1-0-LL simulations for all three climate scenarios SSP1-2.6, SSP3-7.0, and SSP5-8.5. The associated lightning densities were monthly averaged. To maintain the spatial structure of lightning observed at present, lightning anomalies compared to the simulated 2015--2020 climatological reference were added to the observed present-day lightning climatology from WGLC for 2015--2020. The 'varlightning' sensitivity experiment is assumed to start from the default historical group I simulation, assuming the Flash Rate Monthly Climatology (Cecil, 2006), not changing with climate change.

1313 **Table 11:** Future lightning forcing data provided within ISIMIP3b.

Variable	Variable specifier	Unit	Resolution	Datasets
Monthly flash rate	lightning	km ⁻² d ⁻¹	0.5° grid, monthly	Derived from UKESM1-0-LL (SSP1-2.6, SSP3-7.0, and SSP5-8.5) using an empirical relationship between Convective Available Potential Energy (CAPE) and lightning densities (Kaplan et al., 2023).

1314
1315
1316

1317 **3 Conclusions**

1318

1319 This paper gives an overview over the ISIMIP3b, group I and II experiments and the
 1320 provided climate-related forcing data sets. The simulations assuming fixed 2015 direct
 1321 human forcings and a low (ssp126) and two high emission scenarios (ssp370 and ssp585)
 1322 are designed to describe the impacts of different levels of climate change on present day
 1323 natural and human systems. ~~The set-up allows e.g. for testing to what degree the~~
 1324 ~~(bio-)physical impacts scale with global mean temperature change and could therefore be~~
 1325 ~~translated to other global warming pathways than the ones considered here. While a~~
 1326 ~~functional relationship between the considered impact indicator and global mean~~
 1327 ~~temperature change (or other climate variables) could be trained on ssp585 simulations~~
 1328 ~~because of the high warming levels reached, its performance could then be tested on~~
 1329 ~~ssp370 and ssp126. However, in such a setting it has to be taken into account that ssp370~~
 1330 ~~is different from the other scenarios with regard to particularly high aerosol emissions~~
 1331 ~~and high decreases in forest areas going beyond the assumptions in the other models. So~~
 1332 ~~it has been shown that the increase of global mean precipitation with global warming is~~
 1333 ~~much weaker in SSP3-7.0 than in the other scenarios (Shiogama et al., 2023).~~

1334

1335 **This paper is intended to work as a catalogue where the climate impact modellers**
 1336 **can find all relevant information** (data source, formats, resolution, covered time period
 1337 **etc.) about the climate-related forcings selected as input needed as reference for the**
 1338 **impact model simulations generated within the CMIP6-based ISIMIP3b, group I**
 1339 **(historical period) and group II (future projections) framework.** As a continuous
 1340 process we would like to improve or complement these data sets wherever possible. So
 1341 this paper can also be read as a call to either contribute by additional input data that
 1342 allows other sectors to join the current simulation round or by methods that could be

1343 used to generate additional data sets for the next simulation round that will likely build on
1344 CMIP7 simulations. The following climate-related forcings have been identified as still
1345 missing and particularly critical to be added to a fourth simulation round of ISIMIP: i)
1346 temporally resolved lightning data accounting for changes in climate, ii) bias-adjusted
1347 oceanic forcing data, iii) projected coastal water levels in high temporal resolution
1348 accounting for extremes and representing the effects of long term sea level rise in line
1349 with the underlying global climate simulations, and iv) ozone concentration fields in line
1350 with the GCM simulations. While a bias-adjustment of the oceanic forcings is already
1351 suggested in section **2.4.2**, the approach does not preserve the daily variability of the raw
1352 oceanic forcings as it requires atmospheric surface flux only available in monthly
1353 resolution from the ISIMIP3b GCMs. To ensure the consistency on daily time scale, we
1354 have submitted an associated request for CMIP7 whose simulations will be used within
1355 the next round of ISIMIP. The generation of high resolution coastal water levels is ongoing
1356 research described in section **2.2.3**. In particular the generation of the short term
1357 variability that will have to be added to the long term trends in water levels still has to be
1358 developed and prove to fulfill the demands. In addition, it would be great to also provide
1359 estimates of the extreme coastal water levels associated with the tropical cyclone tracks
1360 and wind fields we provide within ISIMIP3b (see section **2.2**). There is a general demand
1361 for higher resolution [CRFclimate-related forcings](#) including both, the oceanic and the
1362 atmospheric components ideally accounting for heat island effects. As the ISIMIP
1363 [CRFclimate-related forcings](#) have to be globally consistent in the sense that they have to
1364 represent the daily variability of the underlying coarse resolution GCMs, we cannot use
1365 data from dynamical downscaling approaches using boundary conditions from different
1366 GCM runs as for example available through CORDEX. However, it seems to be appealing to
1367 harmonize the selection of the ISIMIP GCMs with a priority setting regarding the GCM-
1368 based boundary conditions within CORDEX.

1369
1370 The climate-related forcings described here are also provided as input for the new
1371 ISIMIP3b, group III simulations where the associated Direct Human Forcings (DHF) are not
1372 held constant at 2015 levels but are projected into the future in line with i) the population
1373 growth and economic development associated with the considered Shared Socioeconomic
1374 Pathways (SSPs) and mitigation measures required to reach the prescribed levels of
1375 climate forcings associated with the climate projections ('no adaptation' experiments) and
1376 ii) additionally accounting for the impacts of climate change ('adaptation' experiments).
1377 The collection of the associated DHF will be described in a separate paper.

1379 **Code and data availability.** The two versions of the downscaling and bias-adjustment
1380 algorithms that have been used to generate the data in Figure 4 and 5 are openly
1381 available (v1.0.0 at <https://zenodo.org/records/2586869> and v2.5.2 at
1382 <https://zenodo.org/records/6344911>). The data to reproduce behind Figures 3, 4 and 5 is
1383 openly accessible at <https://zenodo.org/records/17990574> (Quesada-Chacón, 2025). See
1384 Table 4 for detailed references for the ESM simulations used in ISIMIP3b. Figure 2 has
1385 been created on January 24, 2020 with ESMValTool v2.0.0b2 (Andela et al., 2020b, 2020a;
1386 Righi et al., 2020) which is openly accessible on Zenodo at
1387 <https://doi.org/10.5281/zenodo.3759523>.

1388
1389 All generated ISIMIP3 climate-related forcing data described in this paper is publicly
1390 available at the ISIMIP data repository. The repository is hosted by the Potsdam Institute
1391 for Climate Impact Research (PIK) e.V. which is part of the TIB DOI Consortium ensuring
1392 persistent, FAIR-compliant data publication, by committing to adhering to the DataCite
1393 Consortium Agreement. This includes commitments to data persistence (§4 a.) as well as
1394 maintaining and updating metadata (§4 c.), which forbids “withdrawing content without
1395 posting a notification”. In compliance with these rules a system to document and trace
1396 back data issues has been implemented in the repository to comply with this requirement.
1397 Additionally, should PIK be unable to continue hosting the ISIMIP repository, it will take
1398 responsibility for coordinating a timely transfer of the full repository and its DOI
1399 infrastructure to an appropriate, trusted archive or institutional partner to ensure
1400 uninterrupted access and citation continuity. DOIs are used to refer to datasets in a
1401 persistent way. Whenever a dataset is replaced a copy is kept on tape, and a new DOI is
1402 issued, while the old DOI is kept online with information on how to retrieve the archived
1403 data. Whenever we need to replace datasets, we will create a new version of the DOI,
1404 marked by a version number at the end. This ensures that every DOI references exactly
1405 the datasets, which were public at the time of registration. Detailed information can be
1406 found in the ISIMIP terms of use at <https://www.isimip.org/gettingstarted/terms-of-use/>
1407 (ISIMIP terms of use, 2023).

1408 1409 **Author contributions**

1410 KF lead the project and developed the concept with contributions from JS, MM, CO, CPOR,
1411 SH, JLB, CSH, CMP, TDE, KOC, CN, RH, DPT, OM, SJC, JJ, SR, GL, SC, EB, AGS, NS, JC, SH, CB,
1412 AG, FL, SNG, HMS, FH, TH, RM, DP, WT, DMB, RL, AIA, MF, MB, RR, and IDG. JV, MB, JK,
1413 IDVDV, LN, IJS supported the quality control and curation of the climate-related forcing
1414 data and the protocol development together with the sectoral ISIMIP coordinators listed
1415 as co-authors. SL developed the method and generated the downscaled and bias-adjusted

1416 atmospheric climate forcing data. MM and ST provided the description of the approach to
1417 generate the coastal water level data. ML provided the description of the method to bias-
1418 adjust the global oceanic forcings. TV, DQC, CYL, SJC, and KE provided TC data. JOK and AK
1419 provided the future lightning data. KF prepared the manuscript with contributions from all
1420 co-authors.

1421

1422 **Competing interests**

1423 At least one of the (co-)authors is a member of the editorial board of GMD

1424

1425 **Acknowledgements**

1426 This article is based upon work from COST Action CA19139 PROCLIAS (PROcess-based
1427 models for CLimate Impact Attribution across Sectors), supported by COST (European
1428 Cooperation in Science and Technology; <https://www.cost.eu>). SL received funding from
1429 the German Research Foundation (DFG, project number 427397136). MB acknowledges
1430 funding from the BELSPO STEREO IV project SR/00/414. SC, AGS, MB and NS acknowledge
1431 funding through NERC NE/V01854X/1 (MOTHERSHIP). This research has received funding
1432 from the German Federal Ministry of Education and Research (BMBF) under the research
1433 projects QUIDIC (grant agreement no. 01LP1907A) and ISI-Access (16QK05), from the
1434 Horizon 2020 Framework Programme of the European Union under the projects RECEIPT
1435 (grant agreement no. 820712) [and from the Horizon Europe research and innovation
1436 programme under grant agreement No 101135481 \(COMPASS\)](#). C.-Y. L is supported by
1437 Palisades Geophysical Institute (PGI) Young Scientist Award. KOC acknowledges support
1438 from the National Research Foundation of South Africa (grant 136481) and the resources
1439 from the Cluster for High Performance Computing-CSIR. FL is supported by the National
1440 Key Research and Development Program of China (2022YFE0106500). DPT acknowledges
1441 funding from the Jarislowsky Foundation and NSERC. IDG acknowledges funding of the
1442 European Research Council (ERC Starting Grant, GROW-101041110). [This work used
1443 resources of the Deutsches Klimarechenzentrum \(DKRZ\) granted by its Scientific Steering
1444 Committee \(WLA\) under project ID bb0820.](#)

1445

1446

1447

1448

1449

1450 **References**

- 1451 Adler, R. F., Huffman, G. J., Chang, A., Ferraro, R., Xie, P.-P., Janowiak, J., Rudolf, B.,
1452 Schneider, U., Curtis, S., Bolvin, D., Gruber, A., Susskind, J., Arkin, P., & Nelkin, E. (2003).
1453 The Version-2 Global Precipitation Climatology Project (GPCP) Monthly Precipitation
1454 Analysis (1979–Present). *Journal of Hydrometeorology*, 4(6), 1147–1167.
1455 [https://doi.org/10.1175/1525-7541\(2003\)004<1147:TVGPCP>2.0.CO;2](https://doi.org/10.1175/1525-7541(2003)004<1147:TVGPCP>2.0.CO;2)
- 1456 Andela, B., Broetz, B., de Mora, L., Drost, N., Eyring, V., Koldunov, N., Lauer, A., Mueller, B.,
1457 Predoi, V., Righi, M., Schlund, M., Vegas-Regidor, J., Zimmermann, K., Adeniyi, K.,
1458 Arnone, E., Bellprat, O., Berg, P., Bock, L., Caron, L.-P., ... Weigel, K. (2020b).
1459 *ESMValTool*. <https://doi.org/10.5281/zenodo.3970975>
- 1460 Andela, B., Broetz, B., Drost, N., Eyring, V., Koldunov, N., Lauer, A., Predoi, V., Righi, M.,
1461 Schlund, M., Zimmermann, K., Bock, L., Diblen, F., Dreyer, L., Earnshaw, P., Hassler, B.,
1462 & Little, B. (2020a). *ESMValCore*. <https://doi.org/10.5281/zenodo.3952695>
- 1463 Barrier, N., Lengaigne, M., Rault, J., Person, R., Ethé, C., Aumont, O., & Maury, O. (2023).
1464 Mechanisms underlying the epipelagic ecosystem response to ENSO in the equatorial
1465 Pacific ocean. *Progress in Oceanography*, 213, 103002.
1466 <https://doi.org/10.1016/j.pocean.2023.103002>
- 1467 Bock, L., & Lauer, A. (2024). Cloud properties and their projected changes in CMIP models
1468 with low to high climate sensitivity. *Atmospheric Chemistry and Physics*, 24(3), 1587–
1469 1605. <https://doi.org/10.5194/acp-24-1587-2024>
- 1470 Bock, L., Lauer, A., Schlund, M., Barreiro, M., Bellouin, N., Jones, C., Meehl, G. A., Predoi, V.,

1471 Roberts, M. J., & Eyring, V. (2020). Quantifying progress across different CMIP phases
1472 with the ESMValTool. *Journal of Geophysical Research*, 125(21).
1473 <https://doi.org/10.1029/2019jd032321>

1474 Boucher, O., Denvil, S., Levavasseur, G., Cozic, A., Caubel, A., Foujols, M.-A., Meurdesoif, Y.,
1475 Cadule, P., Devilliers, M., Dupont, E., & Lurton, T. (2019). *IPSL IPSL-CM6A-LR model*
1476 *output prepared for CMIP6 ScenarioMIP* [Dataset]. Earth System Grid Federation.
1477 <https://doi.org/10.22033/ESGF/CMIP6.1532>

1478 Boucher, O., Denvil, S., Levavasseur, G., Cozic, A., Caubel, A., Foujols, M.-A., Meurdesoif, Y.,
1479 Cadule, P., Devilliers, M., Ghattas, J., Lebas, N., Lurton, T., Mellul, L., Musat, I., Mignot,
1480 J., & Cheruy, F. (2018). *IPSL IPSL-CM6A-LR model output prepared for CMIP6 CMIP*
1481 [Dataset]. Earth System Grid Federation. <https://doi.org/10.22033/ESGF/CMIP6.1534>

1482 Boucher, O., Servonnat, J., Albright, A. L., Aumont, O., Balkanski, Y., Bastrikov, V., Bekki, S.,
1483 Bonnet, R., Bony, S., Bopp, L., Braconnot, P., Brockmann, P., Cadule, P., Caubel, A.,
1484 Cheruy, F., Codron, F., Cozic, A., Cugnet, D., D'Andrea, F., ... Vuichard, N. (2020).
1485 Presentation and evaluation of the IPSL-CM6A-LR climate model. *Journal of Advances in*
1486 *Modeling Earth Systems*, 12(7). <https://doi.org/10.1029/2019ms002010>

1487 Büchner, M. (2024). *ISIMIP3b ocean input data* [Dataset]. ISIMIP Repository.
1488 <https://doi.org/10.48364/ISIMIP.575744.5>

1489 Büchner, M., & Reyer, C. (2022). *ISIMIP3b atmospheric composition input data* [Dataset].
1490 ISIMIP Repository. <https://doi.org/10.48364/ISIMIP.482153.1>

1491 Buck, A. L. (1981). New Equations for Computing Vapor Pressure and Enhancement Factor.

1492 *Journal of Applied Meteorology and Climatology*, 20(12), 1527–1532.

1493 [https://doi.org/10.1175/1520-0450\(1981\)020<1527:NEFCVP>2.0.CO;2](https://doi.org/10.1175/1520-0450(1981)020<1527:NEFCVP>2.0.CO;2)

1494 Camargo, S. J., Tippett, M. K., Sobel, A. H., Vecchi, G. A., & Zhao, M. (2014). Testing the
1495 Performance of Tropical Cyclone Genesis Indices in Future Climates Using the HiRAM
1496 Model. *Journal of Climate*, 27(24), 9171–9196. [https://doi.org/10.1175/JCLI-D-13-](https://doi.org/10.1175/JCLI-D-13-00505.1)
1497 00505.1

1498 Cannon, A. J. (2018). Multivariate quantile mapping bias correction: an N-dimensional
1499 probability density function transform for climate model simulations of multiple
1500 variables. *Climate Dynamics*, 50(1), 31–49. <https://doi.org/10.1007/s00382-017-3580-6>

1501 Cecil, D. (2006). *LIS/OTD 0.5 Degree High Resolution Monthly Climatology (HRMC)* [Dataset].
1502 NASA Global Hydrometeorology Resource Center DAAC.
1503 <https://doi.org/10.5067/LIS/LIS-OTD/DATA303>

1504 Cucchi, M., Weedon, G. P., Amici, A., Bellouin, N., Lange, S., Müller Schmied, H., Hersbach,
1505 H., & Buontempo, C. (2020). WFDE5: bias-adjusted ERA5 reanalysis data for impact
1506 studies. *Earth System Science Data*, 12(3), 2097–2120. [https://doi.org/10.5194/essd-12-](https://doi.org/10.5194/essd-12-2097-2020)
1507 2097-2020

1508 Dunne, J. P., Horowitz, L. W., Adcroft, A. J., Ginoux, P., Held, I. M., John, J. G., Krasting, J. P.,
1509 Malyshev, S., Naik, V., Paulot, F., Shevliakova, E., Stock, C. A., Zadeh, N., Balaji, V.,
1510 Blanton, C., Dunne, K. A., Dupuis, C., Durachta, J., Dussin, R., ... Zhao, M. (2020). The
1511 GFDL earth system model version 4.1 (GFDL-ESM 4.1): Overall coupled model
1512 description and simulation characteristics. *Journal of Advances in Modeling Earth*

1513 *Systems*, 12(11). <https://doi.org/10.1029/2019ms002015>

1514 Durack, P. J. (n.d.). *CMIP6 source_id values*. Retrieved January 16, 2023, from [https://wcrp-](https://wcrp-cmip.github.io/CMIP6_CVs/docs/CMIP6_source_id.html)

1515 [cmip.github.io/CMIP6_CVs/docs/CMIP6_source_id.html](https://wcrp-cmip.github.io/CMIP6_CVs/docs/CMIP6_source_id.html)

1516 Eddy, T. D., Heneghan, R. F., Bryndum-Buchholz, A., Fulton, E. A., Harrison, C. S., Tittensor,
1517 D. P., Lotze, H. K., Ortega-Cisneros, K., Novaglio, C., Bianchi, D., Büchner, M., Bulman,
1518 C., Cheung, W. W. L., Christensen, V., Coll, M., Everett, J. D., Fierro-Arcos, D., Galbraith,
1519 E. D., Gascuel, D., ... Blanchard, J. L. (2025). Global and regional marine ecosystem
1520 models reveal key uncertainties in climate change projections. *Earth's Future*, 13(3).
1521 <https://doi.org/10.1029/2024ef005537>

1522 Emanuel, K., DesAutels, C., Holloway, C., & Korty, R. (2004). Environmental Control of
1523 Tropical Cyclone Intensity. *Journal of the Atmospheric Sciences*, 61(7), 843–858.
1524 [https://doi.org/10.1175/1520-0469\(2004\)061<0843:ECOTCI>2.0.CO;2](https://doi.org/10.1175/1520-0469(2004)061<0843:ECOTCI>2.0.CO;2)

1525 Emanuel, K., Quesada-Chacón, D., Novak, L., & Otto, C. (2025). *ISIMIP3b tropical cyclone*
1526 *tracks (MIT)* [Dataset]. ISIMIP Repository. <https://doi.org/10.48364/ISIMIP.682793>

1527 Emanuel, K., Sundararajan, R., & Williams, J. (2008). Hurricanes and Global Warming:
1528 Results from Downscaling IPCC AR4 Simulations. *Bulletin of the American*
1529 *Meteorological Society*, 89(3), 347–368. <https://doi.org/10.1175/BAMS-89-3-347>

1530 Eyring, V., Bony, S., Meehl, G. A., Senior, C. A., Stevens, B., Stouffer, R. J., & Taylor, K. E.
1531 (2016). Overview of the Coupled Model Intercomparison Project Phase 6 (CMIP6)
1532 experimental design and organization. *Geoscientific Model Development*, 9(5), 1937–
1533 1958. <https://doi.org/10.5194/gmd-9-1937-2016>

- 1534 Eyring, V., Gillett, N. P., Achuta Rao, K. M., Barimalala, R., Barreiro Parrillo, M., Bellouin, N.,
1535 V. Masson-Delmotte, P. Zhai, A. Pirani, S. L. Connors, C. Péan, S. Berger, &
1536 Intergovernmental Panel on Climate Change (IPCC). (2023). Human Influence on the
1537 Climate System. In *Climate Change 2021 – The Physical Science Basis: Working Group I*
1538 *Contribution to the Sixth Assessment Report of the Intergovernmental Panel on Climate*
1539 *Change* (pp. 423–552). Cambridge University Press.
1540 <https://doi.org/10.1017/9781009157896.005>
- 1541 Forster, P., Storelvmo, T., Armour, K., Collins, W., Dufresne, J.-L., Frame, D., Lunt, D. J.,
1542 Mauritsen, T., Palmer, Watanabe, M., Wild, M., & Zhang, H. (2021). The earth's energy
1543 budget, climate feedbacks and climate sensitivity. In *Climate Change 2021 – The*
1544 *Physical Science Basis* (pp. 923–1054). Cambridge University Press.
1545 <https://doi.org/10.1017/9781009157896.009>
- 1546 Fosu, B., Sobel, A., Camargo, S., Tippet, M., Hemmati, M., Bowen, S., & Bloemendaal, N.
1547 (2024). Assessing future tropical cyclone risk using downscaled 1 CMIP6 projections.
1548 *Journal of Catastrophe Risk and Resilience*, 2(1). <https://doi.org/10.63024/dpva-2pa1>
- 1549 Frieler, K., Lange, S., Piontek, F., Rey, C. P. O., Schewe, J., Warszawski, L., Zhao, F., Chini,
1550 L., Denvil, S., Emanuel, K., Geiger, T., Halladay, K., Hurtt, G., Mengel, M., Murakami, D.,
1551 Ostberg, S., Popp, A., Riva, R., Stevanovic, M., ... Yamagata, Y. (2017). Assessing the
1552 impacts of 1.5 °C global warming – simulation protocol of the Inter-Sectoral Impact
1553 Model Intercomparison Project (ISIMIP2b). *Geoscientific Model Development*, 10(12),
1554 4321–4345. <https://doi.org/10.5194/gmd-10-4321-2017>

1555 Frieler, K., Volkholz, J., Lange, S., Schewe, J., Mengel, M., del Rocío Rivas López, M., Otto, C.,
1556 Reyer, C. P. O., Karger, D. N., Malle, J. T., Treu, S., Menz, C., Blanchard, J. L., Harrison, C.
1557 S., Petrik, C. M., Eddy, T. D., Ortega-Cisneros, K., Novaglio, C., Rousseau, Y., ...
1558 Bechtold, M. (2024). Scenario setup and forcing data for impact model evaluation and
1559 impact attribution within the third round of the Inter-Sectoral Impact Model
1560 Intercomparison Project (ISIMIP3a). *Geoscientific Model Development*, 17(1), 1–51.
1561 <https://doi.org/10.5194/gmd-17-1-2024>

1562 Geiger, T., Gütschow, J., Bresch, D. N., Emanuel, K., & Frieler, K. (2021). Double benefit of
1563 limiting global warming for tropical cyclone exposure. *Nature Climate Change*, 11(10),
1564 861–866. <https://doi.org/10.1038/s41558-021-01157-9>

1565 Gennaretti, F., Sangelantoni, L., & Grenier, P. (2015). Toward daily climate scenarios for
1566 Canadian Arctic coastal zones with more realistic temperature-precipitation
1567 interdependence. *JGR: Atmospheres*, 120(23), 11,862–11,877.
1568 <https://doi.org/10.1002/2015JD023890>

1569 Gillett, N. P., Shiogama, H., Funke, B., Hegerl, G., Knutti, R., Matthes, K., Santer, B. D.,
1570 Stone, D., & Tebaldi, C. (2016). The detection and Attribution Model Intercomparison
1571 Project (DAMIP v1.0) contribution to CMIP6. *Geoscientific Model Development*, 9(10),
1572 3685–3697. <https://doi.org/10.5194/gmd-9-3685-2016>

1573 Good, P., Sellar, A., Tang, Y., Rumbold, S., Ellis, R., Kelley, D., Kuhlbrodt, T., & Walton, J.
1574 (2019). *MOHC UKESM1.0-LL model output prepared for CMIP6 ScenarioMIP* [Dataset].
1575 Earth System Grid Federation. <https://doi.org/10.22033/ESGF/CMIP6.1567>

- 1576 Gregory, J. M., Griffies, S. M., Hughes, C. W., Lowe, J. A., Church, J. A., Fukimori, I., Gomez,
1577 N., Kopp, R. E., Landerer, F., Cozannet, G. L., Ponte, R. M., Stammer, D., Tamisiea, M. E.,
1578 & van de Wal, R. S. W. (2019). Concepts and terminology for sea level: Mean, variability
1579 and change, both local and global. *Surveys in Geophysics*, 40(6), 1251–1289.
1580 <https://doi.org/10.1007/s10712-019-09525-z>
- 1581 Grenier, P. (2018). Two Types of Physical Inconsistency to Avoid with Univariate Quantile
1582 Mapping: A Case Study over North America Concerning Relative Humidity and Its
1583 Parent Variables. *Journal of Applied Meteorology and Climatology*, 57(2), 347–364.
1584 <https://doi.org/10.1175/JAMC-D-17-0177.1>
- 1585 Haerter, J. O., Hagemann, S., Moseley, C., & Piani, C. (2011). Climate model bias correction
1586 and the role of timescales. *Hydrology and Earth System Sciences*, 15(3), 1065–1079.
1587 <https://doi.org/10.5194/hess-15-1065-2011>
- 1588 Hausfather, Z., & Peters, G. P. (2020, January 29). *Emissions – the “business as usual” story is*
1589 *misleading*. Nature Publishing Group UK. <https://doi.org/10.1038/d41586-020-00177-3>
- 1590 Hersbach, H., Bell, B., Berrisford, P., Hirahara, S., Horányi, A., Muñoz-Sabater, J., Nicolas, J.,
1591 Peubey, C., Radu, R., Schepers, D., Simmons, A., Soci, C., Abdalla, S., Abellan, X.,
1592 Balsamo, G., Bechtold, P., Biavati, G., Bidlot, J., Bonavita, M., ... Jean-Noël Thépaut.
1593 (2020). The ERA5 global reanalysis. *Quarterly Journal of the Royal Meteorological Society*,
1594 146(730), 1999–2049. <https://doi.org/10.1002/qj.3803>
- 1595 Holland. (1980). An Analytic Model of the Wind and Pressure Profiles in Hurricanes, *Mon.*
1596 *Mon. Weather Rev*, 108, 1212–1218.

1597 Holland. (2008). A revised hurricane pressure–wind model. *Monthly Weather Review*, 136(9),
1598 3432–3445. <https://doi.org/10.1175/2008mwr2395.1>

1599 *ISIMIP3b simulation protocol*. (2026). <https://protocol.isimip.org/#/ISIMIP3b>

1600 *ISIMIP Repository*. (2020). <https://data.isimip.org>

1601 Jägermeyr, J., Müller, C., Ruane, A. C., Elliott, J., Balkovic, J., Castillo, O., Faye, B., Foster, I.,
1602 Folberth, C., Franke, J. A., Fuchs, K., Guarin, J. R., Heinke, J., Hoogenboom, G., Iizumi, T.,
1603 Jain, A. K., Kelly, D., Khabarov, N., Lange, S., ... Rosenzweig, C. (2021). Climate impacts
1604 on global agriculture emerge earlier in new generation of climate and crop models.
1605 *Nature Food*, 2(11), 873–885. <https://doi.org/10.1038/s43016-021-00400-y>

1606 John, J. G., Blanton, C., McHugh, C., Radhakrishnan, A., Rand, K., Vahlenkamp, H., Wilson,
1607 C., Zadeh, N. T., Dunne, J. P., Dussin, R., Horowitz, L. W., Krasting, J. P., Lin, P.,
1608 Malyshev, S., Naik, V., Ploshay, J., Shevliakova, E., Silvers, L., Stock, C., ... Zeng, Y. (2018).
1609 *NOAA-GFDL GFDL-ESM4 model output prepared for CMIP6 ScenarioMIP* [Dataset]. Earth
1610 System Grid Federation. <https://doi.org/10.22033/ESGF/CMIP6.1414>

1611 Jungclaus, J., Bittner, M., Wieners, K.-H., Wachsman, F., Schupfner, M., Legutke, S.,
1612 Giorgetta, M., Reick, C., Gayler, V., Haak, H., de Vrese, P., Raddatz, T., Esch, M.,
1613 Mauritsen, T., von Storch, J.-S., Behrens, J., Brovkin, V., Claussen, M., Crueger, T., ...
1614 Roeckner, E. (2019). *MPI-M MPIESM1.2-HR model output prepared for CMIP6 CMIP*
1615 [Dataset]. Earth System Grid Federation. <https://doi.org/10.22033/ESGF/CMIP6.741>

1616 Kaplan, J. O., Koch, A., & Lau, K. H.-K. (2023). *Estimated future global lightning strokes (2010-*
1617 *2100)*. <https://doi.org/10.5281/zenodo.7511843>

- 1618 Kaplan, J. O., & Lau, K. H.-K. (2021). The WGLC global gridded lightning climatology and
1619 time series. *Earth System Science Data*, 13(7), 3219–3237. [https://doi.org/10.5194/essd-](https://doi.org/10.5194/essd-13-3219-2021)
1620 13-3219-2021
- 1621 Kaplan, J. O., & Lau, K. H.-K. (2022). World Wide Lightning Location Network (WWLLN)
1622 Global Lightning Climatology (WGLC) and time series, 2022 update. *Earth System*
1623 *Science Data*, 14(12), 5665–5670. <https://doi.org/10.5194/essd-14-5665-2022>
- 1624 Krasting, J. P., John, J. G., Blanton, C., McHugh, C., Nikonov, S., Radhakrishnan, A., Rand, K.,
1625 Zadeh, N. T., Balaji, V., Durachta, J., Dupuis, C., Menzel, R., Robinson, T., Underwood,
1626 S., Vahlenkamp, H., Dunne, K. A., Gauthier, P. P. G., Ginoux, P., Griffies, S. M., ... Zhao,
1627 M. (2018). *NOAA-GFDL GFDL-ESM4 model output prepared for CMIP6 CMIP* [Dataset].
1628 Earth System Grid Federation. <https://doi.org/10.22033/ESGF/CMIP6.1407>
- 1629 Lange, S. (2017). *ISIMIP2b Bias-Correction Code*. <https://doi.org/10.5281/zenodo.1069050>
- 1630 Lange, S. (2018). Bias correction of surface downwelling longwave and shortwave
1631 radiation for the EWEMBI dataset. *Earth System Dynamics*, 9(2), 627–645.
1632 <https://doi.org/10.5194/esd-9-627-2018>
- 1633 Lange, S. (2019a). *Earth2Observe, WFDEI and ERA-interim data merged and bias-corrected for*
1634 *ISIMIP (EWEMBI)* [Dataset]. <https://doi.org/10.5880/pik.2019.004>
- 1635 Lange, S. (2019b). Trend-preserving bias adjustment and statistical downscaling with
1636 ISIMIP3BASD (v1.0). *Geoscientific Model Development*, 12(7), 3055–3070.
1637 <https://doi.org/10.5194/gmd-12-3055-2019>
- 1638 Lange, S. (2021a). *ISIMIP3BASD*. <https://doi.org/10.5281/zenodo.4686991>

1639 Lange, S. (2021b). *ISIMIP3b bias adjustment fact sheet*.
1640 https://www.isimip.org/documents/413/ISIMIP3b_bias_adjustment_fact_sheet_Gnsz7C
1641 [O.pdf](#)

1642 Lange, S., & Büchner, M. (2021). *ISIMIP3b bias-adjusted atmospheric climate input data*
1643 [Dataset]. ISIMIP Repository. <https://doi.org/10.48364/ISIMIP.842396.1>

1644 Lange, S., Menz, C., Gleixner, S., Cucchi, M., Weedon, G. P., Amici, A., Bellouin, N., Schmied,
1645 H. M., Hersbach, H., Buontempo, C., & Cagnazzo, C. (2021). *WFDE5 over land merged*
1646 *with ERA5 over the ocean (W5E5 v2.0)* [Dataset]. ISIMIP Repository.
1647 <https://doi.org/10.48364/ISIMIP.342217>

1648 Lange, S., Quesada-Chacón, D., & Büchner, M. (2023). *Secondary ISIMIP3b bias-adjusted*
1649 *atmospheric climate input data* [Dataset]. ISIMIP Repository.
1650 <https://doi.org/10.48364/ISIMIP.581124.3>

1651 Lan, X., Tans, P., & Thoning, K. W. (2023). *Trends in globally-averaged CO2 determined from*
1652 *NOAA Global Monitoring Laboratory measurements. Version 2023-01 NOAA/GML*
1653 [Dataset]. <https://gml.noaa.gov/ccgg/trends/>

1654 Large W. G., A. S. G. Y. (2004). *Diurnal to decadal global forcing for ocean and sea ice models:*
1655 *the data sets and flux climatologies* (No. NCAR/TN460+STR). CGD Division of the
1656 National Centre for Atmospheric Research (NCAR).
1657 [https://www.researchgate.net/profile/Stephen-Yeager/publication/281588002_Diurnal](https://www.researchgate.net/profile/Stephen-Yeager/publication/281588002_Diurnal_to_Decadal_Global_Forcing_for_Ocean_and_Sea-Ice_Models_The_Data_Sets_and_Flux_Climatologies/links/)
1658 [_to_Decadal_Global_Forcing_for_Ocean_and_Sea-](#)
1659 [Ice_Models_The_Data_Sets_and_Flux_Climatologies/links/](#)

1660 55eede7108ae199d47bfaf41/Diurnal-to-Decadal-Global-Forcing-for-Ocean-and-Sea-
1661 Ice-Models-The-Data-Sets-and-Flux-Climatologies.pdf

1662 Lee, C.-Y., Camargo, S. J., Sobel, A. H., & Tippett, M. K. (2020). Statistical–Dynamical
1663 Downscaling Projections of Tropical Cyclone Activity in a Warming Climate: Two
1664 Diverging Genesis Scenarios. *Journal of Climate*, 33(11), 4815–4834.
1665 <https://doi.org/10.1175/JCLI-D-19-0452.1>

1666 Lee, C.-Y., Camargo, S. J., Sobel, A., Tippett, M. K., Quesada-Chacón, D., Büchner, M., Novak,
1667 L., & Otto, C. (2025). *ISIMIP3b tropical cyclone tracks (CHAZ)* [Dataset]. ISIMIP
1668 Repository. <https://doi.org/10.48364/ISIMIP.808980>

1669 Lee, C.-Y., Tippett, M. K., Camargo, S. J., & Sobel, A. H. (2015). Probabilistic Multiple Linear
1670 Regression Modeling for Tropical Cyclone Intensity. *Monthly Weather Review*, 143(3),
1671 933–954. <https://doi.org/10.1175/MWR-D-14-00171.1>

1672 Lee, C.-Y., Tippett, M. K., Sobel, A. H., & Camargo, S. J. (2016). Rapid intensification and the
1673 bimodal distribution of tropical cyclone intensity. *Nature Communications*, 7, 10625.
1674 <https://doi.org/10.1038/ncomms10625>

1675 Lee, C.-Y., Tippett, M. K., Sobel, A. H., & Camargo, S. J. (2018). An environmentally forced
1676 tropical cyclone hazard model. *Journal of Advances in Modeling Earth Systems*, 10(1),
1677 223–241. <https://doi.org/10.1002/2017ms001186>

1678 Lengaigne, M., Pang, S., Silvy, Y., Danielli, V., Gopika, S., Sadhvi, K., Dutheil, C., Rousset, C.,
1679 Ethé, C., Person, R., Madec, G., Barrier, N., Maury, O., Dalaut, L., Menkes, C., Nicol, S.,
1680 Gorgues, T., Melet, A., & Guihou, K. (2025). Vialard: An ocean modelling framework for

1681 mitigating oceanic projections from global climate models present-day biases. In
1682 *Earth future*.

1683 Liang, Y., Gillett, N. P., & Monahan, A. H. (2024). Accounting for Pacific climate variability
1684 increases projected global warming. *Nature Climate Change*, 14(6), 608–614.
1685 <https://doi.org/10.1038/s41558-024-02017-y>

1686 Li, G., Xie, S.-P., Du, Y., & Luo, Y. (2016). Effects of excessive equatorial cold tongue bias on
1687 the projections of tropical Pacific climate change. Part I: the warming pattern in CMIP5
1688 multi-model ensemble. *Climate Dynamics*, 47(12), 3817–3831.
1689 <https://doi.org/10.1007/s00382-016-3043-5>

1690 Madec, G. (2015). NEMO ocean engine, Version 3.6 stable Note du Pole de modelisation de
1691 l'Institut Pierre-Simon Laplace, vol. 27. *IPSL, Paris: France*.

1692 Maraun, D. (2013). Bias Correction, Quantile Mapping, and Downscaling: Revisiting the
1693 Inflation Issue. *Journal of Climate*, 26(6), 2137–2143. [https://doi.org/10.1175/JCLI-D-12-](https://doi.org/10.1175/JCLI-D-12-00821.1)
1694 [00821.1](https://doi.org/10.1175/JCLI-D-12-00821.1)

1695 Mauritsen, T., Bader, J., Becker, T., Behrens, J., Bittner, M., Brokopf, R., Brovkin, V.,
1696 Claussen, M., Crueger, T., Esch, M., Fast, I., Fiedler, S., Fläschner, D., Gayler, V.,
1697 Giorgetta, M., Goll, D. S., Haak, H., Hagemann, S., Hedemann, C., ... Roeckner, E.
1698 (2019). Developments in the MPI-M Earth System Model version 1.2 (MPI-ESM1.2) and
1699 Its Response to Increasing CO₂. *Journal of Advances in Modeling Earth Systems*, 11(4),
1700 998–1038. <https://doi.org/10.1029/2018MS001400>

1701 Meehl, G. A., Senior, C. A., Eyring, V., Flato, G., Lamarque, J.-F., Stouffer, R. J., Taylor, K. E., &

1702 Schlund, M. (2020). Context for interpreting equilibrium climate sensitivity and
1703 transient climate response from the CMIP6 Earth system models. *Science Advances*,
1704 6(26), eaba1981. <https://doi.org/10.1126/sciadv.aba1981>

1705 Meiler, S., Kropf, C. M., McCaughey, J. W., Lee, C.-Y., Camargo, S. J., Sobel, A. H.,
1706 Bloemendaal, N., Emanuel, K., & Bresch, D. N. (2025). Navigating and attributing
1707 uncertainty in future tropical cyclone risk estimates. *Science Advances*, 11(16),
1708 eadn4607. <https://doi.org/10.1126/sciadv.adn4607>

1709 Meiler, S., Vogt, T., Bloemendaal, N., Ciullo, A., Lee, C.-Y., Camargo, S. J., Emanuel, K., &
1710 Bresch, D. N. (2022). Intercomparison of regional loss estimates from global synthetic
1711 tropical cyclone models. *Nature Communications*, 13(1), 6156.
1712 <https://doi.org/10.1038/s41467-022-33918-1>

1713 Meinshausen, M., Nicholls, Z. R. J., Lewis, J., Gidden, M. J., Vogel, E., Freund, M., Beyerle, U.,
1714 Gessner, C., Nauels, A., Bauer, N., Canadell, J. G., Daniel, J. S., John, A., Krummel, P. B.,
1715 Luderer, G., Meinshausen, N., Montzka, S. A., Rayner, P. J., Reimann, S., ... Wang, R. H.
1716 J. (2020). The shared socio-economic pathway (SSP) greenhouse gas concentrations
1717 and their extensions to 2500. *Geoscientific Model Development*, 13(8), 3571–3605.
1718 <https://doi.org/10.5194/gmd-13-3571-2020>

1719 Meinshausen, M., Smith, S. J., Calvin, K., Daniel, J. S., Kainuma, M. L. T., Lamarque, J.-F.,
1720 Matsumoto, K., Montzka, S. A., Raper, S. C. B., Riahi, K., Thomson, A., Velders, G. J. M.,
1721 & van Vuuren, D. P. P. (2011). The RCP greenhouse gas concentrations and their
1722 extensions from 1765 to 2300. *Climatic Change*, 109(1), 213.

1723 <https://doi.org/10.1007/s10584-011-0156-z>

1724 Meinshausen, M., Vogel, E., Nauels, A., Lorbacher, K., Meinshausen, N., Etheridge, D. M.,
1725 Fraser, P. J., Montzka, S. A., Rayner, P. J., Trudinger, C. M., Krummel, P. B., Beyerle, U.,
1726 Canadell, J. G., Daniel, J. S., Enting, I. G., Law, R. M., Lunder, C. R., O'Doherty, S., Prinn,
1727 R. G., ... Weiss, R. (2017). Historical greenhouse gas concentrations for climate
1728 modelling (CMIP6). *Geoscientific Model Development*, 10(5), 2057–2116.
1729 <https://doi.org/10.5194/gmd-10-2057-2017>

1730 Muis, S., Aerts, J. C. J. H., Á. Antolínez, J. A., Dullaart, J. C., Duong, T. M., Erikson, L.,
1731 Haarsma, R. J., Apecechea, M. I., Mengel, M., Le Bars, D., O'Neill, A., Ranasinghe, R.,
1732 Roberts, M. J., Verlaan, M., Ward, P. J., & Yan, K. (2023). Global projections of storm
1733 surges using high-resolution CMIP6 climate models. *Earth's Future*, 11(9).
1734 <https://doi.org/10.1029/2023ef003479>

1735 Muis, S., Apecechea, M. I., Dullaart, J., de Lima Rego, J., Madsen, K. S., Su, J., Yan, K., &
1736 Verlaan, M. (2020). A High-Resolution Global Dataset of Extreme Sea Levels, Tides, and
1737 Storm Surges, Including Future Projections. *Frontiers in Marine Science*, 7.
1738 <https://doi.org/10.3389/fmars.2020.00263>

1739 O'Neill, B. C., Tebaldi, C., van Vuuren, D. P., Eyring, V., Friedlingstein, P., Hurtt, G., Knutti, R.,
1740 Kriegler, E., Lamarque, J.-F., Lowe, J., Meehl, G. A., Moss, R., Riahi, K., & Sanderson, B.
1741 M. (2016). The Scenario Model Intercomparison Project (ScenarioMIP) for CMIP6.
1742 *Geoscientific Model Development*, 9(9), 3461–3482. [https://doi.org/10.5194/gmd-9-3461-](https://doi.org/10.5194/gmd-9-3461-2016)
1743 2016

1744 O'Neill, B., van Aalst, M., Z., Z. I., Berrang Ford, L., Bhadwal, S., Buhaug, H., Diaz, D., Frieler,
1745 K., Garschagen, M., Magnan, A., Midgley, G., Mirzabaev, A., Thomas, A., & Warren, R.
1746 (2022). Climate Change 2022: Impacts, Adaptation and Vulnerability. Key Risks Across
1747 Sectors and Regions. In H.-O. Pörtner, D. C. Roberts, M. Tignor, E. S. Poloczanska, K.
1748 Mintenbeck, A. Alegría, M. Craig, S. Langsdorf, S. Löschke, V. Möller, A. Okem, & B.
1749 Rama (Eds.), *Contribution of Working Group II to the Sixth Assessment Report of the*
1750 *Intergovernmental Panel on Climate Change* (pp. 2411–2538). Cambridge University
1751 Press. <https://doi.org/10.1017/9781009325844.025>

1752 Ortega-Cisneros, K., Fierros-Arcos, D., Lindmark, M., Novaglio, C., Woodworth-Jefcoats, P.,
1753 Eddy, T. D., Coll, M., Fulton, E., Oliveros-Ramos, R., Reum, J., Shin, Y.-J., Bulman, C.,
1754 Capitani, L., Datta, S., Murphy, K., Rogers, A., Shannon, L., Whitehouse, G. A., Adekoya,
1755 E., ... Blanchard, J. L. (2025). An integrated global-to-regional scale workflow for
1756 simulating climate change impacts on marine ecosystems. *Earth's Future*, 13(2).
1757 <https://doi.org/10.1029/2024ef004826>

1758 Perrette, M., & Mengel, M. (2025). Relative sea level projections constrained by historical
1759 trends at tide gauge sites. *Science Advances*, 11(40), eado4506.
1760 <https://doi.org/10.1126/sciadv.ado4506>

1761 Quesada-Chacón, D. (2025). *Data for Figure 3, 4 and 5 of ISIMIP3b, group I + II protocol paper*
1762 [Dataset]. Zenodo. <https://doi.org/10.5281/ZENODO.17990574>

1763 Quesada-Chacón, D., Hamester, L., & Vogt, T. (2025b). *Code to generate the rain and*
1764 *windfields presented in the ISIMIP3b protocol paper*. Zenodo.

1765 <https://doi.org/10.5281/ZENODO.17570410>

1766 Quesada-Chacón, D., Novak, L., Hamester, L., & Otto, C. (2025a). *ISIMIP3b tropical cyclone*
1767 *wind and rain fields (MIT)* [Dataset]. ISIMIP Repository.
1768 <https://doi.org/10.48364/ISIMIP.779038>

1769 Righi, M., Andela, B., Eyring, V., Lauer, A., Predoi, V., Schlund, M., Vegas-Regidor, J., Bock,
1770 L., Brötz, B., de Mora, L., Diblen, F., Dreyer, L., Drost, N., Earnshaw, P., Hassler, B.,
1771 Koldunov, N., Little, B., Loosveldt Tomas, S., & Zimmermann, K. (2020). Earth System
1772 Model Evaluation Tool (ESMValTool) v2.0 – technical overview. *Geoscientific Model*
1773 *Development*, 13(3), 1179–1199. <https://doi.org/10.5194/gmd-13-1179-2020>

1774 Ruosteenoja, K., Jylhä, K., Räisänen, J., & Mäkelä, A. (2017). Surface air relative humidities
1775 spuriously exceeding 100% in CMIP5 model output and their impact on future
1776 projections. *JGR Atmospheres*, 122(18), 9557–9568.
1777 <https://doi.org/10.1002/2017JD026909>

1778 Ruosteenoja, K., Jylhä, K., Räisänen, J., & Mäkelä, A. (2018). Reply to comment by genthon
1779 et al. On “surface air relative humidities spuriously exceeding 100% in CMIP5 model
1780 output and their impact on future projections.” *Journal of Geophysical Research*,
1781 123(16), 8728–8734. <https://doi.org/10.1029/2018jd028680>

1782 Schupfner, M., Wieners, K.-H., Wachsmann, F., Steger, C., Bittner, M., Jungclaus, J., Früh, B.,
1783 Pankatz, K., Giorgetta, M., Reick, C., Legutke, S., Esch, M., Gayler, V., Haak, H., de
1784 Vrese, P., Raddatz, T., Mauritsen, T., von Storch, J.-S., Behrens, J., ... Roeckner, E. (2019).
1785 *DKRZ MPI-ESM1.2-HR model output prepared for CMIP6 ScenarioMIP* [Dataset]. Earth

1786 System Grid Federation. <https://doi.org/10.22033/ESGF/CMIP6.2450>

1787 Séférian, R., Berthet, S., Yool, A., Palmiéri, J., Bopp, L., Tagliabue, A., Kwiatkowski, L.,
1788 Aumont, O., Christian, J., Dunne, J., Gehlen, M., Ilyina, T., John, J. G., Li, H., Long, M. C.,
1789 Luo, J. Y., Nakano, H., Romanou, A., Schwinger, J., ... Yamamoto, A. (2020). Tracking
1790 Improvement in Simulated Marine Biogeochemistry Between CMIP5 and CMIP6.
1791 *Current Climate Change Reports*, 6(3), 95–119. [https://doi.org/10.1007/s40641-020-](https://doi.org/10.1007/s40641-020-00160-0)
1792 00160-0

1793 Sellar, A. A., Jones, C. G., Mulcahy, J. P., Tang, Y., Yool, A., Wiltshire, A., O'Connor, F. M.,
1794 Stringer, M., Hill, R., Palmieri, J., Woodward, S., Mora, L., Kuhlbrodt, T., Rumbold, S. T.,
1795 Kelley, D. I., Ellis, R., Johnson, C. E., Walton, J., Abraham, N. L., ... Zerroukat, M. (2019).
1796 UKESM1: Description and evaluation of the U.k. earth system model. *Journal of*
1797 *Advances in Modeling Earth Systems*, 11(12), 4513–4558.
1798 <https://doi.org/10.1029/2019ms001739>

1799 Shakespeare, C. J., & Roderick, M. L. (2022). Diagnosing instantaneous forcing and
1800 feedbacks of downwelling longwave radiation at the surface: A simple methodology
1801 and its application to CMIP5 models. *Journal of Climate*, 35(12), 3785–3801.
1802 <https://doi.org/10.1175/jcli-d-21-0865.1>

1803 Shiogama, H., Fujimori, S., Hasegawa, T., Hayashi, M., Hirabayashi, Y., Ogura, T., Iizumi, T.,
1804 Takahashi, K., & Takemura, T. (2023). Important distinctiveness of SSP3–7.0 for use in
1805 impact assessments. *Nature Climate Change*, 13(12), 1276–1278.
1806 <https://doi.org/10.1038/s41558-023-01883-2>

- 1807 Sobel, A. H., Lee, C.-Y., Bowen, S. G., Camargo, S. J., Cane, M. A., Clement, A., Fosu, B., Hart,
1808 M., Reed, K. A., Seager, R., & Tippett, M. K. (2021). Near-term tropical cyclone risk and
1809 coupled Earth system model biases. *Proceedings of the National Academy of Sciences of
1810 the United States of America*, *120*(33), e2209631120.
1811 <https://doi.org/10.1073/pnas.2209631120>
- 1812 Sobel, A. H., Lee, C.-Y., Camargo, S. J., Mandli, K. T., Emanuel, K. A., Mukhopadhyay, P., &
1813 Mahakur, M. (2019). Tropical Cyclone Hazard to Mumbai in the Recent Historical
1814 Climate. *Monthly Weather Review*, *147*(7), 2355–2366. [https://doi.org/10.1175/MWR-D-
1815 18-0419.1](https://doi.org/10.1175/MWR-D-18-0419.1)
- 1816 Stewart, K. D., Kim, W. M., Urakawa, S., Hogg, A. M., Yeager, S., Tsujino, H., Nakano, H.,
1817 Kiss, A. E., & Danabasoglu, G. (2020). JRA55-do-based repeat year forcing datasets for
1818 driving ocean–sea-ice models. *Ocean Modelling*, *147*, 101557.
1819 <https://doi.org/10.1016/j.ocemod.2019.101557>
- 1820 Swaminathan, R., Schewe, J., Walton, J., Zimmermann, K., Jones, C., Betts, R. A., Burton, C.,
1821 Jones, C. D., Mengel, M., Reyer, C. P. O., Turner, A. G., & Weigel, K. (2024). Regional
1822 impacts poorly constrained by climate sensitivity. *Earth's Future*, *12*(12).
1823 <https://doi.org/10.1029/2024ef004901>
- 1824 Switanek, M. B., Troch, P. A., Castro, C. L., Leuprecht, A., Chang, H.-I., Mukherjee, R., &
1825 Demaria, E. M. C. (2017). Scaled distribution mapping: a bias correction method that
1826 preserves raw climate model projected changes. *Hydrology and Earth System Sciences*,
1827 *21*(6), 2649–2666. <https://doi.org/10.5194/hess-21-2649-2017>

- 1828 Tagliabue, A., Kwiatkowski, L., Bopp, L., Butenschön, M., Cheung, W., Lengaigne, M., &
1829 Vialard, J. (2021). Persistent Uncertainties in Ocean Net Primary Production Climate
1830 Change Projections at Regional Scales Raise Challenges for Assessing Impacts on
1831 Ecosystem Services. *Frontiers in Climate*, 3. <https://doi.org/10.3389/fclim.2021.738224>
- 1832 Tang, Y., Rumbold, S., Ellis, R., Kelley, D., Mulcahy, J., Sellar, A., Walton, J., & Jones, C. (2019).
1833 *MOHC UKESM1.0-LL model output prepared for CMIP6 CMIP* [Dataset]. Earth System Grid
1834 Federation. <https://doi.org/10.22033/ESGF/CMIP6.1569>
- 1835 Themeßl, M. J., Gobiet, A., & Heinrich, G. (2012). Empirical-statistical downscaling and error
1836 correction of regional climate models and its impact on the climate change signal.
1837 *Climatic Change*, 112(2), 449–468. <https://doi.org/10.1007/s10584-011-0224-4>
- 1838 Thrasher, B., Maurer, E. P., McKellar, C., & Duffy, P. B. (2012). Technical Note: Bias
1839 correcting climate model simulated daily temperature extremes with quantile
1840 mapping. *Hydrology and Earth System Sciences*, 16(9), 3309–3314.
1841 <https://doi.org/10.5194/hess-16-3309-2012>
- 1842 Tippett, M. K., Camargo, S. J., & Sobel, A. H. (2011). A Poisson Regression Index for Tropical
1843 Cyclone Genesis and the Role of Large-Scale Vorticity in Genesis. *Journal of Climate*,
1844 24(9), 2335–2357. <https://doi.org/10.1175/2010JCLI3811.1>
- 1845 Treu, S., Muis, S., Dangendorf, S., Wahl, T., Oelsmann, J., Heinicke, S., Frieler, K., & Mengel,
1846 M. (2023). Reconstruction of hourly coastal water levels and counterfactuals without
1847 sea level rise for impact attribution. In *Earth System Science Data Discussions*.
1848 <https://doi.org/10.5194/essd-2023-112>

1849 Tsujino, H., Urakawa, L. S., Griffies, S. M., Danabasoglu, G., Adcroft, A. J., Amaral, A. E.,
1850 Arsouze, T., Bentsen, M., Bernardello, R., Böning, C. W., Bozec, A., Chassignet, E. P.,
1851 Danilov, S., Dussin, R., Exarchou, E., Fogli, P. G., Fox-Kemper, B., Guo, C., Ilicak, M., ...
1852 Yu, Z. (2020). Evaluation of global ocean–sea-ice model simulations based on the
1853 experimental protocols of the Ocean Model Intercomparison Project phase 2 (OMIP-
1854 2). *Geoscientific Model Development*, 13(8), 3643–3708. [https://doi.org/10.5194/gmd-13-](https://doi.org/10.5194/gmd-13-3643-2020)
1855 3643-2020

1856 Tsujino, H., Urakawa, S., Nakano, H., Small, R. J., Kim, W. M., Yeager, S. G., Danabasoglu, G.,
1857 Suzuki, T., Bamber, J. L., Bentsen, M., Böning, C. W., Bozec, A., Chassignet, E. P.,
1858 Curchitser, E., Boeira Dias, F., Durack, P. J., Griffies, S. M., Harada, Y., Ilicak, M., ...
1859 Yamazaki, D. (2018). JRA-55 based surface dataset for driving ocean–sea-ice models
1860 (JRA55-do). *Ocean Modelling*, 130, 79–139.
1861 <https://doi.org/10.1016/j.ocemod.2018.07.002>

1862 Watanabe, M., Kang, S. M., Collins, M., Hwang, Y.-T., McGregor, S., & Stuecker, M. F. (2024).
1863 Possible shift in controls of the tropical Pacific surface warming pattern. *Nature*,
1864 630(8016), 315–324. <https://doi.org/10.1038/s41586-024-07452-7>

1865 Weedon, G. P., Gomes, S., Viterbo, P., Österle, H., Adam, J. C., Bellouin, N., Boucher, O., &
1866 Best, M. (2010). *The watch forcing data 1958-2001: a meteorological forcing data set for*
1867 *land surface- and hydrological-models*. 41.
1868 https://publications.pik-potsdam.de/pubman/item/item_16400

1869 Woodworth-Jefcoats, P. (2022). *therMizer-FishMIP-2022-HI: Code and data for FishMIP 2022*

1870 *ISIMIP 3a - Hawaii longline fishing ground regional model*. Github.
1871 <https://github.com/pwoodworth-jefcoats/therMizer-FishMIP-2022-HI>

1872 Yukimoto, S., Kawai, H., Koshiro, T., Oshima, N., Yoshida, K., Urakawa, S., Tsujino, H.,
1873 Deushi, M., Tanaka, T., Hosaka, M., Yabu, S., Yoshimura, H., Shindo, E., Mizuta, R.,
1874 Obata, A., Adachi, Y., & Ishii, M. (2019). The Meteorological Research Institute Earth
1875 System Model Version 2.0, MRI-ESM2.0: Description and Basic Evaluation of the
1876 Physical Component. *Journal of the Meteorological Society of Japan. Ser. II*, 97(5), 931–
1877 965. <https://doi.org/10.2151/jmsj.2019-051>

1878 Yukimoto, S., Koshiro, T., Kawai, H., Oshima, N., Yoshida, K., Urakawa, S., Tsujino, H.,
1879 Deushi, M., Tanaka, T., Hosaka, M., Yoshimura, H., Shindo, E., Mizuta, R., Ishii, M.,
1880 Obata, A., & Adachi, Y. (2019a). *MRI MRI-ESM2.0 model output prepared for CMIP6 CMIP*
1881 [Dataset]. Earth System Grid Federation. <https://doi.org/10.22033/ESGF/CMIP6.621>

1882 Yukimoto, S., Koshiro, T., Kawai, H., Oshima, N., Yoshida, K., Urakawa, S., Tsujino, H.,
1883 Deushi, M., Tanaka, T., Hosaka, M., Yoshimura, H., Shindo, E., Mizuta, R., Ishii, M.,
1884 Obata, A., & Adachi, Y. (2019b). *MRI MRI-ESM2.0 model output prepared for CMIP6*
1885 *ScenarioMIP* [Dataset]. Earth System Grid Federation.
1886 <https://doi.org/10.22033/ESGF/CMIP6.638>

1887 Zelinka, M. D., Myers, T. A., McCoy, D. T., Po-Chedley, S., Caldwell, P. M., Ceppi, P., Klein, S.
1888 A., & Taylor, K. E. (2020). Causes of higher climate sensitivity in CMIP6 models.
1889 *Geophysical Research Letters*, 47(1). <https://doi.org/10.1029/2019gl085782>

1890 Zhang, L., & Li, T. (2014). A simple analytical model for understanding the formation of sea

1891 surface temperature patterns under global warming. *Journal of Climate*, 27(22), 8413–
1892 8421. <https://doi.org/10.1175/jcli-d-14-00346.1>

1893 Zhu, L., Quiring, S. M., & Emanuel, K. A. (2013). Estimating tropical cyclone precipitation
1894 risk in Texas. *Geophysical Research Letters*, 40(23), 6225–6230.
1895 <https://doi.org/10.1002/2013gl058284>

